THE ROLE OF HETEROCHROMATIN IN RNAi-MEDIATED TRANSCRIPTION REPRESSION IN *C. ELEGANS*

By

NATALLIA KALINAVA

A dissertation submitted to the

School of Graduate Studies

Rutgers, The State University of New Jersey

In partial fulfillment of the requirements

For the degree of

Doctor of Philosophy

Graduate Program in Cell and Developmental Biology

Written under the direction of

Dr. Sam Guoping Gu

And approved by

_____

_____

_____

_____

New Brunswick, New Jersey

January, 2018

ABSTRACT OF THE DISSERTATION

THE ROLE OF HETEROCHROMATIN IN RNAi-MEDIATED TRANSCRIPTION REPRESSION IN *C. ELEGANS*

by NATALLIA KALINAVA

Dissertation Director:

Dr. Sam Guoping Gu

The germline nuclear RNAi pathway in *C. elegans* can lead to histone H3 lysine 9 trimethylation (H3K9me3) and transcriptional silencing at target genes. H3K9me3 heterochromatin induced by either exogenous double-stranded RNA (dsRNA) or endogenous siRNA (endo-siRNA) is highly specific to the target loci and is trans-generationally heritable. Despite these features, the role of H3K9me3 in siRNA-mediated establishment and maintenance of transcriptional silencing and its inheritance in *C. elegans* is unclear. It is also not known which of H3K9me3 histone methyltransferases (HMT) function in an RNAi-dependent manner. In this study, we took combined genetic, biochemical, CRISPR-Cas9 genome editing, cell biology and computational approaches to address these questions.

Here we demonstrate that siRNA-mediated H3K9me3 requires combined activities of three H3K9 histone methyltransferases (HMTs): MET-2, SET-25, and SET-32. Surprisingly, loss of high-magnitude of H3K9me3 in *set-32; met-2 set-25* mutant worms has no effect on the transcriptional silencing at the native nuclear RNAi targets. In addition, the exogenous dsRNA-induced transcriptional silencing and heritable RNAi at *oma-1*, a well-established nuclear RNAi reporter gene, are completely resistant to the loss of H3K9me3. Repair of germline nuclear Argonaut HRDE-1 fully restore silencing of nuclear RNAi targets. However, loss of SET-32 showed trans-generational delay in re-establishment of transcriptional silencing. We propose that H3K9me3 is dispensable for the maintenance of siRNA-mediated transcriptional silencing. However, H3K9me HMT SET-32 promotes the onset of nuclear RNAi-mediated transcriptional silencing.

Acknowledgments

This work reflects my major projects that I have been working over the years of my graduate training. Chapter I is a literature review and an introduction to this thesis. Chapter II was adopted from my published work (Kalinava et. al., 2017). Chapter III was adopted from the manuscript for another paper, which is still in development for submission.

I would like to express deep appreciation and gratitude to my advisor, Dr. Sam Gu, for his patience, guidance, encouragement and support over the years of my PhD work. I enjoyed working on the projects, our brainstorming discussions and could always rely on his thoughtful advice. I am grateful to Dr. Sam Gu for teaching me bioinformatics, which made this work possible. Friendly and stimulating environment in his lab helped me to grow as a graduate student and as a person.

I also would like to thank Dr. Julie Ni for her help and opportunity to collaborate with her on several projects. Dr. Julie Ni taught me many molecular biology techniques and helped with troubleshooting when experiments did not work. She taught me imaging techniques and performed the key imaging experiments for my projects. Dr. Sam Gu and Dr. Julie Ni both trained me to become persistent scientist and a productive collaborator. With their help, I participated in several collaboration projects, expanded my professional network, made new friends and experienced great science.

I would like to thank my committee advisers, Dr. Marc Gartenberg, Dr. Monika Driscoll and Dr. Michael Hampsey for the challenging questions, insightful suggestions and constructive feedback. With their help I was able to develop and shape my dissertation. In addition, I want to express my gratitude to Dr. Vincenzo Pirrotta and Dr.

Mikel Zaratiegui for the productive discussions and guidance with my projects.

I would like to thank Esteban Chen for the technical support and help during the late nights and weekends. Helen Ushakov performed most of the injections; I thank her for her hard work and expertise. I also want to thank all the members in Dr. Sam Gu's lab, in particular Alex Huang, Kim Peterman and Zoran Gajic for helping with CRISPR screens and other projects.

I want to thank my parents for bringing me up with love and career and supporting my curiosity and passion to science. Neither of them knows English, so I want to say "спасибо".

Finally, I want to express my gratitude to my family, my husband Jean-Francois, daughters Nicole and Victoria and all close relatives and friends, for being encouraging in my choice to pursue graduate studies and for the continuous support to finish my PhD degree. This work would have not happened without their optimism and cheer.

Table of Contents

List of Figures

List of Tables

1. CHAPTER I - Introduction to Nuclear RNAi

1.1. Introduction to RNAi

RNAi or RNA interference is a phenomenon in which an exogenously introduced double stranded RNA (dsRNA) leads to a potent and specific gene silencing (Fire et al. (1998); (Kennerdell and Carthew, 1998). Although RNAi was first observed in plants (Napoli et al., 1990) and then discovered *C. elegans*, RNAi is conserved in most eukaryotes and serves as an endogenous cellular pathway that regulates activity of repetitive DNA sequences and transposable elements (TEs) (Brennecke et al., 2008; Das et al., 2008; Sienski et al., 2012; Slotkin and Martienssen, 2007). RNAi is also involved in many cellular processes, such as stress response, genome surveillance and stability, heterochromatin assembly, maintenance of germline immortality, epigenetic memory, and others (Bayne and Allshire, 2005; Buckley et al., 2012; Castel and Martienssen, 2013; Hammond, 2005; Moazed, 2009; Ni et al., 2016).

When introduced into a cell, dsRNA is first recognized by the RNase III-like enzyme Dicer, which cuts dsRNA into short interfering RNAs (siRNAs) (Bernstein et al., 2001). These siRNAs are loaded into a RNA-induced silencing complex (RISC), which targets mRNA for degradation, which called post-transcriptional gene silencing (PTGS) (Hammond et al., 2000). An Argonaut family protein is at the core of the RISC complex. It contains an RNaseH-like 'PIWI' domain, which often has a slicing activity, and a 'PAZ' domain, which binds siRNAs (Hammond et al., 2001). RNAi specificity is determined by siRNAs, which are antisense complementing to the target RNA. In addition, in some organisms (*C. elegans, S. pombe,* plants, etc.), RNA-dependent RNA

polymerase (RdRP) can use target RNAs as a template and further amplify antisense siRNAs (Elbashir et al., 2001; Pak and Fire, 2007; Sijen et al., 2007; Tuschl et al., 1999). Therefore, a small number of dsRNAs can often yield a potent gene silencing.

1.2. Nuclear RNAi

In addition to post-transcriptional gene silencing (PTGS), siRNA can function in the nucleus at the transcription and chromatin level. Nuclear RNAi leads to the transcriptional gene silencing (TGS) and heterochromatin formation at the target sequence. The RNAi can lead to the formation of the repressive heterochromatin by either DNA methylation or histone modifications, such as methylation of histone H3 lysine 9 (H3K9me3) or in some cases histone H3 lysine 27 methylation (H3K27me3). RNAi-triggered heterochromatin response was first reported in plants, where it was discovered that a viral RNA or a transgene can lead to the heritable DNA-methylation of the homologous sequence (Mette et al., 2000; Wassenegger et al., 1994). Later studies showed that nuclear RNAi is conserved from fungi to mammals, which often suppress transcription of repetitive DNA sequences and transposable elements (TEs) and therefore, maintains genome integrity and stability (Brennecke et al., 2008; Castel and Martienssen, 2013; Das et al., 2008; Holoch and Moazed, 2015; Sienski et al., 2012; Slotkin and Martienssen, 2007). Moreover, RNAi-mediated transcriptional gene silencing and heterochromatin marks are heritable. Hence, an understanding of nuclear RNAi pathways may provide insights into the mechanism of epigenetic inheritance (Holoch and Moazed, 2015).

1.2.1 Role of heterochromatin in transcriptional silencing

The effect of heterochromatin on transcription repression was first demonstrated in *Drosophila* by the phenomenon called position effect variegation. It was found that an active gene, when trans-located into heterochromatin domain, becomes inactive by the local heterochromatin spreading. Extensive research of position effect variegation helped to identify *Suppressors of variegation* [*Su(var)s*] - the key players for the heterochromatin formation and transcriptional silencing. Among them, SU(VAR)3-9 is a conserved H3K9 histone methyltransferase (HMT) and SU(VAR)2-5 – a heterochromatin protein 1 (HP1) (Eissenberg et al., 1990; Tschiersch et al., 1994). HP1 protein has two domains: a chromo domain and a shadow domain. The chromo domain recognizes H3K9me3, while the shadow domain facilitates homodimerization of HP1 and recruitment of more HMTs, leading to the propagation of H3K9me3 marks and compaction of the region. The mechanism of chromatin compaction is conserved and became a conventional model for transcriptional repression by heterochromatin (Ekwall et al., 1996) (Grewal and Jia, 2007). However, recent studies indicate that siRNA plays an important role in heterochromatin assembly and maintenance. The mechanism of transcriptional repression by heterochromatin is far more complex than the conventional compaction model and in many cases includes intermediate nascent RNA and siRNA-dependent steps.

1.2.2 Role of heterochromatin in RNAi-mediated transcriptional silencing in different model organisms

Several model organisms have been used to study the mechanism of RNAi-mediated transcription regulation. The role of heterochromatin in nuclear RNAi is

complex and is often difficult to decouple from the nuclear RNAi-mediated repression effect. Perhaps the nuclear RNAi pathway is best understood in fission yeast (*S. pombe)*. In *S. pombe*, nuclear RNAi can lead to the H3K9me3 heterochromatin formation (Bühler et al., 2006) and is required for the heterochromatin at pericentromere regions and mating type loci (Martienssen and Moazed, 2015). Clr-4, the sole H3K9me3 HMT, is required for both the RNAi-directed transcriptional silencing and H3K9me responses in *S. pombe* (Verdel et al., 2004; Zhang et al., 2008). The RNAi complex contains chromodomain proteins (Swi6 and Chp1), which can bind to H3K9me3 and provide more recruitment and stable interactions of the RNAi complex (Martienssen and Moazed, 2015). Therefore, RNAi-guided heterochromatin is an integral part of self-reinforcing RNAi targeting loop. RNAi is required for the initiation of heterochromatin, but the maintenance of pericentromere heterochromatin can be achieved by both RNAi-dependent and RNAi-independent mechanisms (Hall et al., 2002; Irvine et al., 2006; Partridge et al., 2007). Tethering of Clr-4 to an active gene results in RNAi-independent silencing, indicating that H3K9me3 heterochromatin alone is potent for silencing (Audergon et al., 2015; Ragunathan et al., 2015). In addition, several other mechanisms ensure silencing of heterochromatin at the pericentromer repetitive regions in *S. pombe*: Rdp1 and Dcr1 mediate degradation of target RNA via RNAi mechanisms and degradation of RNA transcripts by TRAMP polyadenylation complex (Buhler et al., 2007; Buhler et al., 2008; Yamanaka et al., 2013). While these regions are recognized by the antisense siRNAs for transcriptional silencing and heterochromatin, it is still not clear what triggers the *de novo* production of siRNAs.

In plants, the nuclear RNAi pathway involves plant-specific RNA Polymerases IV and V, several proteins of the Argonaut and Dicer family, DNA methyltransferases and histone modifying enzymes (Haag and Pikaard, 2011). Silencing of an active transposable element (TE) involves siRNA-based recognition of Pol IV transcription, which triggers siRNA amplification. These siRNAs target Pol V transcripts and promote DNA methylation at these regions (Cuerda-Gil and Slotkin, 2016; Fultz et al., 2015; Slotkin, 2014). As a result, DNA methylation is tightly linked to the initiation and the maintenance of RNAi-mediated transcriptional silencing and is required for the nuclear RNAi re-enforcement loop.

In *Drosophila*, nuclear RNAi is represented by two main classes: siRNA and piRNA (Piwi-interacting RNAs). Unlike siRNA, piRNA biogenesis does not involve Dicer or RdRP enzymes and instead are originate from the piRNA clusters – a depository of TEs in the host genome as "non-self" sequences (Izumi and Tomari, 2014). In *Drosophila*, piRNAs and nuclear siRNA associated complexes target TEs and lead to PTGS, transcriptional gene silencing (TGS) and H3K9me3 responses (Huang et al., 2013; Le Thomas et al., 2013; Rozhkov et al., 2013). Unlike the repressive role of heterochromatin in gene regulation, it is not clear if RNAi-directed heterochromatin also plays a silencing role in nuclear RNAi in *Drosophila*. Surprisingly, H3K9me3 at the piRNA clusters promotes transcription and biogenesis of piRNA in *Drosophila* (Le Thomas et al., 2014; Mohn et al., 2014) and in some cases H3K9me3 heterochromatin at the RNAi targets is accompanied by transcription (Sienski et al., 2012). These results undermine the assumption that RNAi-mediated heterochromatin has silencing function in nuclear RNAi in *Drosophila*.

Mammals too have RNAi components, which can lead to TGS, H3K9me3 and DNA methylation of target regions (Bayne and Allshire, 2005; Castellano and Stebbing, 2013; Kim et al., 2006; Morris et al., 2004). Some studies showed that nuclear siRNAs can target promoter and 3' end sequences of genes, leading to gene silencing (TGS) or in some cases gene activation (TGA) (Chu et al., 2010; Gagnon and Corey, 2012). In mice, piRNA are expressed in the male germ line and are required for DNA methylation and transposon silencing (Aravin et al., 2008; Carmell et al., 2007; Kuramochi-Miyagawa et al., 2008). There is some evidence of nuclear RNAi-directed H3K9me3 heterochromatin formation and recruitment of HP1 to the target genes in somatic mammalian cells as well (Ameyar-Zazoua et al., 2012). The most recent study indicated that heterochromatin regions of mammalian cells are accompanied by RNA transcripts, which are required for the heterochromatin assembly at these regions (Johnson et al., 2017). However, the mechanism of RNAi-mediated transcriptional silencing and the role of heterochromatin in this process in mammals remain unclear.

1.2.3 Nuclear RNAi function

1.2.3.1 Genome stability. Active TEs can disrupt genes, regulatory elements and cause genome instability. While siRNA mediated PTGS can disable TE translation events, nuclear RNAi is the front line of defense, which represses TEs at the transcriptional level (reviewed in (Slotkin and Martienssen, 2007)). In addition to TE silencing, siRNA pathways are involved in other cellular pathways that also promote genome stability.

For instance, nuclear RNAi is directly involved into assembly of constitutive heterochromatin. Loss of RNAi-mediated heterochromatin at pericentromer regions in *S.*

pombe leads to defects in chromosome segregation during mitosis (Volpe et al., 2003). Furthermore, nuclear RNAi promotes condensation of chromosomes in *Drosophila* and *S. pombe* (Gullerova and Proudfoot, 2008; Pek and Kai, 2011); therefore, nuclear RNAi ensures proper genome structure.

Repetitive regions are highly prone to recombination events, which can yield deletions, duplications and other genomic rearrangements. Studies in *S. pombe* and *Drosophila* also showed that RNAi-directed heterochromatin can inhibit recombination between repetitive regions and therefore ensure genome stability (Ellermeier et al., 2010). In addition, there is some evidence of RNAi responding to the double stranded breaks and promoting DNA repair events (Wei et al., 2012). Thus, nuclear RNAi pathways are involved into maintenance of genome integrity.

1.2.3.2 Role of nuclear RNAi in epigenetic inheritance. Epigenetic inheritance is a non-DNA-based change that alters gene expression, which can be passed on from parent to the progeny. There are several examples in which nuclear RNAi plays a central role in epigenetic changes.

Both RNAi-mediated transcriptional silencing and heterochromatin responses are heritable. dsRNA-induced gene silencing in *C. elegans* is often heritable for more than four generations. In addition, dsRNA-induced H3K9me3 is also maintained for several generations in the absence of a dsRNA trigger (more in the later section). siRNA transmission is thought to be required for germline RNAi-mediated epigenetic inheritance in *C. elegans* (Burton and Burkhart, 2011; Gu et al., 2012).

Transgene based silencing of the endogenous copy is called co-suppression, another example of epigenetic gene regulation. Both *C. elegans* and plants are

notoriously known for efficient and heritable transgene silencing and co-suppression effects. There are multiple mechanisms for transgene silencing; siRNA is one of them (Dernburg et al., 2000; Ketting and Plasterk, 2000; Rajeevkumar et al., 2015; Robert et al., 2005). Transgene silencing became a common approach to study the mechanism of the endogenous siRNA and piRNA pathways and helped to identify many nuclear RNAi factors in *C. elegans* and plants.

Paramutation is a phenomenon, by which a silenced allele can induce silencing of a homologous region in *trans*, thus altering gene expression in the heritable generations. In plants paramutation is mediated by nuclear RNAi (siRNA-directed DNA-methylation) (Chandler, 2010). There are some examples of paramutation in animals too. In *Drosophila* paramutation is accompanied with the *de novo* produced piRNA, which can be inherited through maternal germline and can transgenerationally maintain silencing of the homologous region (Brennecke et al., 2008; de Vanssay et al., 2012). Thus understanding of nuclear RNAi may help to uncover the mechanism of epigenetic regulation.

1.3. Nuclear RNAi in *C. elegans*

1.3.1 *C. elegans* as a model organism to study RNAi pathways

The *C. elegans* is a model organism that widely used for basic research studies in many fields of biology. The *C. elegans* genome is well annotated, containing about 20,000 genes, with ~50% conserved in mammals, and provides a strong foundation for the whole genome studies (Spieth et al., 2014). *C. elegans* are self-fertile hermaphrodites with a short reproductive cycle (about 3 days at 19°C) and serve as a good model

organism to study the mechanism of transgenerational changes (Corsi et al., 2015). dsRNA can be efficiently delivered to animals by several ways: injection, soaking worms in the solution with dsRNA or simply feeding bacteria producing dsRNA (Fire et al., 1998; Tabara et al., 1998; Timmons and Fire, 1998).

Screens using dsRNA-induced silencing of a transgene reporter helped to identify many RNAi players in *C. elegans* (Dernburg et al., 2000). Many endogenous active genes respond to dsRNA with efficient gene silencing and heterochromatin responses. *C. elegans* is widely used as a model to study the RNAi pathway too (Gu et al., 2012). *C. elegans* has a large number of endogenously produced siRNA, which define endogenous native targets and became an important tool to understand the endogenous function of RNAi (Ni et al., 2014). While exogenously introduced dsRNA against transgenes or native genes are good model systems to track and measure RNAi-induced changes, it is also important to test native endo-siRNA targets when studying components of RNAi pathway and their function.

After the discovery of the RNAi phenomenon in *C. elegans,* similar dsRNA events were reported in plants, *S. pombe*, *Drosophila* and other organisms. Early efforts failed to find nuclear transcriptional gene silencing effects in *C. elegans*. Targeting promoter or intron sequences by dsRNA resulted in no effect on gene expression (Fire et al., 1998). In addition, targeting one gene of a polycistronic message had no effect on the expression of the coupled genes (Montgomery et al., 1998), indicated that dsRNA silencing is predominantly through PTGS mechanism. One hint for nuclear RNAi came from the observation that dsRNA leads to the reduction of both mRNA and pre-mRNA transcripts of the target gene (Fire et al., 1998; Montgomery et al., 1998). Moreover,

similar to plants, several RNAi factors in *C. elegans* are required for the transgene silencing and co-suppression of the endogenous native gene *in trans*, which include transcriptional repression and chromatin changes (Tabara et al., 1999) (Ketting and Plasterk, 2000) (Robert et al., 2005), indicating the conservation of the nuclear RNAi function in *C. elegans* too. Later studies found that dsRNA leads to the H3K9me3 (Gu et al., 2012) and H3K27me3 (Mao et al., 2015) heterochromatin responses and Pol II pausing at the target gene in *C. elegans* (Burkhart et al., 2011; Guang et al., 2010).

1.3.2 Endo siRNA and piRNA in *C. elegans*

Exogenously introduced dsRNA in *C. elegans* is processed into siRNA by RNase III enzyme Dicer (DCR-1, the sole ortholog in *C. elegans*) (Zamore et al., 2000). RdRP amplifies siRNA signal into secondary siRNA, which load into Argonaut proteins and lead to potent gene silencing by diverse mechanisms (Sijen et al., 2001). There are several types of small RNAs in *C. elegans*. Small RNAi analysis revealed a large group of 5' guanosine antisense siRNA in *C. elegans*, which is divided into two major subpopulations: primary 26G and secondary 22G siRNAs (Pak and Fire, 2007). 26G primary siRNAs mostly function in cytoplasm and trigger 22G biogenesis, which can function in nucleus. Another large class of small RNA is 21U RNAs, which maintain epigenetic memory of non-self (Ashe et al., 2012; Bagijn et al., 2012; Lee et al., 2012; Shirayama et al., 2012). 21U RNAs associate with PRG-1, a PIWI subclass of Ago proteins and called piRNA. PRG-1 with 21U RNAs initiate transcriptional silencing and 22G siRNA further maintain silencing (Ashe et al., 2012; Lee et al., 2012; Luteijn et al., 2012; Shirayama et al., 2012). Therefore, 22G siRNA can be generated downstream of either 26G primary siRNA from the exo-dsRNA, or 21U piRNA trigger. However, PRG-

1 mutants, which lack piRNAs, do not loose 22G endo siRNAs, indicating that there are other triggers for endo siRNAs biogenesis (Ni et al., 2014).

1.3.3 Nuclear RNAi effects in *C. elegans*

In *C. elegans* there are 27 Argonaut proteins, half of which are worm specific or so called WAGO proteins (Yigit et al., 2006). Many RNAi factors and Argonauts when mutated result in adverse effects in germline and sterility (Ashe et al., 2012; Buckley et al., 2012; Knight and Bass, 2001; Ni et al., 2016).

Nuclear RNAi can lead to transcriptional silencing and heterochromatin in *C. elegans* (Ashe et al., 2012; Buckley et al., 2012; Burton and Burkhart, 2011; Gu et al., 2012). Genetic screens identified several *n*uclear *R*NAi *de*ficient factors (NRDE-1, 2, 3 and 4) (Burkhart et al., 2011; Guang et al., 2008). NRDE-3 is a nuclear Argonaut in somatic cells, which transport siRNA into nucleus and together with other NRDE factors inhibit elongation of RNA Pol II (Burkhart et al., 2011; Guang et al., 2010). NRDE-2 is a nuclear RNAi factor, which is required for RNAi-directed H3K9me3 response (Gu et al., 2012; Ni et al., 2014). dsRNA-induced H3K9me3 can spread several kilobases flanking the dsRNA trigger, supporting the idea of co-transcriptional RNAi-mediated heterochromatin formation.

Both transcriptional silencing and heterochromatin response are maintained for several generations, even in the absence of the initial dsRNA trigger (Burton and Burkhart, 2011; Gu et al., 2012). Genetic screens for *H*eritable *R*NAi *de*ficient outcomes identified germline nuclear Argonaut – HRDE-1 (also known as WAGO-9) (Ashe et al., 2012; Buckley et al., 2012). HRDE-1 Argonaut and NRDE-2 are required for transcriptional silencing, H3K9me3 and H3K27me3 heterochromatin responses (Mao et

al., 2015; Ni et al., 2014). Several reports indicated that PRG-1 is required for the initiation of transcriptional silencing, while HRDE-1 is required for the maintenance of these silencing events (Ashe et al., 2012; Lee et al., 2012; Shirayama et al., 2012). dsRNA-induced siRNA response precedes H3K9me3 response in heritable generations, indicating that siRNA is the heritable epigenetic factor, where heterochromatin is maintained by the siRNA-mediated mechanism (Burton and Burkhart, 2011). Although, both RNAi-directed H3K9me3 and H3K27me3 accompany RNAi-mediated transcriptional silencing, it is not clear if these heterochromatin marks are required for RNAi-mediated silencing in *C. elegans*.

Many RNAi mutants, including *hrde-1*, show progressive loss of fertility and sterility after exposure to high temperatures (23-25°C) for several generations (Buckley et al., 2012; Ni et al., 2016). This phenomenon is called *Mrt* phenotype (mortal germline) and is characteristic of other NRDE mutants, but not NRDE-3. Whole genome analysis of *hrde-1* mutants in early and late generations of heat stress revealed that *Mrt* phenotype is accompanied with genome wide defects of heterochromatin assembly and miss-regulation of a large number of genes and genomic regions (Ni et al., 2016). Surprisingly, *Mrt* phenotype in *hrde-1* mutants is reversible, indicating that heat induced changes are not permanent. Therefore, the germline nuclear RNAi pathway is essential for maintaining homeostasis of gene expression under stress conditions (Ni et al., 2016).

1.3.4 Native targets of endo-siRNA mediated nuclear RNAi

Several approaches have been used to define native nuclear RNAi targets. Mapping of Argonaut-bound siRNA sequences is one of the methods. HRDE-1 bound siRNAs align to a large number of regions through out the genome, highlighting the

potential of nuclear RNAi to regulate many endogenous genes and intergenic regions (Buckley et al., 2012). Another way to define nuclear RNAi targets is to map genomic regions that show functional changes dependent on nuclear RNAi components. We performed whole genome characterization of *hrde-1* mutants and defined native germline nuclear RNAi targets at permissive temperature (19°C) (Ni et al., 2014). Regions that showed strong transcriptional de-silencing in *hrde-1* mutants were called GRTS – germline RNAi-dependent transcriptional silencing targets; regions that showed strong H3K9me3 heterochromatin depletion in *hrde-1* and *nrde-2* mutants were classified as GRH – germline RNAi-dependent heterochromatin targets (Ni et al., 2014). Both GRTS and GRH targets are further used in this work as native nuclear RNAi targets. HRDE-1 is also required for H3K27me3 at GRH regions, indicating that both H3K9me3 and H3K27me3 responses are triggered by the same signals (Mao et al., 2015; Ni et al., 2014). Both GRTS and GRH are enriched with repetitive DNA and LTR retrotransposon sequences. Surprisingly, only 18% of GRTS regions overlap with GRH regions (Ni et al., 2014), suggesting that RNAi-mediated transcriptional silencing and heterochromatin are not linked with each other, challenging the assumption that RNAi-directed heterochromatin plays a silencing role in nuclear RNAi in *C. elegans*. This observation leads to the aim of my work: to investigate if RNAi-directed heterochromatin is the cause of the RNAi-mediated transcriptional silencing.

1.4. Chromatin factors and RNAi-directed heterochromatin in *C. elegans*

H3K9me3, the hallmark of constitutive heterochromatin, is enriched at the distal arms of autosomal chromosomes and at one end of sex chromosome in *C. elegans* (Gu

and Fire, 2010; Ho et al., 2014). There are 38 putative histone methyltransferases (HMT) in *C. elegans* genome; many are predicted to carry H3K9me activity (Andersen and Horvitz, 2007; Greer et al., 2014). SET-25, a tri-methylation HMT, and MET-2, a mono- and di-methylation HMT, are responsible for all H3K9me3 in the *C. elegans* embryo stage, which was measured by mass spectrometry (Bessler et al., 2010; Garrigues et al., 2015; Towbin et al., 2012). Surprisingly, *met-2* mutants have normal H3K9me3 levels in germline and intestinal nuclei, but lack H3K9me2, indicating that other HMTs with mono-, di- and trimethylation activity must function (Bessler et al., 2010; Snyder et al., 2016). Indeed, other studies found additional H3K9 HMTs: SET-32, which was tested by immunofluorescence (IF) and SET-26 – by *in vitro* biochemistry analysis (Greer et al., 2014; Snyder et al., 2016).

The relationship of different HMTs to the RNAi pathway was best tested by a candidate screen using dsRNA-induced transgene silencing and a piRNA reporter. These screens identified a potential role for SET-25 and SET-32 in the RNAi pathway (Ashe et al., 2012; Shirayama et al., 2012). A recent study showed that *met-2 set-25* double mutants have H3K9me3 depletion in the germline, which results in transcriptional activation and genome instability (Zeller et al., 2016). However, this study reported no changes of transcription in *met-2 set-25* mutants at LTR retrotransposons, which are also regulated by the nuclear RNAi pathway. However, the role of these and other HMTs in RNAi-dependent H3K9me3 have not been tested.

1.5. Outstanding question and an overview of this study

Different heterochromatin factors have been identified in the RNAi pathway of *S. pombe*, *Drosophila*, plants and other organisms; however, RNAi-directed H3K9me3 HMTs in *C. elegans* have not been investigated. The pressing question remains open: does RNAi-directed H3K9me3 lead to the RNAi-mediated transcriptional silencing in *C. elegans*?

The first goal of my work is to identify nuclear RNAi-dependent H3K9me3 HMTs, specifically the ones that function downstream of the HRDE-1 Argonaute and the germline endo-siRNA pathway. The next goal is to test if these HMTs are required for the initiation or the maintenance stages of RNAi transcriptional silencing of native nuclear RNAi targets and/or the exogenous dsRNA target gene *oma-1*. Finally, we want to test the requirement of H3K9me3 HMTs for heritable RNAi.

My work made significant progress in understanding the role of H3K9me3 HMTs in germline RNAi-mediated transcriptional silencing in *C. elegans.* We determined that MET-2, SET-25 and SET-32 are H3K9me3 HMTs function in an RNAi-dependent manner. Surprisingly, we found that H3K9me3 is dispensable for RNAi-mediated transcriptional silencing. Full genome analysis revealed differential roles for MET-2, SET-25 and SET-32 HMTs in global and RNAi-dependent H3K9me3 levels in *C. elegans*. Furthermore, we found that H3K9me3 HMT SET-32 promotes trans-generational onset of transcriptional silencing. Surprisingly, well studied H3K9me3 HMTs MET-2 and SET-25 showed little effect on the transcription of native nuclear RNAi targets. Together, these results define requirement for H3K9me3 HMTs in the

initiation and maintenance of nuclear RNAi-mediated transcriptional silencing in *C. elegans*.

2. CHAPTER II - Decoupling the downstream effects of germline nuclear RNAi reveals that H3K9me3 is dispensable for heritable RNAi and the maintenance of endogenous siRNA-mediated transcriptional silencing in *Caenorhabditis elegans*

Natallia Kalinava, Julie Zhouli Ni, Kimberly Peterman, Esteban Chen, and Sam Guoping Gu

Department of Molecular Biology and Biochemistry, Rutgers the State University of New Jersey, Piscataway, New Jersey, 08854, United States of America

Epigenetics & Chromatin 2017 Feb15, Volume 10, pg. 6

Author contributions: NK and SG designed the experiments. NK, EC, JN, and KP collected the samples and performed the experiments. NK and SG performed data analysis and wrote the manuscripts. All authors read and approved the final manuscript.

2.1. Summary

Background: Germline nuclear RNAi in *C. elegans* is a transgenerational gene-silencing pathway that leads to H3K9 trimethylation (H3K9me3) and transcriptional silencing at the target genes. H3K9me3 induced by either exogenous double-stranded RNA (dsRNA) or endogenous siRNA (endo-siRNA) is highly specific to the target loci and transgenerationally heritable. Despite these features, the role of H3K9me3 in siRNA-mediated transcriptional silencing and inheritance is unclear. In this study, we took combined genetic and whole-genome approaches to address this question.

Results: Here we demonstrate that siRNA-mediated H3K9me3 requires combined activities of three H3K9 histone methyltransferases (HMTs): MET-2, SET-25, and SET-32. *set-32* single, *met-2 set-25* double, and *met-2 set-25;set-32* triple mutant adult animals all exhibit prominent reductions in H3K9me3 throughout the genome, with *met-2 set-25;set-32* mutant worms losing all detectable H3K9me3 signals. Surprisingly, loss of high-magnitude H3K9me3 at the native nuclear RNAi targets has no effect on the transcriptional silencing state. In addition, the exogenous dsRNA-induced transcriptional silencing and heritable RNAi at *oma-1,* a well-established nuclear RNAi reporter gene, are completely resistant to the loss of H3K9me3.

Conclusions: Nuclear RNAi-mediated H3K9me3 in *C. elegans* requires multiple histone methyltransferases, including MET-2, SET-25, and SET-32. H3K9me3 is not essential for dsRNA-induced heritable RNAi or the maintenance of endo-siRNA-mediated transcriptional silencing in *C. elegans*. We propose that siRNA-mediated transcriptional silencing in *C. elegans* can be maintained by an H3K9me3-independent mechanism.

2.2. Introduction

In this chapter, we combined genetic and whole-genome approaches to characterize the requirement of H3K9me3 for transcriptional silencing at nuclear RNAi targets. *C. elegans* has 38 putative histone methyltransferases (HMTs) (Andersen and Horvitz, 2007; Greer et al., 2014). It is unclear which of these are required for the H3K9me3 response associated with nuclear RNAi. MET-2 (a H3K9 mono- and dimethylation HMT) (Bessler et al., 2010) and SET-25 (a H3K9 trimethylation HMT) are required for all detectable H3K9me3 at the embryonic stage, as shown by mass spectrometry analysis (Garrigues et al., 2015; Towbin et al., 2012). A recent study also showed a complete loss of H3K9me3 in the adult germline of *met-2 set-25* mutants by immunofluorescence (IF) analysis; de-silencing in the *met-2 set-25* mutants leads to increased genome-instability and mutation (Zeller et al., 2016). Interestingly, many H3K9me3-eniched loci, including LTR retrotransposons, remain silenced in *met-2 set-25* mutant worms (Zeller et al., 2016). Despite the prominent loss of H3K9me3 in *met-2 set-25* mutants, SET-32 and SET-26 were also shown to be H3K9 HMTs by IF (Snyder et al., 2016) and *in vitro* HMT assay (Greer et al., 2014), respectively. A candidate screen using a transgene reporter showed that SET-25 is required for exogenous dsRNA-induced heritable RNAi and SET-32 is required for piRNA-induced gene silencing (Ashe et al., 2012). The H3K9me3 status at nuclear RNAi reporter transgenes is unclear. In addition, the requirement of H3K9me3 for nuclear RNAi-mediated transcriptional silencing at native genes has not been tested.

2.3. Results

2.3.1. MET-2, SET-25, and SET-32 are required for exogenous dsRNA-triggered H3K9me3

We first performed H3K9me3 ChIP-seq in *met-2 set-25* double mutant worms to examine the requirement of these two HMTs for exogenous dsRNA-triggered H3K9me3. We chose a germline-specific gene *oma-1* as the target gene as it is sensitive to dsRNA-induced nuclear RNAi (Buckley et al., 2012; Mao et al., 2015). Despite the popular usage of *oma-1* in nuclear RNAi and heritable silencing studies (Alcazar et al., 2008; Buckley et al., 2012; Houri-Ze'evi et al., 2016; Mao et al., 2015), a high-resolution profile of dsRNA-induced H3K9me3 at this locus has not been reported before. A combination of control samples, including wild type and *hrde-1* mutant animals, both with *oma-1* RNAi, as well as wild type animals with control RNAi (*gfp*), were used to indicate the full extent of HRDE-1-dependent H3K9me3 response at the *oma-1* locus. Synchronized young adult animals, of which over 50% of total cells are germline (Hirsh et al., 1976), were used throughout this study. (Table A-1 lists all samples and sequencing libraries used in this thesis.)

The *oma-1* dsRNA-induced H3K9me3 response was analyzed using coverage plot (Fig. 1a) and whole-genome 1-kb-resolution scatter plot (Fig. 1b-f). In WT, *oma-1* dsRNA-induced H3K9me3 peaked at the dsRNA trigger region (0.52 kb) (Fig. 1a) and was limited to *oma-1* (Fig. 1b), a degree of specificity similar to the ones observed for other targets in our previous study (Gu et al., 2012). The H3K9me3 response spread throughout the *oma-1* gene (~ 2 kb) and dropped to the background level around the putative *oma-1* promoter and the polyadenylation site, without spreading into either of

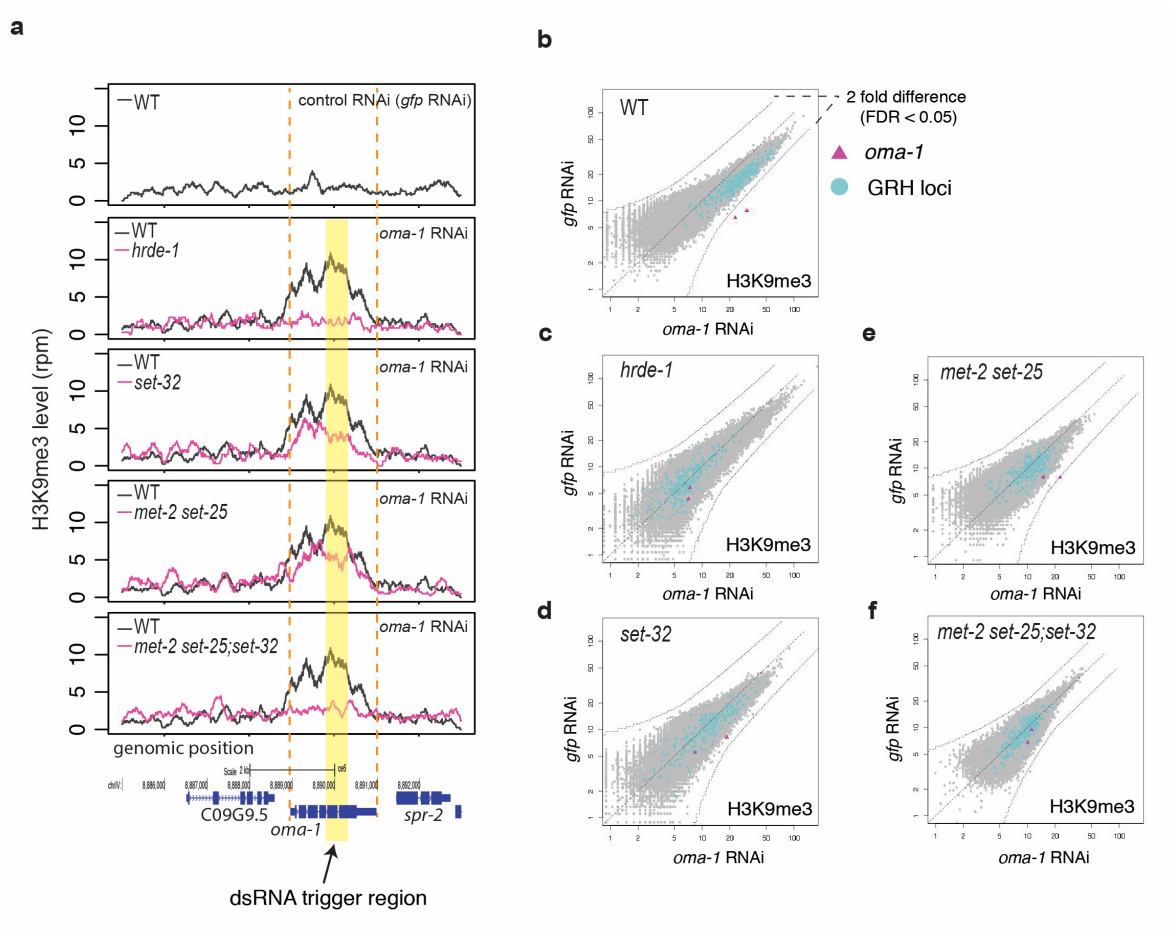

Figure 1 **MET-2, SET-25, and SET-32 are required for the dsRNA-triggered H3K9me3 response at the *oma-1* locus**

(a) H3K9me3 levels in different samples are plotted as a function of position along the *oma-1* locus. The WT response (*oma-1* RNAi) is shown in all panels, except the top one (WT with *gfp* RNAi), to facilitate comparison with mutant ones. A yellow block indicates the region targeted by dsRNA. (b-f) Scatter plots that compare whole-genome H3K9me3 levels in *oma-1* RNAi and *gfp* RNAi samples at 1kb resolution for WT and various mutant strains. *oma-1* regions (2 kb) and GRH loci (215 kb) are highlighted. Curved dotted lines indicate the 2-fold change (FDR<0.05). Synchronized young adult animals (19˚C) were used throughout this study.

the adjacent genes, both of which are less than 0.5 kb away (Fig. 1a). The H3K9me3 response was absent in the *hrde-1* mutant (*oma-1* RNAi) or WT (control RNAi) worms (Fig. 1a, b, and c), as expected (Buckley et al., 2012; Mao et al., 2015).

Compared to WT, *met-2 set-25* mutants showed only a partial defect in the H3K9me3 response at the *oma-1* locus (Fig. 1a, b, and e), suggesting that additional H3K9 HMT(s) are involved. This was somewhat surprising because of the more severe H3K9me3 defect at the whole-genome level observed in the same mutant sample (Fig. 4a and see later section). In addition, previous studies showed that *met-2 set-25* double mutants were devoid of H3K9me3 at the embryo stage (Garrigues et al., 2015; Towbin et al., 2012), as well as in adult germline (Zeller et al., 2016).

We then performed *oma-1* RNAi and H3K9me3 ChIP-qPCR to screen additional H3K9 HMT mutants (Fig. A-1), among which only *set-32* mutant and *met-2 set-25;set-32* triple mutant worms showed defects in the H3K9me3 response at the *oma-1* locus (Fig. S1). *met-2* or *set-25* single mutants did not show any defect in the H3K9me3 response (Fig. A-1). We further confirmed the requirement of *set-32* by H3K9me3 ChIP-seq analysis (Fig. 1a). Compared to *met-2 set-25* mutants (*oma-1* RNAi), *set-32* mutants (*oma-1* RNAi) showed a stronger defect in the H3K9me3 response at the *oma-1* locus (ΔH3K9me3$_{oma\text{-}1}$ [*set-32*/WT] = 0.32 and ΔH3K9me3 $_{oma\text{-}1}$ [*met-2 set-25*/WT] = 0.55) (Fig. 1a, d, and e), indicating that SET-32 plays a more prominent role than MET-2 SET-25 in dsRNA-induced H3K9me3. Similar to *hrde-1* mutants (*oma-1* RNAi), *met-2 set-25;set-32* mutants (*oma-1* RNAi) showed a background level of H3K9me3 ChIP-seq signal at the *oma-1* locus (Fig. 1a, c, and f), suggesting that MET-2, SET-25, and SET-

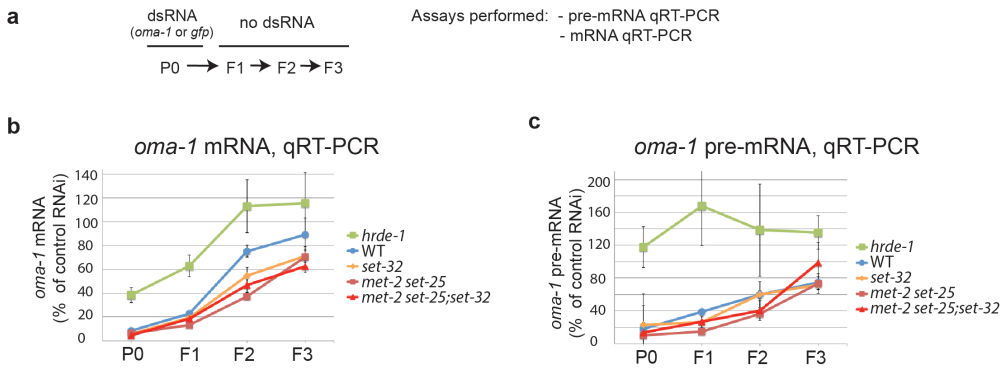

Figure 2* The requirement of H3K9me3 in heritable RNAi and transcriptional silencing of *oma-1

(a) Experimental scheme. (b and c) mRNA and pre-mRNA levels of *oma-1* RNAi samples, normalized to the control RNAi, are plotted as a function of generations for WT or various mutant strains.

32, in combination, contribute to the full H3K9me3 response induced by exogenous dsRNA.

2.3.2. H3K9me3 is not required for exogenous dsRNA-induced transcriptional silencing and heritable RNAi

To investigate the role of H3K9me3 in nuclear RNAi and heritable silencing, we performed a set of heritable RNAi experiments using wild type, *hrde-1, met-2 set-25, set-32,* and *met-2 set-25;set-32* mutant strains with *oma-1* or *gfp* RNAi (Fig. 2a). qRT-PCR analyses of *oma-1* mRNA and pre-mRNA were performed for the dsRNA-exposed animals (P0 generation) and their descendants (F1, F2, and F3) that were cultured without dsRNA exposure.

In the WT animals, *oma-1* RNAi caused heritable silencing of the target gene in F1, F2, and F3 at both mRNA and pre-mRNA levels (Fig. 2b and c). The heritable

silencing was dependent on HRDE-1 (Fig. 2b and c), as expected (Alcazar et al., 2008; Buckley et al., 2012).

All three HMT mutant strains (*met-2 set-25, set-32, and met-2 set-25;set-32*) showed wild type-like multigenerational profiles of *oma-1* pre-mRNA (Fig. 2c), despite various degrees of H3K9me3 defect at the *oma-1* locus. These results indicate that heritable transcriptional silencing can occur in the absence of the H3K9me3 response. We note that all three HMT mutant strains had a modest but consistently enhanced heritable RNAi at the mRNA level (Fig. 2b).

To further examine nuclear RNAi-mediated transcriptional silencing at *oma-1*, we performed RNA polymerase II (Pol II) ChIP-seq for the P0 generation samples, using an antibody against the phosphorylated C-terminal domain (CTD) repeat YSPTSPS at the S2 position (S2P), a modification associated with the elongating Pol II. Our scatter plot analysis showed that, compared to *gfp* RNAi, *oma-1* RNAi did not change the overall Pol II levels at the *oma-1* locus in wild type, *set-32,* or *met-2 set-25;set-32* mutant worms (Fig. 3a, c, and d). (A modest reduction in the Pol II level was observed in the *oma-1* RNAi sample for *met-2 set-25* mutants [Fig. 3b].) However, coverage plot analysis showed that *oma-1* RNAi changed the Pol II profile at the target gene. Specifically, it led to a reduction in the Pol II level at the 3' end (for WT and all three HMT mutant strains) and an increase in the gene body (all samples except *met-2 set-25* mutants) (Fig. 3e). Such Pol II shift is consistent with a model in which exogenous dsRNA-induced transcriptional silencing occurs at the elongation step, as previously suggested (Guang et al., 2010).

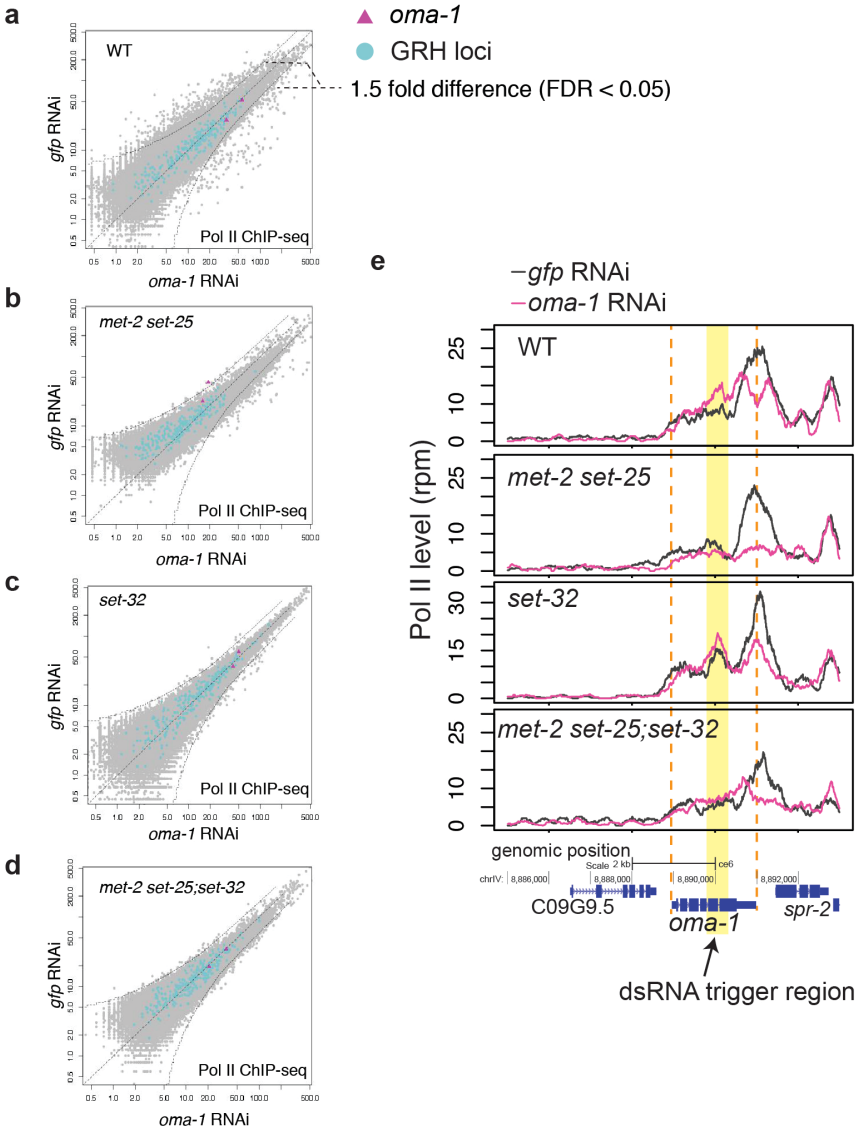

Figure 3 **The impact of RNAi on Pol II profile at the *oma-1* locus.**

(a-d) Scatter plots that compare whole-genome Pol II levels in *oma-1* RNAi and *gfp* RNAi samples at 1kb resolution for WT and various mutant strains. *oma-1* regions (2 kb) and GRH loci (215 kb) are highlighted. Curved dotted lines indicate the 1.5-fold change (FDR<0.05). (e) Pol II levels are plotted as a function of position along the *oma-1* locus.

Taken together, these results indicate that MET-2, SET-25, and SET-32 in combination are responsible for the full H3K9me3 response for exogenous dsRNA-triggered H3K9me3. However, these HMTs are not required for dsRNA-induced transcription silencing or heritable silencing.

2.3.3. MET-2, SET-25, and SET-32 in combination contribute to all of the detectable H3K9me3 at the native nuclear RNAi targets in adult animals

When examined at the global level, *set-32, met-2 set-25*, and *met-2 set-25;set-32* mutant worms all showed significant reduction in the H3K9me3 ChIP-seq signal compared to WT (Fig. 4a and Fig. A-2). *met-2 set-25;set-32* triple mutants had the most severe global H3K9me3 loss among the three HMT mutant strains and showed H3K9me3 depletion throughout each of the six chromosomes (Fig. 4a and Fig. A-2). *met-2 set-25* double mutants ranked the second, and had a severity of H3K9me3 loss similar to *met-2 set-25;set-32* mutants. *set-32* mutants showed the least global H3K9me3 loss among the three HMT mutant strains. To quantify the loss of H3K9me3, we defined the top 5 percentile regions of H3K9me3 in WT as the H3K9me3(+) regions. The 0.25, and 0.17 for *set-32*, *met-2 set-25*, and *met-2 set-25;set-32* mutants, respectively (Fig. 5a and Fig. A-3a, all p-values $< 2.2 \times 10^{-16}$).

By using ΔH3K9me3[WT/mutant] ≥ 2 fold (FDR < 0.05) as the cut off, we identified 816 kb regions with SET-32-dependent H3K9me3, which were much less than the ones that required MET-2 SET-25 (2,677 kb) or all three HMTs (3,290 kb) (Fig. 4b, Fig. A-4a-b). Regions with SET-32-dependent H3K9me3 largely

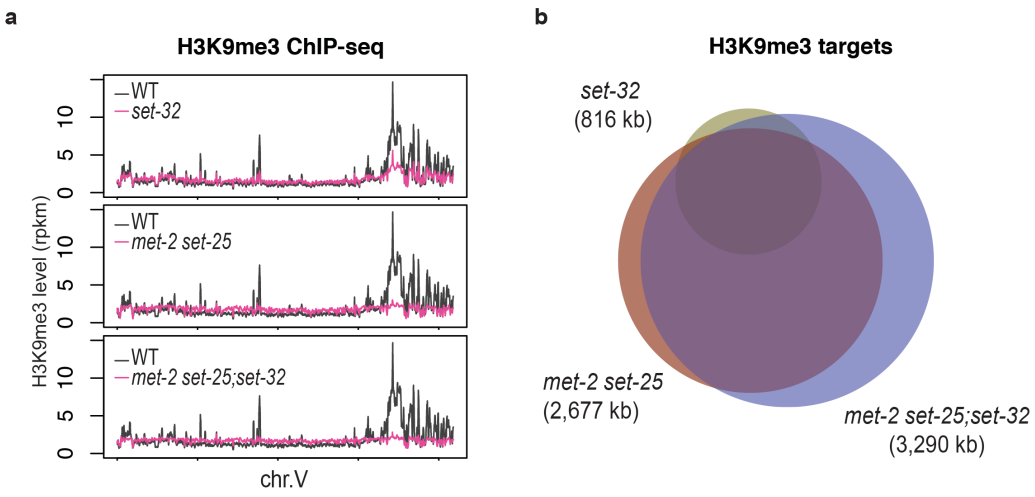

***Figure 4* Global H3K9me3 contribution of MET-2, SET-25, and SET-32.**
(a) H3K9me3 levels are plotted as a function of position in chromosome V for WT and HMT mutant strains (the effect is the same for other chromosomes, see Fig. A-2). A moving average with a sliding window of 50 kb was used to plot H3K9me3 levels. (b) A Venn diagram of H3K9me3 regions that are dependent on SET-25, MET-2 SET-25, and MET-2 SET-25;SET-32. Targets were identified as regions with ΔH3K9me3[mutant/WT]≥2 (FDR<0.05) in two replica (Fig. A-3).

overlapped with the MET-2 SET-25-dependent ones (Fig.4b). Taken together, these results indicate that MET-2, SET-25, and SET-32, in combination, contribute to all detectable level of H3K9me3 ChIP-seq signal in adult *C. elegans*. Interestingly, both *set-32* and *met-2 set-25* mutants had more than 50% H3K9me3 loss in many regions throughout the genome compared to wild type animals, suggesting a synergistic relationship between SET-32 and MET-2 SET-25.

We then limited our analysis to the native targets of germline nuclear RNAi. Consistent with our previous work (Ni et al., 2014), *hrde-1* mutation led to a much stronger loss of H3K9me3 in GRH than GRTS loci, as shown in exemplary targets in Fig.

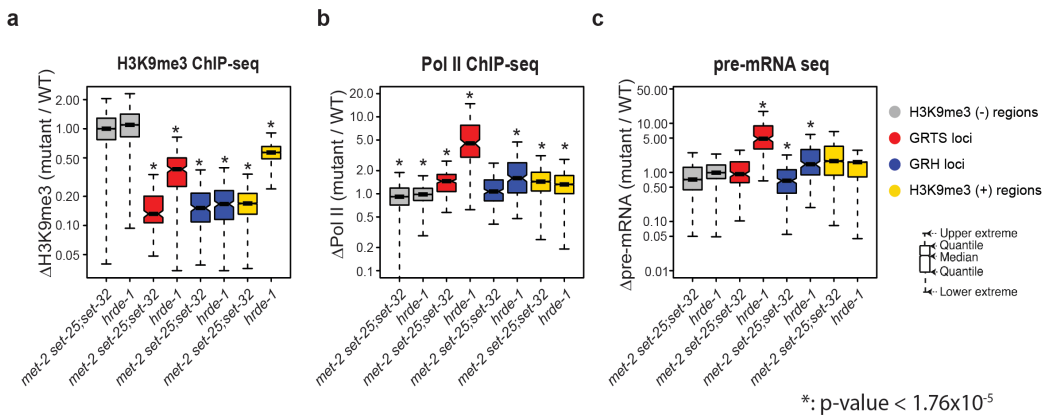

***Figure 5* The impact of *met-2 set-25;set-32* mutations and *hrde-1* mutation on H3K9me3, Pol II and pre-mRNA levels.**

(a) H3K9me3, (b) Pol II, and (c) pre-mRNA in different subsets of the genome: GRTS loci (191 kb), GRH loci (215 kb), top 5-percentile H3K9me3 regions in WT (H3K9me3(+) regions, 4,775 kb), and bottom 5 to 25-percentile H3K9me3 regions in WT (H3K9me3(-) regions, 20,200 kb). Boxplot analysis is used to describe the ratios between mutant and WT for H3K9me3, Pol II, and pre-mRNA.

6a-b. Similar results were obtained when GRTS and GRH loci were analyzed as groups: the median values of ΔH3K9me3[*hrde-1*/WT] were 0.17 for GRH and 0.38 for GRTS loci (both p-values < $2.2\text{x}10^{-16}$, Fig. 5a and Fig. A-3a). The partial H3K9me3 loss in *hrde-1* mutants indicates that GRTS carry both HRDE-1-dependent and HRDE-1-independent H3K9me3.

met-2 set-25;set-32 triple mutants showed a background-level of H3K9me3 at HRDE-1-dependent loci (Fig. 6a-b). This is expected because of the aforementioned genome-wide depletion of H3K9me3 in the same mutant worms. *met-2 set-25* double mutant and *set-32* mutant worms both showed strong H3K9me3 loss at both GRTS and GRH loci (Fig. 6a-b). The median values of ΔH3K9me3[mutant/WT] for *set-32, met-2 set-25,* and *met-2 set-25;set-32* mutants were 0.21, 0.25 and 0.15 in GRH loci (0.23, 0.20,

and 0.13 in the GRTS loci, respectively) (Fig. 5a and A-3a, all p-values < $2.2x10^{-16}$). Therefore, these HMTs together are required for HRDE-1-dependent and HRDE-1-independent H3K9me3 at the native germline nuclear RNAi targets.

2.3.4. H3K9me3 is not required for transcriptional silencing at the native nuclear RNAi targets

To determine the impact of H3K9me3 loss on the transcriptional silencing in the native germline nuclear RNAi targets, we performed coverage analyses of Pol II ChIP-seq, and pre-mRNA-seq for two exemplary native targets and a control region (Fig 6a-c). *set-32, met-2 set-25,* and *met2 set-25;set-32* mutants all showed background levels of Pol II occupancy and pre-mRNA at these two targets, similar to WT, despite partial or complete H3K9me3 loss in the mutants. In contrast, *hrde-1* mutant worms showed dramatic increases in both Pol II occupancy and pre-mRNA at these two targets, even though it had only partial H3K9me3 loss at *cer8,* a GRTS locus (Fig. 6a).

Consistent with our previous study, *hrde-1* mutant worms showed strong transcriptional de-silencing in GRTS loci: the median values of ΔPol II [*hrde-1*/WT] and Δpre-mRNA [*hrde-1*/WT] were 4.52 and 4.85, respectively (p-values < 3.42×10^{-15}) (Fig. 5b-c). In contrast, *met-2 set-25;set-32* mutants showed only a modest increase in Pol II occupancy at GRH loci overall: the median value of ΔPol II [*met2 set-25;set-32* /WT] was 1.46 (p-value < 3.01×10^{-13}). Importantly, *met-2 set-25;set-32* mutants did not show any increase in pre-mRNA at GRTS loci: the median value of Δpre-mRNA [*met2 set-25;set-32* /WT] was 0.93 (p-value = 0.062). In addition, GRH loci showed unchanged Pol

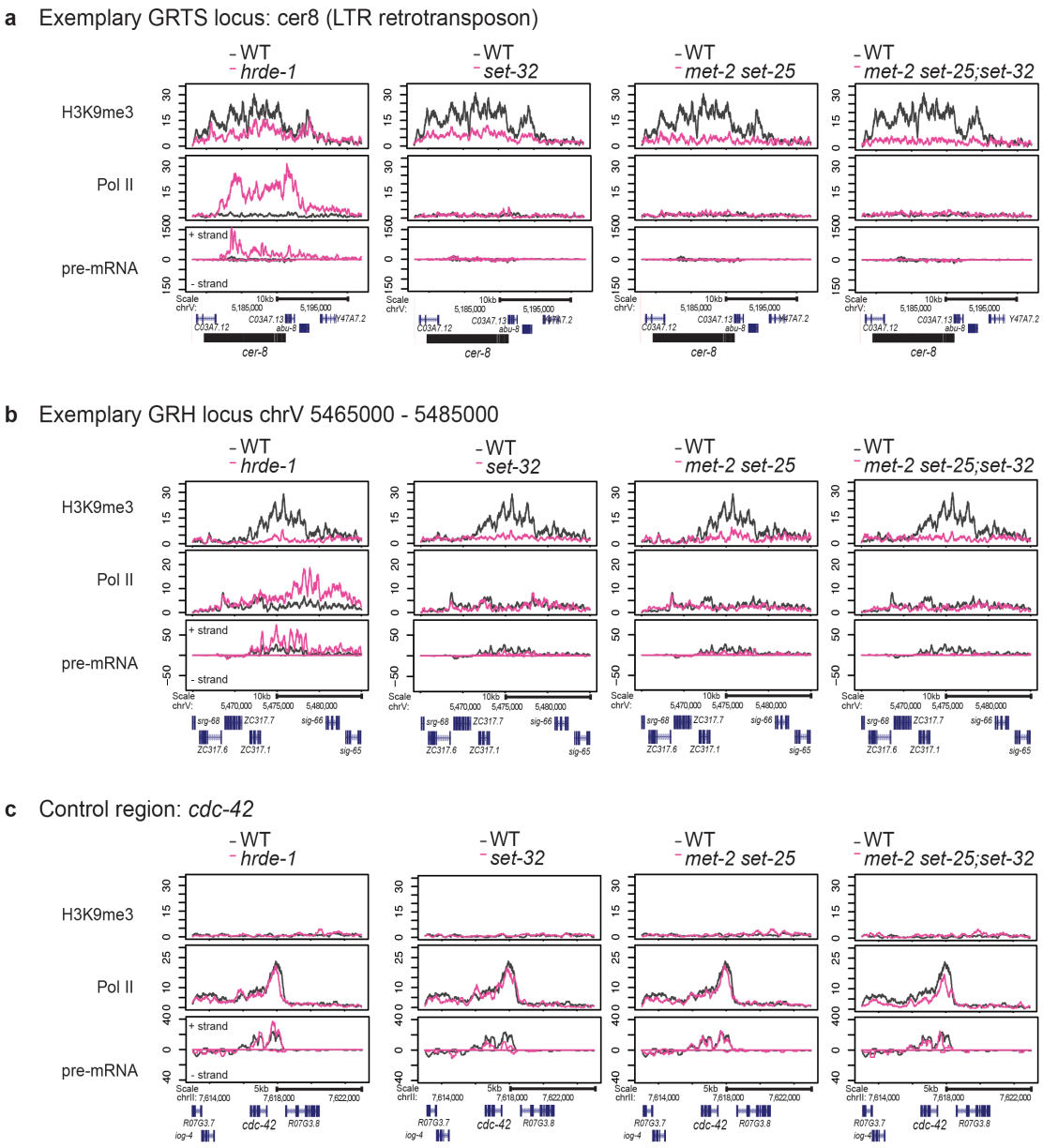

***Figure 6* Coverage plots of H3K9me3, Pol II, and pre-mRNA in exemplary native nuclear RNAi targets and control regions.**

(a) an exemplary GRTS locus, (b) an exemplary GRH locus, and (c) a control region. For pre-mRNA coverage plots, sense reads are plotted above the y=0 line (antisense bellow).

II occupancy in *met-2 set-25;set-32* mutants (the median value of ΔPol II [*met2 set-25;set-32* /WT] = 1.07, p-value = 0.16) and an unexpected decrease in pre-mRNA (the median value of Δpre-mRNA [*met2 set-25;set-32* /WT] was 0.68, p-value = 7.59×10^{-10}) (Fig. 5b-c and Fig. A-3b-c).

We note that the H3K9me3(+) regions in *met-2 set-25;set-32* mutants, on average, showed a modest increase in the Pol II level over WT: the median value of ΔPol II [*met2 set-25;set-32* /WT] was 1.44 (p-value = 1.47×10^{-11}) (Fig. 5b-c and Fig. A-3b-c). However, the pre-mRNA increase in these regions was not statistically significant: the median value of Δpre-mRNA [*met2 set-25;set-32* /WT] was 1.70 (p-value = 0.63). Scatter plot analyses of H3K9me3 ChIP-seq, Pol II ChIP-seq, pre-mRNA-seq, and mRNA-seq confirmed that the loss of H3K9me3 was not associated with transcriptional de-silencing in most of the H3K9me3(+) regions (Fig. A-5). Furthermore, the overall germline chromosome morphology was similar between *met-2 set-25;set-32* mutant and wild type worms (Fig. A-6). These data suggest that H3K9me3 plays, at most, a very limited role in germline chromatin condensation or transcription silencing at the global level.

2.3.5. Germline nuclear RNAi-mediated H3K9me3 is accompanied with H3K27me at the native targets

To characterize the other known germline nuclear RNAi-mediated heterochromatin mark in *C. elegans*, H3K27me3 (Mao et al., 2015), at the whole-genome level, we performed H3K27me3 ChIP-seq in the wild type and *hrde-1* mutant worms. Consistent with a previous study (Mao et al., 2015), we found that H3K27me3 was

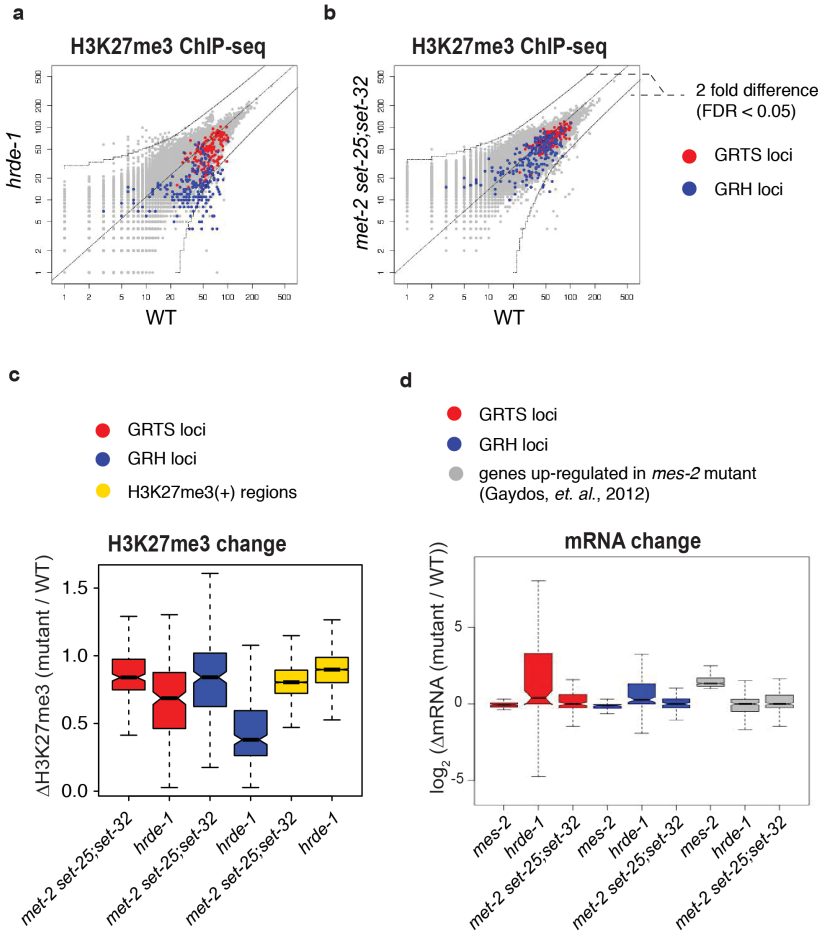

Figure 7 **H3K27me3 is associated with native germline nuclear RNAi targets and not affected in *met-2 set-25;set-32* mutant worms**

(a, b) Scatter plots comparing whole-genome H3K27me3 levels in WT and *hrde-1* or *met-2 set-25;set-32* mutants at 1 kb resolution. (c) Boxplot analysis showing H3K27me3 changes between WT and *met-2 set-25;set-32* or *hrde-1* mutant worms in different subsets of the genome: GRTS loci (191 kb), GRH loci (215 kb), top 5-percentile H3K27me3 regions in WT (H3K27me3 + regions, 4966 kb). (d) Boxplot analysis comparing mRNA expression between WT and *mes-2, hrde-1, or met-2 set-25;set-32* mutants in different subsets of the genome: GRTS loci (121 genes), GRH loci (142 genes), genes that are up-regulated in *mes-2* mutant worms (355 genes, ≥2 fold, FDR < 0.05). Published microarray data (Gaydos et al., 2012) were used for mRNA expression changes between *mes-2* mutant and WT worms.

associated with both GRH and GRTS loci and was dependent on HRDE-1 (Fig. 7a, c). The median values for ΔH3K27me3 [*hrde-1*/WT] at GRTS and GRH loci were 0.68 and 0.38 respectively (all p-values < 2.2×10^{-16}).

Just like H3K9me3, the correlation between HRDE-1-dependent-H3K27me3 and transcriptional silencing was different between the GRTS and GRH loci: GRTS loci showed a much weaker H3K27me3 loss than GRH loci in *hrde-1* mutants (Fig. 7a, c), comparing with a much stronger transcriptional de-silencing in GRTS than GRH loci [Fig. 5b-c]. In addition, GRTS and GRH loci did not show de-silencing at mRNA level in *mes-2* mutants by using a published microarray data (Gaydos et al., 2012) (Fig. 7d), or in *met-2 set-25;set-32* mutants by mRNA-seq analysis in this study (Fig. 7d). In contrast, these targets were activated in *hrde-1* mutants (Fig. 7d). Taken together, these results suggest that transcriptional silencing at HRDE-1 targets is likely to be independent of H3K27me3, as well.

We note that, by performing H3K27me3 ChIP-seq in *met-2 set-25;set-32* mutant worms, we found no evidence of any H3K27me3-based compensating mechanism for the H3K9me3 loss – the triple HMT mutant worms did not show increased H3K27me3 in GRTS and GRH loci (Fig. 7b-c).

2.4. Discussion

In plants, *S. pombe*, as well as *Drosophila,* nuclear RNAi-mediated H3K9me3 is essential to maintain transcriptional silencing state at target loci. Here, we show that H3K9me3 is completely dispensable for the maintenance of endo-siRNA-mediated transcriptional silencing at the whole-genome level in *C. elegans*. In addition, H3K9me3

is not required for exogenous-dsRNA triggered transcriptional silencing and heritable RNAi in a well-established native gene target. These findings shift the paradigm of the *C. elegans* nuclear RNAi pathway, a key model system for studying RNA-mediated transcriptional silencing and transgenerational epigenetics.

2.4.1 The H3K9me3 contributions of MET-2, SET-25, and SET-32 in HRDE-1-dependent regions and elsewhere in the genome

C. elegans has several H3K9 HMTs. Before this study, it was unclear which of these HMTs are required for siRNA-mediated H3K9me3. Here, we provide experimental evidence supporting that germline nuclear RNAi-dependent H3K9me3 requires MET-2, SET-25, and SET-32.

Interestingly, the relative H3K9me3 contributions of these three HMTs are not the same at different targets. Their activities appear to be synergistic at the native targets (endo-siRNA-targeted), as each of the two mutant strains, *met-2 set-25* and *set-32,* showed >50% of H3K9me3 loss compared to the wild type. Such synergy may be the underlying mechanism that allows the high level of H3K9me3 at the native targets. The synergistic relationship is also evident for essentially all H3K9me3-enriched regions in the genome. The underlying mechanism for such apparent synergy is currently unknown. We also note that MET-2 SET-25 and SET-32 activities are not entirely mutually dependent, as the triple HMT mutant worms showed greater H3K9me3 loss than *met-2 set-25* or *set-32* mutants. For exogenous-dsRNA-induced H3K9me3, MET-2 SET-25-dependent H3K9me3 and SET-32-dependent H3K9me3 are additive, suggesting that the two are independently triggered by dsRNA.

2.4.2 RNAi-mediated transcriptional (or co-transcriptional) silencing at different types of targets

Our ChIP-seq analyses show that HRDE-1-dependent silencing at native targets (endo-siRNA targeted) leads to depletion of Pol II throughout the regions, suggesting that transcription initiation is prevented. In contrast, exogenous dsRNA-triggered RNAi does not significantly change the overall Pol II level at the target gene, but causes a shift of the Pol II profile instead (a reduction at the 3' end and a gain in the gene body). This suggests that exogenous dsRNA-triggered RNAi does not block transcription initiation, but rather occurs during transcription elongation (also suggested previously by (Guang et al., 2010)) or co-transcriptionally. It is conceivable that the actual effect of RNAi on transcriptional silencing (and perhaps the degree of heritable silencing) is dependent on various features associated with the target gene (*e.g.,* promoter, chromatin landscape, and siRNA).

2.4.3 The role of H3K9me3 in *C. elegans* germline nuclear RNAi

Our findings are consistent with two models. Model 1: H3K9me3 is not involved in siRNA-mediated transcription silencing and its function lies in another not yet identified aspect of germline nuclear RNAi. Model 2: H3K9me3 is involved in siRNA-mediated transcription silencing, together with an H3K9me3-independent silencing mechanism. Although these two models are mutually exclusive at any given target locus, they may both occur in *C. elegans* and used by different loci/silencing mechanisms that involve siRNA. A previous study showed that SET-32 and SET-25 are required for HRDE-1-dependent silencing using a GFP transgene as the piRNA reporter or exogenous dsRNA-induced heritable RNAi reporter (Ashe et al., 2012). In our study, these HMTs

are not required for heritable silencing at a native reporter gene, *oma-1*. Future studies are required to explain this difference. Transgene reporter is a powerful tool in studying RNAi. However, the efficacy of small RNA-mediated silencing on a transgene reporter appears to be dependent on a variety of factors, such as transgene structure (Shirayama et al., 2012), epigenetic history (Leopold et al., 2015; Seth et al., 2013), and DNA sequence (Bagijn et al., 2012). On the other hand, detailed characterization of additional native targets is needed to address whether heritable RNAi is regulated in a target-specific, context-dependent manner.

2.4.4 Conclusions

We found that three H3K9 HMTs, MET-2, SET-25, and SET-32, are required for germline nuclear RNAi-mediated H3K9me3 in *C. elegans.* Loss of the prominent H3K9me3 response in *met-2 set-25;set-32* mutant worms is not associated with any defect in germline nuclear RNAi-mediated transcriptional silencing at the native targets. Therefore, a high level of H3K9me3 is dispensable for the maintenance of the HRDE-1-dependent transcriptional silencing in *C. elegans* germline. In addition, we found that dsRNA-induced H3K9me3 is not required for transgenerational silencing at *oma-1*. We propose that transcriptional and heritable silencing of the germline nuclear RNAi pathway in *C. elegans* can be maintained in an H3K9me3-independent manner. Our discovery that H3K9me3 can be decoupled from transcriptional silencing in *C. elegans* provides a unique opportunity to study an H3K9me3-independent silencing mechanism, particularly the direct biochemical effect of AGO-siRNA complex on transcription and co-transcriptional processes.

2.5. Material and methods

2.5.1 Strains

Bristol strain N2 was used as a standard wild type strain. This study used the following mutations: LGI: *set-32(ok1457)*; LGII: *set-13(ok2697);* LGIII: *set-25(ok5021), hrde-1(tm1200);* LGIV: *set-21(ok2327), set-26(tm3526),* and *set-9(red8);* LGV: *met-2(n4256).* The *set-9(red8)* mutation has a stop codon and a frame shift in the first exon, which was generated in this study using the CRISPR-cas9-mediated genome editing (Arribere et al., 2014; Paix et al., 2015). Genotyping primers and other relevant sequences are listed in Table A-2. All strains were cultured at 19°C.

2.5.2 Worm grind preparation

Worms were cultured on NGM plates with OP50 *E.coli* as food source (Brenner, 1974). Synchronized young adult hermaphrodite animals were obtained by first using the bleaching method to collect worm embryos, which were hatched in M9 buffer without food, and then releasing L1 larvae onto NGM plates with OP50 *E. coli*. Young adult worms were ground by mortar and pestle in liquid nitrogen and stored at -80°C. Worm grind from ~5000 young adult worms was used for each assay in this study.

2.5.3 Multigenerational heritable RNAi

Heritable RNAi experiments were conducted as previously described (Gu et al., 2012). *oma-1* and *gfp* RNAi trigger sequences are reported in Table A-2. For *oma-1* RNAi, single nucleotide mismatch at every 30 nt was used to distinguish the trigger sequence from the native *oma-1* gene. All animals at P0 (with dsRNA feeding) and F1, F2, F3 (without dsRNA feeding) generations were collected at young adult stage and ground in liquid nitrogen.

2.5.4 H3K9me3 ChIP-qPCR

Worm grinds of P0 generation of *oma-1* RNAi and *gfp* RNAi samples at young adult stage were used for crosslinking, sonication and ChIP according to the protocol described in (Ni et al., 2016). H3K9me3 ChIP from ~5000 worms per grind yield 5-10 ng of DNA. 1 ng of ChIP DNA was used per qPCR reaction. qPCR was set up using KAPA SYBR FAST Universal 2× PCR Master Mix (KAPA Biosystems) on a Mastercycler EP Realplex realtime PCR system (Eppendorf) according to the manufacturer's instructions. qPCR primers are listed in Table A-2. Each sample was processed in triplicate. Reported values for the oma-1 RNAi H3K9me3 fold change were calculated using ΔΔCT analysis.

2.5.5 mRNA and pre-mRNA qRT-PCR

Worm grinds of P0 (RNAi+) and F1, F2, F3 (RNAi-) generations were used for total RNA extraction with Trizol reagent (Life Technologies).

mRNA reverse transcription (RT). 1 μg of total RNA was used for the first strand cDNA synthesis with SuperScript III RT kit (Life Technologies) and oligo(dT)20 primer (to enrich for mRNA).

Pre-mRNA RT. 2 μg of total RNA was used for the first strand cDNA synthesis with SuperScript III RT kit (Life Technologies) and random hexamer primer mix (to capture pre-mRNA).

qRT-PCR. qRT-PCR was performed using KAPA SYBR FAST Universal 2× PCR Master Mix (KAPA Biosystems) on a Mastercycler EP Realplex realtime PCR system (Eppendorf) according to the manufacturer's instructions. qPCR primers are listed in Table A-2. Each sample was processed in triplicate. Reported values for the fold change of mRNA and pre-mRNA at oma-1 gene were calculated using ΔΔCT analysis.

2.5.6 High-throughput sequencing

H3K9me3, Pol II, and H3K27me3 ChIP-seq. Crosslinking, sonication and ChIP were performed using the protocol described in (Ni et al., 2014; Ni et al., 2016). Worm grind sample (~5000 young adult worms) was used as starting material. IP was performed using anti-H3K9me3 (ab8898, Abcam), anti-RNA Pol II S2 (ab5095, Abcam), and anti-H3K27me3 (39535, Active Motif) antibodies for the H3K9me3, Pol II, and H3K27me3 ChIP respectively. 10 ng or less ChIP DNA was used to prepare DNA library using KAPA Hyper Prep Kit (KAPA Biosystems) according to the manufacturer's instruction.

Pre-mRNA-seq. Pre-mRNA library was prepared as described in (Ni et al., 2014). Anti-RNA Pol II S2 (ab5095, Abcam) antibodies were used for Pol II IP, followed by RNA isolation and library preparation.

mRNA-seq. Worm grinds (~5000 young adult worms) were used for total RNA extraction with Trizol reagent (Life Technologies). mRNA was enriched using the Poly(A) Purist MAG kit (Life Technologies) according to the manufacturer's instructions. 0.5–1 μg of mRNA was used for mRNA-seq library preparation as described in (Ni et al., 2014). A mixture of four different 4-mer barcodes were used for the 5'-end ligation in both mRNA and pre-mRNA-seq as indicated Table A-1.

All libraries were sequenced using Illumina HiSeq 2500 platform, with 50-nt single-end run and dedicated index sequencing. Dedicated 6-mer indexes were used to demultiplex DNA ChIP-seq and RNA-seq libraries for different samples.

Data availability: De-multiplexed raw sequencing data in fastq format for all libraries, normalized 1kb tables for H3K9me3 ChIP-seq, pre-mRNA-seq and normalized gene-by-gene table for mRNA-seq were deposited in NCBI (GEO accession number: GSE86517).

2.5.7 Data analysis

Sequencing reads were aligned to *C. elegans* genome (WS190 version) by using Bowtie (0.12.7) (Langmead et al., 2009). Only perfect alignments were used for data analysis. If a read was aligned to N different loci, it was counted as 1/N. Normalization based on sequencing depth of each library was used for all data analysis. In Fig. 5a and Fig. A-3a, besides sequencing depth, we also used the median values of H3K9me3(-) regions for data normalization. Otherwise, the background H3K9me3 levels in HMT mutants are artificially higher than the WT one, due to a high degree of H3K9me3 loss in a large fraction of the genome in the HMT mutants (e.g., Fig. 4a). The three-region Venn diagram was generated using a web-based software (http://www.benfrederickson.com/venn-diagrams-with-d3.js/). Custom R and python scripts were used in this study.

Curves that indicate 2-fold or 1.5-fold changes (FDR<0.05) in all scatter plots were calculated using a script from (Maniar and Fire, 2011). Welch Two Sample t-test was used to calculate all p-values.

3. CHAPTER III - SET-32 promotes the transgenerational establishment of nuclear RNAi-mediated transcriptional silencing in *C. elegans*

Natallia Kalinava, Julie Zhouli Ni, Zoran Gajic and Sam Gouping Gu

Department of Molecular Biology and Biochemistry, Rutgers the State University of New Jersey, Piscataway, New Jersey, 08854, United States of America

Author contribution: NK and SG designed experiments. NK wrote manuscript and performed data analysis. NK, ZN and ZG performed all experiments. All authors reviewed and approved the final manuscript.

3.1. Summary

Here we study endogenous targets of the nuclear RNA interference (RNAi) pathway as a model of establishment and maintenance of transcriptional silencing in *C. elegans*. We show that RNAi-dependent H3K9 HMTs SET-32, MET-2 and SET-25 are dispensable for the maintenance of RNAi-mediated repression, but required for some transcriptional silencing when the dominant RNAi-mediated mechanism of silencing is absent. Furthermore, we show that despite the strong transcriptional de-silencing in *hrde-1* mutant animals, repair of HRDE-1 Argonaut can fully recover transcriptional silencing in the early post-repair generations. We demonstrate that the putative H3K9 histone methyltransferase (HMT) SET-32 is required for the robust transgenerational establishment of the transcriptional repression at nuclear RNAi targets. This work defines the role of H3K9me3 HMTs in initiation and maintenance of RNAi-mediated transcriptional silencing in *C. elegans*.

3.2. Introduction

In *C. elegans*, nuclear RNAi can lead to the prominent target-specific H3K9me3 heterochromatin response at target regions (Buckley et al., 2012; Gu et al., 2012). There are many putative HMTs in *C. elegans* genome (Andersen and Horvitz, 2007; Greer et al., 2014). MET-2 and SET-25 are known major H3K9me HMTs which are required for nearly all H3K9me3, tested in embryo (Towbin et al., 2012), germline (dissected gonads) (Bessler et al., 2010) and in whole young adult animals (Kalinava et al., 2017). MET-2 HMT is required for H3K9 mono and di-methylation (Bessler et al., 2010); SET-25 HMT – for H3K9 tri-methylation (Towbin et al., 2012). SET-32 is a putative H3K9me HMT,

and is required for more than 50% of the dsRNA-induced H3K9me3 response (Kalinava et al., 2017; Spracklin et al., 2017). Together, MET-2, SET-25 and SET-32 HMTs are required for all RNAi-directed H3K9me3 response and the bulk of H3K9me3 in young adult animals (Kalinava et al., 2017). Complete depletion of H3K9me3 in *set-32; met-2 set-25* mutants does not lead to transcriptional desilencing of native nuclear RNAi targets (GRTS or GRH) (Kalinava et al., 2017). Interestingly, H3K9me2 and H3K9me3 only partially overlap and have distinct distributions in the genome. H3K9me2 is enriched at DNA transposon sequences and required for their silencing (McMurchy et al., 2017). H3K9me3 marks LTR retrotransposons (many are native nuclear RNAi targets) and is dispensable for transcriptional silencing of these regions (Kalinava et al., 2017; McMurchy et al., 2017; Zeller et al., 2016). Therefore, maintenance of RNAi-mediated transcriptional silencing in *C. elegans* can be achieved in the absence of RNAi-directed heterochromatin. However, combinations of H3K9me3 HMT and *hrde-1* mutants have never been tested.

The mechanism for the onset of germline nuclear RNAi silencing in *C. elegans* is not well understood. Previously it was reported that dsRNA triggered RNAi responses in the P0 generation are weaker than in subsequent F1 generation (Burton and Burkhart, 2011; Zhuang et al., 2013), suggesting that there is a trans-generational initiation of RNAi-mediated transcriptional silencing. Another study using a soma-expressed gene showed that dsRNA exposure as early as embryonic or L1 stages results in a more potent nuclear RNAi-mediated silencing response (Shiu and Hunter, 2017), indicating that there is a sensitive stage for efficient initiation of nuclear RNAi effects. However, the onset of

nuclear RNAi-dependent transcriptional silencing at native nuclear RNAi targets in *C. elegans* and the role of H3K9me3 HMTs in this process has not been tested.

CRISPR/Cas9-mediated genome editing has become a powerful genetic tool (Sander and Joung, 2014) with a potential for gene therapy to combat numerous genetic disorders. However, little is known about the influence of epigenetic history and whether a gene repair can fully restore normal function of the whole pathway.

In this chapter, we further tested the requirement of H3K9me3 for RNAi-mediated transcriptional silencing. While HRDE-1-dependent silencing plays a dominant role, MET-2, SET-2 and SET-32 contribute to repression and become essential for silencing in the *hrde-1* mutants. Furthermore, using CRISPR/Cas9-mediated repair of mutant *hrde-1(tm1200)* allele to *hrde-1* wild type sequence, we found that transcriptional silencing at native nuclear RNAi targets can be fully restored by nuclear RNAi as soon as in the F3 generation. We tested the requirement of RNAi-dependent H3K9me HMTs MET-2, SET-25 and SET-32 for such HRDE-1-dependent re-establishment of RNAi-mediated transcriptional silencing. We found that SET-32 is necessary for the efficient transgenerational onset of RNAi-mediated silencing at native nuclear RNAi targets. Remarkably well-characterized *C. elegans* H3K9me HMTs MET-2 and SET-25 appeared to be dispensable for the re-establishment of repression. This work identified differential roles of the H3K9me HMTs in transgenerational onset of RNAi-mediated transcriptional silencing and its maintenance in *C. elegans*.

3.3. Results

3.3.1. Mutations in H3K9me3 HMT genes enhance the silencing defect in the *hrde-1* mutant

Our previous work identified that *met-2*, *set-25* and *set-32* together are required for the nuclear RNAi-dependent H3K9me3 in *C. elegans* adults (Kalinava et al., 2017). Although, HRDE-1 is required for both transcriptional silencing and H3K9me3 heterochromatin at many endogenous regions, depletion of H3K9me3 in *set-32; met-2 set-25* mutants did not result in transcriptional de-silencing of native nuclear RNAi targets (Kalinava et al., 2017). These results indicated that H3K9me3 is dispensable for the maintenance of RNAi-mediated transcriptional silencing.

We decided to test if MET-2, SET-25 and SET-32 HMTs have any effect on transcription in the absence of nuclear RNAi-mediated repression. For that we generated combination HMT+*hrde-1* mutants. We used genetic crossed *set-32; hrde-1* and *met-2 set-25 hrde-1* mutants. We generated the *set-32; met-2 set-25 hrde-1* quadruple mutants using CRISPR-Cas9. For that we created a loss-of-function allele *set-32(red11)*, which has a stop codon followed by a frame shift mutation in exon 3 of the *set-32* gene (Table A-2). We verified that the *set-32(red11)* allele shows the same ~50% loss of dsRNA-induced H3K9me3 response at *oma-1* and no heritable RNAi defect, as it was previously reported for the *set-32(ok1457)* mutants (Fig. A-7a, b and c) (Kalinava et al., 2017). We then created *set-32(red11); hrde-1* double mutants. All the data and figures labeled bellow with "*set-32*" refer to the *set-32(red11)* allele, unless indicated otherwise.

To evaluate transcriptional changes in various combination mutants of *set-32, met-2, set-25* and *hrde-1* we performed Pol II ChIP-seq and RNA-seq using young adult

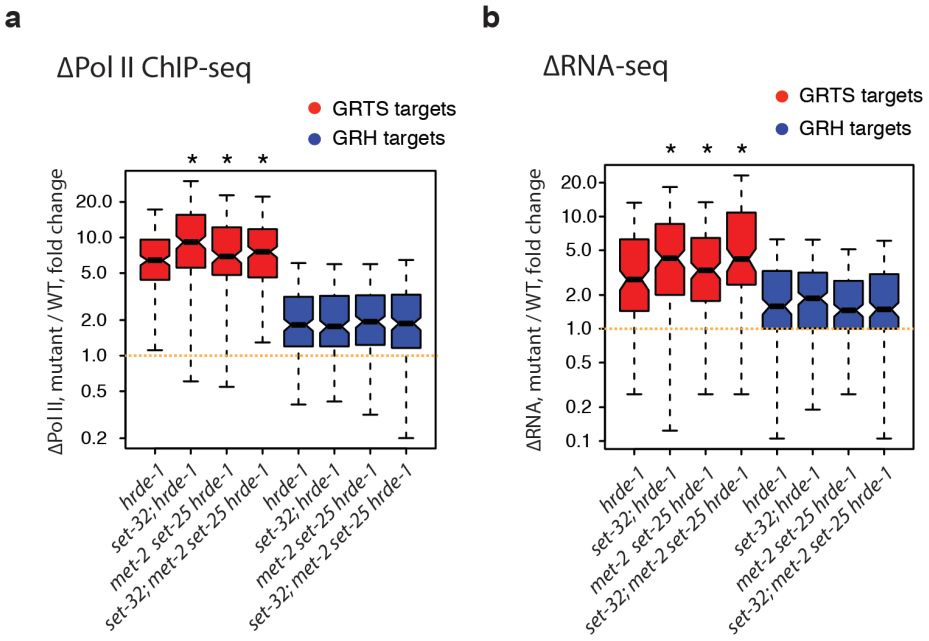

***Figure 8* Synthetic genetic effect of various combination mutants of *set-32*, *met-2, set-25* and *hrde-1* on the transcription of native nuclear RNAi targets**

Boxplot analysis is used to describe the ratios between different mutants and WT for (a) Pol II and (b) RNA levels at germline RNAi transcriptional silencing (GRTS, 191 kb regions) and heterochromatin (GRH, 215 kb regions) targets.

animals raised at 19°C. We used the WT, *hrde-1*, various HMT mutants (*set-32, met-2 set-25* and *set-32;met-2 set-25*) and various combination mutants of HMT+*hrde-1* (*set-32;hrde-1, met-2 set-25;hrde-1* and *set-32;met-2 set-25 hrde-1*). We performed the whole genome Pol II ChIP-seq 1kb analysis and highlighted previously characterized two classes of nuclear RNAi targets: GRTS and GRH. We observed stronger Pol II increase at GRTS regions in all animals with HMT+*hrde-1* combination mutant genotype when compared to *hrde-1* single mutants (Fig. A-8a). Boxplot analysis (Fig. 8a) showed that ΔPol II (mutant/WT) at GRTS in *set-32;hrde-1*, *met-2 set-25 hrde-1* and *set-32;met-2 set-*

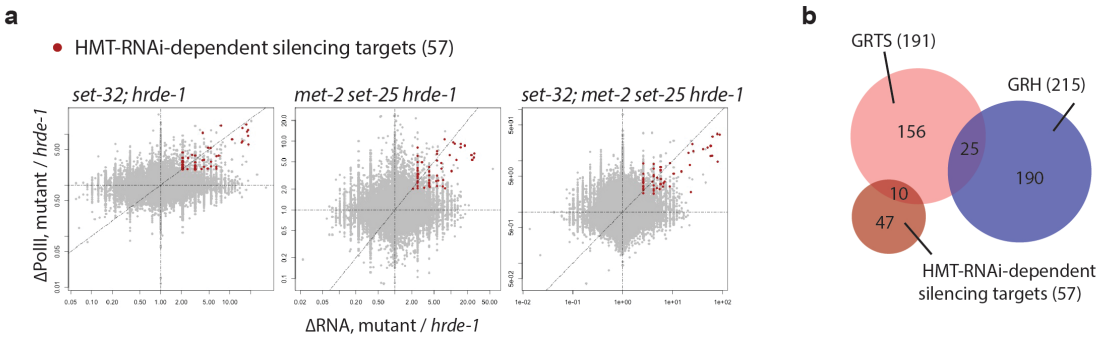

Figure 9 **Identification of regions with enhanced transcriptional desilencing in various combination mutants of *set-32*, *met-2, set-25* and *hrde-1***

(a) Scatter plot analysis comparing ratio of (x-axis) RNA changes in various combination mutants over single *hrde-1* mutant with (y-axis) Pol II changes in various combination mutants over single *hrde-1* mutant. (b) Venn diagram of different type of targets: GRTS (191 kb), GRH (215 kb), HMT-RNAi-dependent silencing targets (57 kb).

25 hrde-1 mutants were 9.15, 6.92 and 7.57 respectively, compared to ΔPol II in *hrde-1* single mutants 6.41 (p-value < 0.018). We did not find statistical significant difference of ΔPol II (mutant/WT) levels at GRH regions in compound HMT+*hrde-1* mutants when compared to *hrde-1* mutants. Median values for the ΔPol II at GRH in *set-32;hrde-1, met-2 set-25 hrde-1* and *set-32;met-2 set-25 hrde-1* mutants were 1.77, 1.94 and 1.87 respectively, compared to ΔPol II in *hrde-1* single mutants 1.82 (p-value = 0.727).

Both boxplot and scatter plot analyses of RNA-seq data (Fig. 8b and A-8b) also showed strong desilencing at GRTS, but not GRH, regions in all HMT+*hrde-1* compound mutants when compared to single *hrde-1* mutants.

We note that not all GRTS targets showed synthetic de-silencing in HMT+*hrde-1* compound mutants; some additional regions appeared in these analyses as well (Fig. A-8). We identified 57 regions (1kb) which consistently showed 2 fold and more increase in both RNA and Pol II levels in all combinations of HMT+*hrde-1* mutants (*set-32; hrde-1* or *met-2 set-25 hrde-1* or *set-32;met-2 set-25 hrde-1*) when compared to *hrde-1* (Fig. 9a). As a result of the synthetic combination of HMT mutations with *hrde-1*, these regions consistently showed enhanced transcriptional desilencing, here called HMT-RNAi-dependent silencing targets. Venn diagram analysis of GRTS, GRH and HMT-RNAi-dependent silencing targets showed that only some GRTS regions (10 regions, p-value = 1.53x10-19) exhibit the synthetic transcriptional de-silencing effect, but none of GRH (Fig. 9b). This is expected since GRTS, but not GRH, showed additive de-silencing in Fig. 8a and 8b analyses.

We used the *Cer3* LTR retrotransposon region (Gypsy family) as an example of such enhanced transcription in HMT+*hrde-1* compound mutants and presented coverage plots of H3K9me3, Pol II and RNA levels (Fig. 10a-c and Fig. A-9). We observed high levels of H3K9me3 at *Cer3* region in WT, partially reduced H3K9me3 levels in *hrde-1* mutants and near background levels of H3K9me3 in *set-32; met-2 set-25* (Fig. 10a). Pol II and RNA coverage plots showed that *Cer3* region is silent in WT and HMT mutants: *set-32, met-2 set-25* and *set-32; met-2 set-25* (Fig. 10b, c and Fig. A-9), confirming that H3K9me3 is dispensable for the maintenance of transcriptional silencing at *Cer3* LTR retrotransposon. All HMT+*hrde-1* mutant combinations showed higher Pol II and RNA levels at *Cer3* locus than in *hrde-1* single mutant, demonstrating the enhanced desilencing effect (Fig. 10b, c and Fig. A-9).

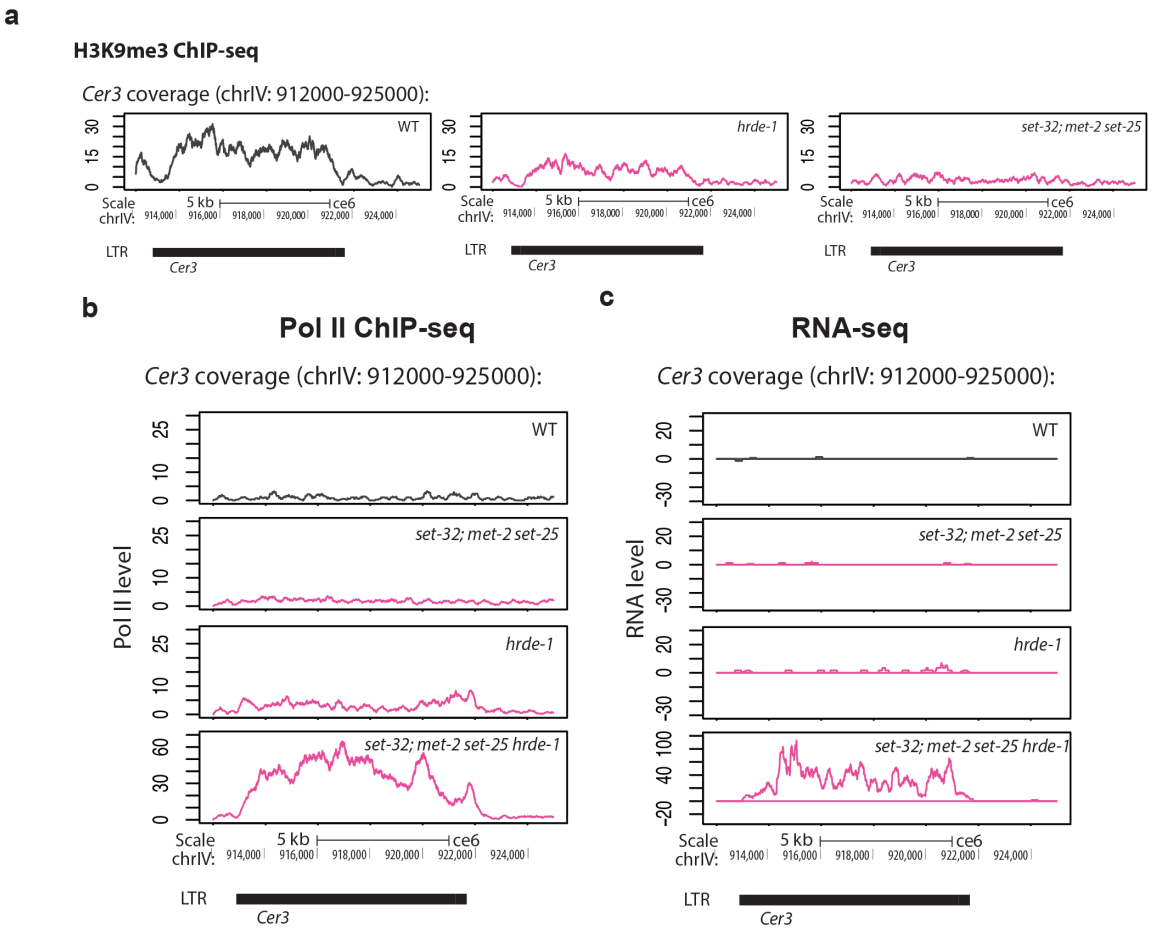

Figure 10 **H3K9me3, Pol II and RNA characterization of an exemplary region with enhanced desilencing (*Cer3* locus)**

(a) Coverage plots of H3K9me3 in WT and *hrde-1* and *set-32(ok1457);met-2 set-25* mutants (raw data for this analysis was used from Kalinava et al., 2017). Coverage plot of (b) Pol II and (c) RNA levels at *Cer3* locus in WT and *hrde-1*, *set-32; met-2 set-25* and *set-32; met-2 set-25 hrde-1* mutants. For RNA coverage plots sense reads are plotted above the $y = 0$ line (antisense bellow).

Thus, MET-2, SET-2 and SET-32 H3K9me HMTs are required for some transcriptional silencing as a backup mechanism to suppress transcription of a subset of genomic regions (57 kb), including some nuclear RNAi targets. Since whole genome analysis reflects an average signal from all tissues of synchronized young adult worms, we cannot determine if the enhanced desilencing in HMT+*hrde-1* mutants is the result of transcription in somatic cells, or increased transcription in the germline. These questions are currently under investigation (Ni et al., unpublished data).

3.3.2. CRISPR-mediated *hrde-1* repair reveals requirement of H3K9me HMTs for the efficient establishment of transcriptional silencing at native nuclear RNAi targets

We then decided to test if SET-32, MET-2 and SET-25 HMTs are required for the re-establishment of transcriptional silencing at native nuclear RNAi targets. Since *hrde-1* mutants show strong desilencing of many regions (GRTS native nuclear RNAi targets), we asked the question whether transcriptional silencing can be fully restored in H3K9me3 deficient mutant background by re-introducing HRDE-1 Argonaut. To eliminate the effect of epigenetic factors that can be introduced by a genetic cross, we took an approach of CRISPR-Cas9 mediated genome editing and repaired the mutant *hrde-1(tm1200)* allele to the wild type allele, here called *hrde-1*($+^{R}$) (Fig. 11a). We collected homozygous samples with the *hrde-1*($+^{R}/+^{R}$) genotype in early and late post-repair generations (Fig. 11b). This allowed us to create animals with identical genotypes, but with different epigenetic history for different conditions: WT HMT background as a control and different HMT mutant backgrounds as test samples (Fig. 11b).

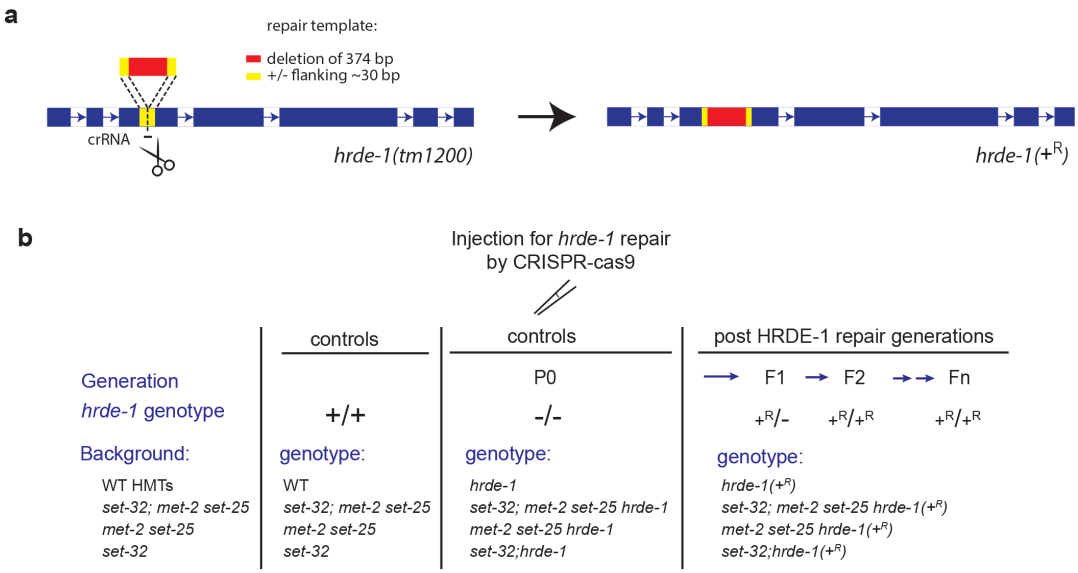

Figure 11 **Experimental scheme for the CRISPR-Cas9-mediated *hrde-1* repair**
(a) Scheme for the *hrde-1* gene editing from the deletion sequence *(tm1200)* to the wild type sequence. (b) Scheme of multigenerational sample collection of animals with WT HMT or various mutant HMT genetic backgrounds. All animals were raised at 19°C and collected at young adult stage.

We performed CRISPR-Cas9-mediated *hrde-1(-)* repair using *hrde-1* mutants for samples with WT HMT background; and *set-32;met-2 set-25 hrde-1* mutants for samples with HMT mutant background. We collected F5, F10 and F20 post-repair generations of synchronized young adult animals of *hrde-1(+^{R})* samples for WT HMT background samples and *set-32;met-2 set-25 hrde-1(+^{R})* for HMT mutant background samples, here collectively called *hrde-1(+^{R})* samples. Using qRT-PCR we measured RNA levels at exemplary regions of previously defined two types of nuclear RNAi targets (Ni et al., 2014): (1) Cer8 – a LTR retrotransposon as an example of GRTS target, and (2) a repetitive region on chromosome V position 5,470,000-5,480,000, as an example of GRH target.

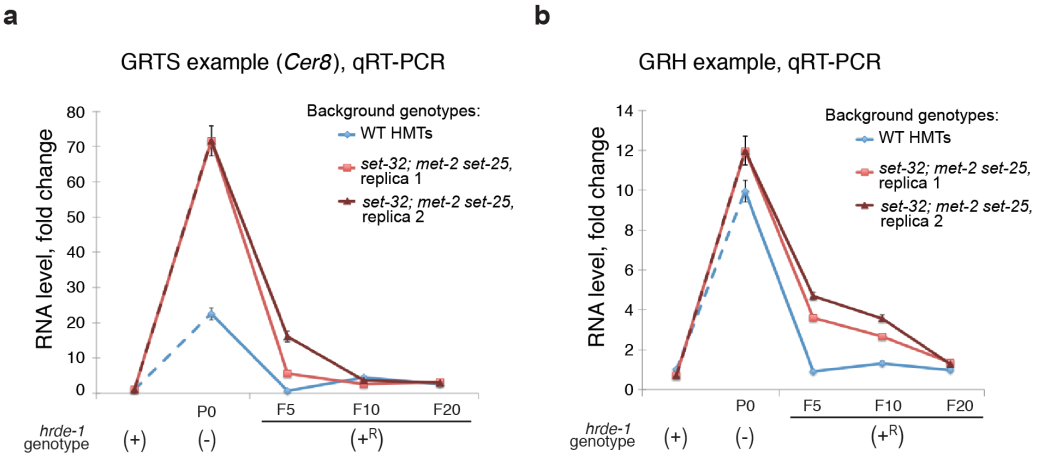

Figure 12 **Requirement of SET-32, MET-2 and SET-25 for the re-establishment of transcriptional silencing of exemplary native nuclear RNAi targets**

RT-qPCR analysis of RNA levels of *hrde-1(+)* controls, *hrde-1(-)* controls and *hrde-1(+^{R})* samples in animals with WT HMT genetic background and triple HMT mutant background at (a) GRTS exemplary region and GRH exemplary region. RNA levels for all samples are normalized by the *hrde-1(+)* control with WT HMT background (N2 strain).

qRT-PCR results of RNA levels at GRTS and GRH examples in *hrde-1(+)* controls were low (Fig. 12), i.e. transcriptionally silent for both WT HMT background and a triple HMT background. These results confirm that MET-2 SET-25 and SET-32 are dispensable for the maintenance of transcriptional silencing at these regions. We observed high level of RNA at GRTS and GRH examples, indicating de-silencing in all *hrde-1(-)* controls samples (Fig. 12). GRTS example (Fig. 12a), but not GRH (Fig. 12b), showed stronger de-silencing in *set-32;met-2 set-25 hrde-1* mutants than *hrde-1* alone. These results are consistent with the results in the previous section, which also indicate that H3K9me HMTs contribute to some silencing when the dominant RNAi-mediated repression is absent.

RNA levels in *hrde-1(+^{R})* samples of F5, F10 and F20 generations in WT HMT background showed full recovery of transcriptional silencing at both GRTS and GRH examples (Fig. 12). Interestingly, RNA levels in two independent replicas of *hrde-1 (+^{R})* F5 generation in *set-32; met-2 set-25* mutant background (*set-32;met-2 set-25 hrde-1(+^{R})* samples) were higher than in the corresponding *hrde-1(+)* control samples (*set-32; met-2 set-25* mutants) (Fig. 12). All late post-repair generations (>F10) showed full recovery of transcriptional silencing at both GRTS and GRH examples in samples with mutant HMT background (Fig. 12). These results indicate that re-establishment of the transcriptional silencing at both the *Cer8* GRTS and GRH examples is a transgenerational process and depend on at least one of the H3K9me HMTs. Transcriptional repression can be fully re-established by HRDE-1 as early as in F5 generation in WT HMT background. However this process takes more than 10 generations in samples with SET-32, MET-2, SET-25 mutant HMT background.

To verify that SET-32, MET-2 and SET-25 HMTs facilitate trans-generational establishment of silencing by nuclear RNAi, we performed total RNA-seq analysis of native nuclear RNAi targets in *hrde-1(+)* and *hrde-1(+^{R})* samples in F5 generation for animals with WT HMT background and mutant HMT background. We did 1kb whole genome analysis and highlighted two classes of previously characterized nuclear RNAi targets: GRTS and GRH. Scatter and boxplot analysis were used to compare RNA levels in animals with identical genotypes, but different transcriptional history: WT vs *hrde-1(+^{R})* F5 generation for WT HMT background, and *set-32; met-2 set-25* vs *set-32; met-2 set-25 hrde-1(+^{R})* F5th generation for mutant HMT background (Fig. 13a-c). WT HMT background animals showed no obvious difference in RNA levels (Fig. 13a), but we

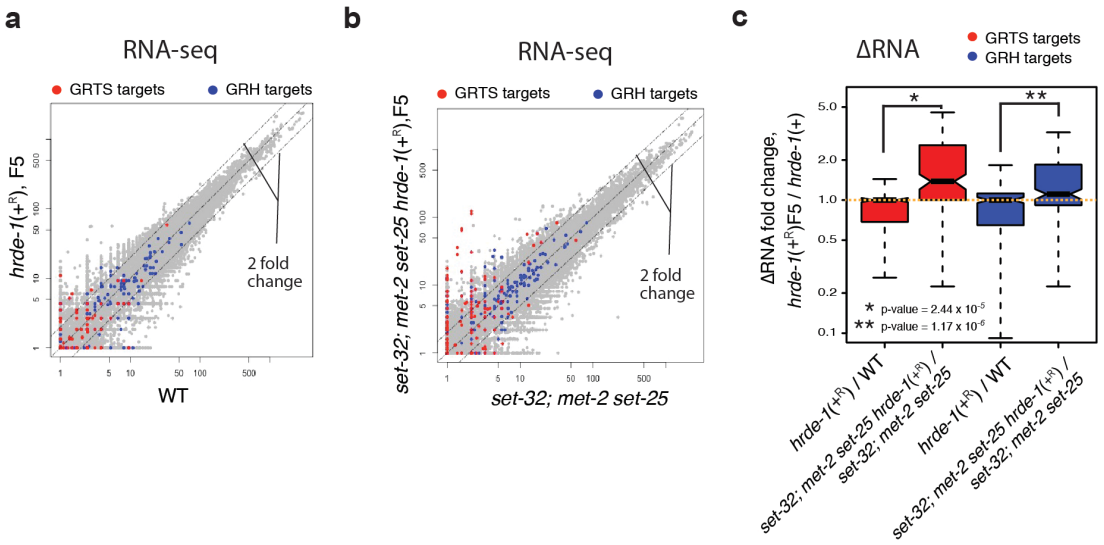

Figure 13 **Impact of *set-32; met-2 set-25* mutations on re-establishment of transcriptional silencing at native nuclear RNAi targets**

Scatter plot analysis comparing RNA levels of *hrde-1(+)* controls vs *hrde-1(+^{R})* in F5 generation for samples with (a) WT HMT background and (b) *set-32; met-2 set-25* mutant HMT background. (c) Boxplot analysis comparing RNA levels of *hrde-1(+)* and *hrde-1(+^{R})* F5 generation in samples with WT HMT or *set-32; met-2 set-25* mutant HMT background in GRTS loci (191 kb) and GRH loci (215 kb).

found higher RNA levels at many native nuclear RNAi targets (more GRTS than GRH) in samples with mutant HMT background (Fig. 13b). The median values for GRTS in samples with WT HMT background were ΔRNA (*hrde-1(+^{R})*/WT) = 1.00, compared to samples with mutant HMT background ΔRNA (*set-32;met-2 set-25 hrde-1(+^{R})/set-32;met-2 set-25*) = 1.38 (p-value <2.44x10-5) (Fig. 13c). The median values for GRH targets in samples with WT HMT background were ΔRNA (*hrde-1(+^{R})*/WT) = 1.00, compare to samples with mutant HMT background ΔRNA (*set-32;met-2 set-25 hrde-1(+^{R})/set-32;met-2 set-25*) = 1.11 (p-value <1.68x10-6) (Fig. 13c). These results further support that H3K9me HMTs MET-2, SET-25 and SET-32 promote re-establishment of

nuclear RNAi-mediated transcriptional silencing. The next question is, which one of these HMTs is required for this process?

3.3.3. SET-32 promotes the onset of the transgenerational repression of nuclear RNAi targets

To test which mutations (*met-2, set-25 or set-32)* are responsible for the delayed re-establishment of silencing, we performed CRISPR-Cas9-mediated *hrde-1(-)* repair experiment in the WT HMT background, *set-32(ok1457)* or *set-32(red11)* mutant background and *met-2 set-25* double mutant background. We collected post-repair *hrde-1 (+^{R})* samples in various post-repair generations (F3, F4, F5, F8 or late >F20) and measured RNA changes by qRT-PCR at the GRH and GRTS exemplary regions (Fig. 14a, b).

Both WT HMT background samples (Fig. 14a, b) and two replicas of *met-2 set-25* mutant background (Fig. 14a) showed full recovery of transcriptional silencing in *hrde-1(+^{R})* samples as early as F3 generation and remained silenced in all tested post-repair generations (F5, F8 and >F20).

qRT-PCR analysis using samples with *set-32(ok1457)* mutant background showed a strong defect in re-establishment of transcriptional silencing at both GRH and GRTS exemplary regions. The delays were apparent in the F3, F5 and F8 generations (Fig. 14a). Both targets were completely silenced in the late (>F20) generation in the *set-32(ok1457)* mutant background. qRT-PCR results of RNA levels at GRH and GRTS regions in *hrde-1* repair experiment in the *set-32(red11)* mutant background were also higher in the early post-repair generations than in the corresponding *set-32(red11)* control sample (Fig. 14b). The late post-repair generations (>F20) in the *set-32(red11)* mutant HMT background

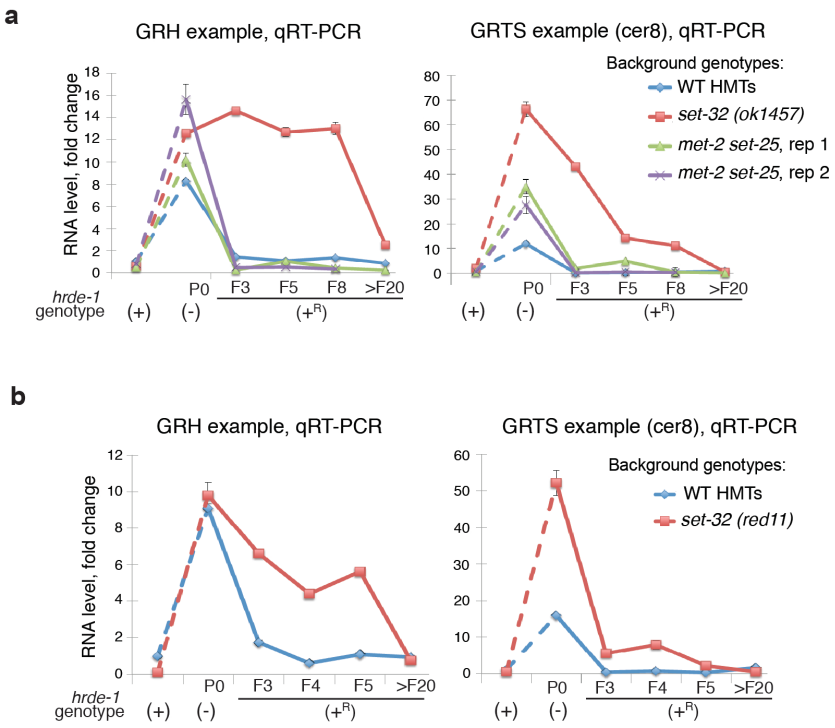

Figure 14 **Requirement of SET-32 for the re-establishment of transcriptional silencing at the exemplary GRH and GRTS regions**

RT-qPCR analysis of RNA levels at GRTS (*Cer8*) and GRH (chr.V: 5,470,000-5,480,000) exemplary regions of *hrde-1(+)* controls, *hrde-1(-)* controls and *hrde-1(+^{R})* samples in animals with WT HMT genetic background and (a) *set-32(ok1457)* or *met-2 set-25* mutant backgrounds (b) *set-32(red11)* mutant background. RNA levels for all samples are normalized by the *hrde-1(+)* WT control.

showed complete silencing, similar to the results observed in the *set-32(ok1457)* mutant background (Fig. 14b). Together these results indicate that the efficient re-establishment of transcriptional repression at exemplary GRH and GRTS regions is dependent on SET-32, but not MET-2 and SET-25.

To verify that SET-32, but not MET-2 SET-25, promote transcriptional silencing across all native nuclear RNAi targets we performed RNA-seq using *hrde-1(+)* control samples and *hrde-1(+^{R})* of selected post-repair generations in *met-2 set-25* mutant

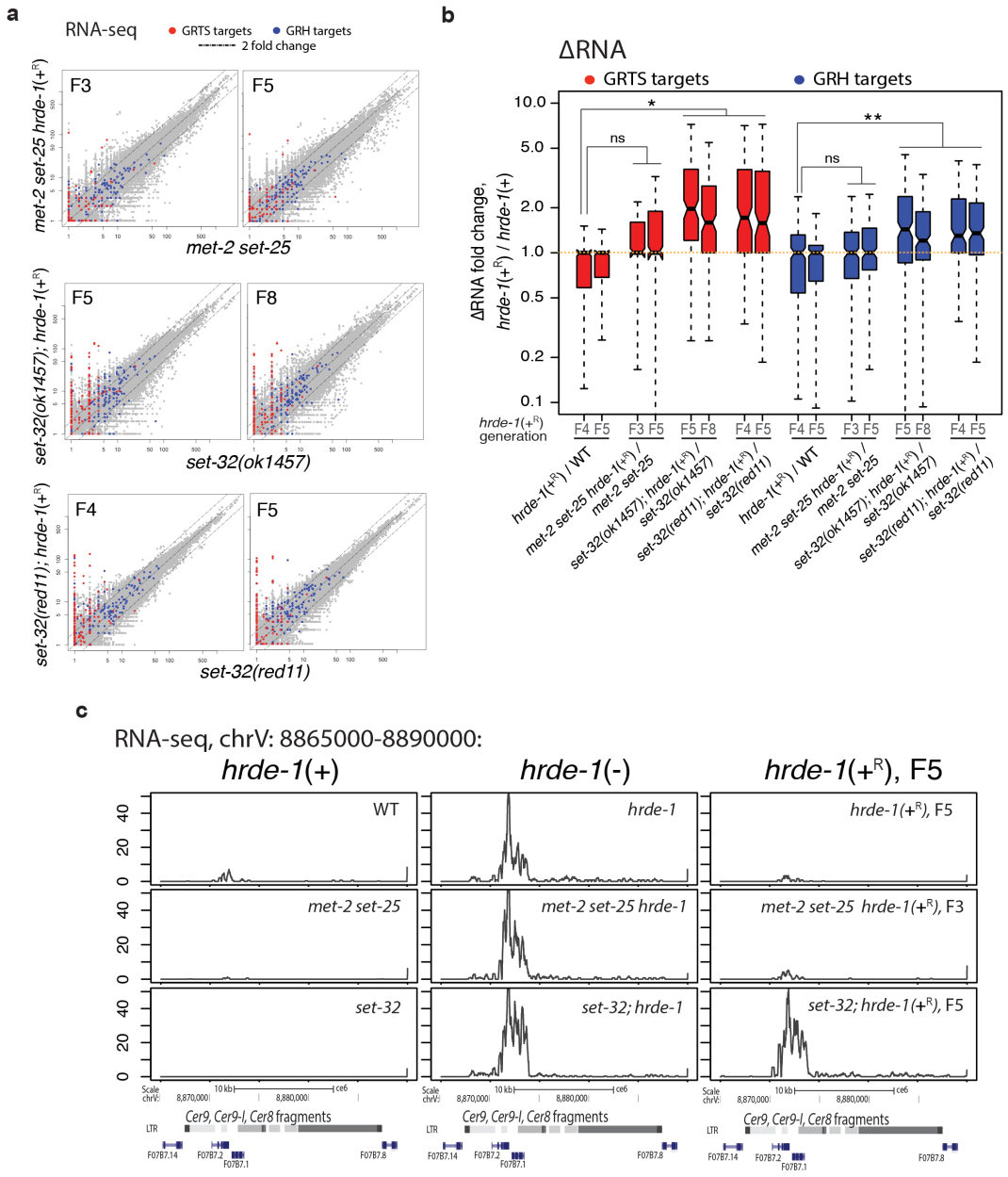

Figure 15 **Impact of different H3K9me3 HMTs on the re-establishment of nuclear RNAi-mediated transcriptional silencing**

(a) Scatter plots comparing whole-genome RNA levels changes in various HMT mutants and corresponding *hrde-1(+^{R})* samples at 1kb resolution in different generations after *hrde-1* repair. (b) Boxplot analysis showing RNA changes in *hrde-1(+^{R})* samples compared to the corresponding *hrde-1(+)* controls at GRTS loci (191 kb) and GRH loci (215 kb). X-axis indicates the genotypes used for the calculation of ratios. (c) Coverage plot of RNA levels of an exemplary GRTS target (*Cer9*) before and after *hrde-1* repair.

background and *set-32* mutant backgrounds (*ok1457* and *red11*). Comparison of RNA levels in samples with identical genotypes, but different history (WT vs. *hrde-1(+^{R})* or *set-32* vs *set-32;hrde-1(+^{R})* or *met-2 set-25* vs *met-2 set-25 hrde-1(+^{R})*), showed that many nuclear RNAi target regions displayed strong defects in the re-establishment of transcriptional silencing in both *set-32* mutant alleles backgrounds, but not in *met-2 set-25* mutant background or WT HMT background samples (Fig. 15a, b). The median values of GRTS and GRH in WT HMT background for F4 and F5 post-repair generations and *met-2 set-25* mutant background for F3 and F5 post-repair generations were each ΔRNA (*hrde-1(+^{R})*/*hrde-1(+)* control) = 1.00 (p-value >0.12, not significant). The median values for GRTS and GRH regions in *set-32* mutant backgrounds were all significantly higher than in WT HMT background. For instance median values for GRTS and GRH in *set-32(ok1457)* mutant background for *hrde-1(+^{R})* F5 generation were ΔRNA (*set-32(ok1457);hrde-1(+^{R})*F5/*set-32(ok1457)*)= 1.97 (p-value = 8.91x10-8) and 1.43 (p-value = 7.14x10-5) respectively (Fig. 12b). Coverage plot of the RNA-sequencing data at the GRTS region with *Cer9*, *Cer9-I* LTR retrotransposon fragments, further shows the SET-32-dependent defect of the transgenerational onset of transcriptional silencing in *set-32; hrde-1(+^{R})* samples (Fig. 15c).

Three replicates of *hrde-1(+^{R})* and two independent replicates of *met-2 set-25 hrde-1(+^{R})* revealed no defect in the re-establishment of transcriptional silencing in all tested generations. However, all *set-32; hrde-1(+^{R})* samples showed active transcription in the early post-repair generations and complete silencing in the late post-repair generations, arguing against a permanent off-target CRISPR-induced damage, which might have caused the observed delayed silencing.

To verify that the delay in establishment of transcriptional silencing in *set-32; hrde-1 (+^{R})* samples is not due to the defect of HRDE-1 transcription after *hrde-1* repair, we performed qRT-PCR and measured RNA levels at *hrde-1* gene in *hrde-1(+^{R})* and *set-32; hrde-1(+^{R})* samples (*ok1457* and r*ed11* alleles) (Fig. A-10a, b). All samples showed similar *hrde-1* transcription, when compared to the corresponding *hrde-1(+)* control (Fig. A-10a, b). We also evaluated *hrde-1* transcription levels using our RNA-seq data in WT HMT, *met-2 set-25* and *set-32(red11)* background genotypes for *hrde-1(+)* and *hrde-1(+^{R})* samples (Fig. A-10c). We observed that RNA levels at *hrde-1* gene in *hrde-1(+^{R})* samples was consistent with corresponding *hrde-1(+)* control samples. These results show that transcriptional defects observed in *set-32; hrde-1(+^{R})* samples were not due to the reduced transcription of *hrde-1*.

Together these results show that SET-32 is required for the robust trans-generational establishment of transcriptional silencing. Although we observed a defect in establishment of silencing in *set-32* mutants, late post-repair generations (>F20) in *set-32* mutants show full silencing, indicating that transcriptional defects in *set-32* mutants are not permanent. We note that the degree of the defect in re-establishment of transcriptional silencing varies between generations, but it is consistently observed in all tested generations of samples with *set-32* mutant background.

3.3.4. SET-32 is co-expressed with HRDE-1 Argonaut in germline

Our current results identified a role of SET-32 H3K9me3 HMT in trans-generational establishment of nuclear RNAi-mediated transcriptional silencing. Next we tested whether SET-32 is expressed in germline, where HRDE-1 is expressed. Using

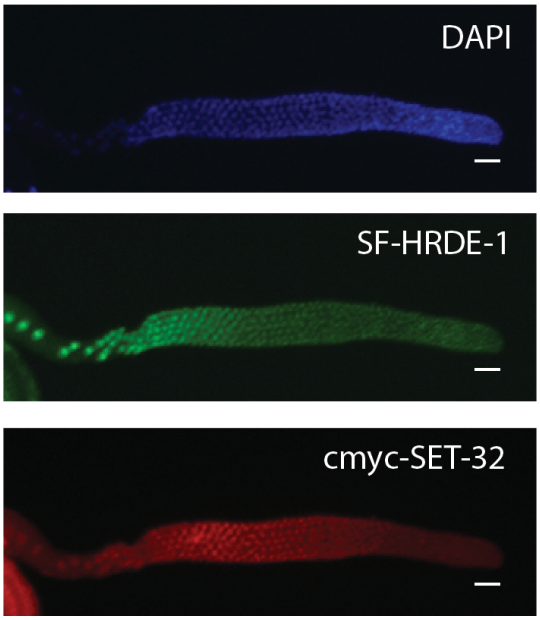

Figure 16 **Immunofluorescence (IF) confirms SET-32 and HRDE-1 expression in germline nuclei**

IF images of a dissected gonad (bar, 20 µm).

CRIPR-mediated gene editing, we tagged the endogenous copy of SET-32 with a c-myc tag at the C-terminus and an endogenous copy of HRDE-1 with a SF tag at the N-terminus (all relevant sequences are in Table A-2). Using immunofluorescence (IF) of the dissected gonads of young adult hermaphrodite animals, we tested both SET-32 and HRDE-1 expression in the germline. Consistent with previously reported expression of HRDE-1:GFP transgene in germline (Buckley et al., 2012), the endogenous copy of SF-HRDE-1 was also expressed in the germline of young hermaphrodite animals (Fig. 16). We observed HRDE-1 signal in nuclei of all stages of oogenesis with the peak in the late pachytene and diplotene stages. The cmyc-SET-32 signal was in all stages of oogenesis in germline nuclei too, with the peak in pachytene stage (Fig. 16). Thus, both SET-32 and HRDE-1 are co-expressed in germline, which is consistent with their function in the germline nuclear RNAi pathway.

3.4. Discussion

In plants and *S. pombe*, RNAi-directed heterochromatin is necessary to initiate and to maintain the transcriptional repression at the target locus. This work investigated the requirement of H3K9me HMTs for transcriptional silencing at native nuclear RNAi targets at two distinct stages: the initiation and the maintenance in *C. elegans*. H3K9me3 heterochromatin is dispensable for the maintenance of RNAi-mediated repression. This is due to the dominant HRDE-1-dependent silencing. However, when HRDE-1 Argonaut is mutated, the role of H3K9me3 in the maintenance of transcriptional silencing becomes evident. We observed synthetic genetic interactions between *hrde-1* and *met-2*, *set-25* and *set-32* mutations that yield enhanced de-silencing of many native nuclear RNAi target loci. Furthermore, transcriptional silencing can be efficiently re-established by the cooperative function of SET-32, the putative H3K9me3 HMT, and HRDE-1, the germline nuclear Argonaut. These findings demonstrate the differential roles of H3K9me3 HMTs in the chronological events of the initiation and the maintenance of the nuclear RNAi-mediated transcriptional repression in *C. elegans*.

3.4.1 Enhanced transcriptional de-silencing in HMT+*hrde-1* mutants

Genome wide loss of H3K9me3 in young adults stage of the *set-32; met-2 set-25* triple HMT mutants indicate that both soma and germline are deficient in H3K9me3 heterochromatin marks. That includes the RNAi-directed heterochromatin in both soma and germline. Yet, *set-32; met-2 set-25* mutants did not show transcriptional activation at native nuclear RNAi targets. All combination mutants, HMT+*hrde-1*, yield enhanced desilencng of these regions, stronger than in the single *hrde-1* mutants. There are several sources of the enhanced desilencing observed. It could be the result of the cooperative

silencing by both the dominant RNAi-mediated and the H3K9me3-dependent mechanisms in germline. Alternatively, the additional desilencing may come from the transcriptional activation in somatic tissue in HMT+*hrde-1* mutants. Therefore, it is important to define the source of the additional desilencing, soma or germline, for the various combinations of HMT+*hrde-1* samples.

3.4.2 CRISPR-mediated gene repair approach

We used CRISPR-mediated gene editing to repair *hrde-1* gene and to restore function of HRDE-1 Argonaut. Here are several alternative and more common ways to restore function of protein of interest: genetic cross, transgene, and inducible system. However, transgenes are subjects of nuclear RNAi-mediated silencing. They can lead to the co-suppression of the endogenous gene, which is also heritable. Genetic cross can introduce epigenetic factors with the gametes of the WT strain. Unlike genetic cross, CRISPR-mediated repair of *hrde-1* allows to create samples that have identical genotypes, but different epigenetic makeup. An inducible gene expression has potential problems: a 'leaky' repression, side effects induced by the drug or the heat when induce the gene 'on' or 'off', etc. CRISPR-mediated gene repair approach can be used as a genetic tool to study epigenetic changes. It can help to address several important questions of epigenetics and adaptation. In this work, using CRISPR we reversed a mutation and investigated transcriptional consequences. Can the function of the pathway be fully restored despite of the mutation history? Can the epigenetic make up be returned with the function of the pathway or it finds a new equilibrium state? Although, natural physiological process is an acquiring of mutations, the understanding of the reverse process is equally important, particular from the therapeutic standpoint.

3.4.3 The onset of nuclear RNAi-mediated transcription regulation

As we investigated the requirement of RNAi-directed H3K9me HMTs for the onset of transcriptional repression by nuclear RNAi in *C. elegans*, we found that nuclear RNAi-mediated transcriptional silencing can be fully restored by the repaired nuclear Argonaut HRDE-1 at least in the F3 post-repair generation. Yet, the onset of silencing of native nuclear RNAi targets in WT HMT background in the immediate post-repair generations remains unclear and requires additional testing. Although CRISPR-Cas9-mediated gene editing serves as a genetic tool to modulate HRDE-1 function, this approach is limited to study early post-repair generations or even hours after HRDE-1 restores its function. Therefore, different experimental approaches need to be developed to study immediate effects of HRDE-1 on transcription of nuclear RNAi targets.

Our results showed that SET-32, a putative H3K9me HMT, promotes the trans-generational establishment of nuclear RNAi-mediated silencing. We also show that transcriptional silencing in post-repair generations in the absence of SET-32 is fully restored in the late generations, therefore, the role of SET-32 in RNAi-mediated repression is temporal, only at the early onset of silencing. However, it is not clear what is the mechanism of the delay of transcriptional repression. One logical explanation is that there is a lack of siRNAs and they are necessary for the proper HRDE-1 targeting. Another reason for the delayed onset of silencing could be the lack of SET-32-dependent H3K9me3, which could potentially serve as an epigenetic mark to propagate silencing from one generation to another, thereby ensuring stronger silencing in the following generations. Each of these questions requires further tests.

In addition, the mechanism of the nuclear RNAi-mediated transcriptional silencing is still elusive. RNAi-directed H3K9me3 response can be decoupled from the maintenance of RNAi-mediated repression, allowing to investigate the mechanism of silencing in-depth. Furthermore, *set-32* mutants have transgenerational delay in the onset of silencing, which provide a longer timeline to study the mechanism of the onset of transcriptional repression by nuclear RNAi.

It is surprising that MET-2 and SET-25 together did not show any effect on the onset of nuclear RNAi silencing, especially since these two HMTs are known major H3K9me HMT in *C. elegans*. While SET-32, MET-2 and SET-25 are required for all dsRNA-induced H3K9me3 response at the *oma-1* locus, the role of MET-2 and SET-25 HMTs in the nuclear RNAi pathway is still unclear. We want to note that this work only tested *met-2 set-25* double mutants; thus, we don't know the effect of the individual mutation on the initiation or maintenance of nuclear RNAi-mediated repression and the Pol II and RNA profiles at native nuclear RNAi targets.

3.4.4 Heritable RNAi in *set-32* mutants

Our current and previous studies both showed no defects of heritable RNAi in the *set-32* mutants (two different alleles). However, genetic screens for RNAi heritable deficient outcomes using GFP reporter expression found several new alleles of *set-32* mutants with heritable RNAi defects (Spracklin et al., 2017). These results are contrary to our heritable RNAi results in *set-32* mutants. In the light of our finding that SET-32 promotes the transgenerational establishment of nuclear RNAi silencing response, it is possible that different heritable RNAi experiments capture different stages of the onset of nuclear RNAi silencing and result with the different heritable RNAi outcomes. It is also

possible that GFP reporter and endogenous gene target have differences in nuclear RNAi responses. Further studies need to be done to address these ideas.

3.4.5 Conclusion

RNAi-mediated transcriptional silencing can be divided into two distinct stages: the initiation and the maintenance. We found that HRDE-1-induced transcriptional silencing (of the unknown mechanism) is very potent and sufficient for both the initiation and the maintenance of the repression of many LTR retrotransposons. RNAi-directed H3K9me3 is dispensable for the maintenance of this repression, but necessary for some repression in the absence of HRDE-1. MET-2, SET-25 and SET-32 H3K9me HMTs all can function in RNAi-dependent manner and deposit RNAi-directed H3K9me3 marks. Only SET-32 HMT is required for the transgenerational initiation stage of RNAi-mediated silencing, therefore, we found another player for the RNAi-mediated epigenetic inheritance.

3.5. Material and methods

3.5.1 Strains

Bristol strain N2 was used as a standard wild type strain. This study used the following mutations: LGI: *set-32(ok1457)*; LGII: *met-2(n4256);* LGIII: *set-25(ok5021), hrde-1(tm1200).* The *set-32(red11)* mutation has a stop codon and a frame shift in the third exon, which was generated in this study using CRISPR-cas9-mediated genome editing (Arribere et al., 2014; Paix et al., 2015). The *hrde-1::SF(red3)III* and *set-32::c-Myc(red10)I* alleles were generated in this study by plasmid-based CRISPR (Arribere et al., 2014; Paix et al., 2015). For that endogenous gene *hrde-1* was tagged with *SF*-tag at

the N-terminal and endogenous *set-32* gene was tagged with *c-Myc*-tag at the C-terminal. The combined strain *set-32(red10)I; hrde-1(red3)III* was generated by the genetic cross and was used for the immunofluorescence (IF) assay in this study. Genotyping primers and other relevant sequences are listed in Table A-2. All strains for all experiments were cultured at 19°C.

3.5.2 Worm grind preparation

Worms were cultured on NGM plates with OP50 *E.coli* or *oma-1* RNAi (where indicated) as food source (Brenner, 1974). Synchronized young adult hermaphrodite animals were obtained by first using the bleaching method to collect worm embryos, which were hatched in M9 buffer without food, and then releasing L1 larvae onto NGM plates with OP50 *E. coli* or *oma-1* RNAi. Young adult worms were ground by mortar and pestle in liquid nitrogen and stored at -80°C.

3.5.3 *hrde-1* repair using CRISPR

We repaired the *hrde-1(tm1200)* mutation in the *hrde-1* mutants, *set-32; hrde-1* mutants, *met-2 set-25 hrde-1* mutants and *set-32; met-2 set-25 hrde-1* mutants to wild-type *hrde-1* sequence using purified Cas-9 ribonuclease complex (Paix et al., 2015) that targets deletion site in *hrde-1(tm1200)* and PCR fragment as a repair template (relevant sequences are listed in Table A-2). *dpy-10(cn64)* co-conversion marker was used. In the each set of experiments, 10-15 animals for each mutant were used for injection. 48-96 F1s with WT or *dpy* or *roller* phenotypes were genotyped by single-worm PCR, resulting with 2-8 F1s with putative *hrde-1(+)/hrde-1(tm1200)* genotype. For each F1 hit, 12-24 F2 worms with only WT phenotype were transferred as single L3-L4 worms onto new OP50 *E.coli* NGM plates and allowed to lay eggs for the next F3 generation. These adult

F2 worms were genotyped by single-worm PCR, followed by Sanger sequencing, and down-selected to those that have wild type *hrde-1* sequence. Each CRISPR screen resulted with 1 outcome for the control line with WT HMT genetic background and 1 or 2 independent lines for various mutant HMT background as indicated in the results section. We refer to the CRISPR/Cas-9-generated wide type *hrde-1* sequence as *hrde-1(+^{R})* to distinguish it from wide type *hrde-1* sequence that has not experienced genome editing, referred to as *hrde-1(+)*.

3.5.4 Sample collection

F3 and F4 post-repair sample collection: we collected into 50 μl of M9 ~20 young adult worms, which were progeny of the identified F2 positive hit. Since F3 progeny was unsynchronized, we collected F3 young adult progeny with ~3hr intervals and were able to obtain about 2-4 aliquots for each sample. About 20 young adult worms in 50 ul of M9 samples were snap frozen by liquid nitrogen and stored at -80°C. F4 generation was collected as ~20 young adult worms in ~50 μl of M9, same as described for the F3 generation.

F5, F8, F10 and >F20 post-repair sample collection: leftover unsynchronized F3 animals for each positive *hrde-1(+^{R})* CRISPR line were transferred to a large OP50 plate and cultured at 19°C for 5 days. At this time, the majority of animals were F4 adults. These animals were egg-preped and shaked in M9 without food to produce synchronized L1s, then released onto large OP50 plates and cultured at 19°C till reaching young adult stage. These animals were F5. F5 young adults were collected and ground in liquid nitrogen. Similarly, subsequent samples for F8, F10 or >F20 generations were collected as synchronized young adults and ground in liquid nitrogen.

Control *hrde-1(+)*: WT, *set-32*, *met-2 set-25*, *set-32; met-2 set-25*, and *hrde-1(-)* samples: *hrde-1*, *set-32; hrde-1*, *met-2 set-25 hrde-1* and *set-32; met-2 set-25 hrde-1* for the CRISPR *hrde-1* repair experiments were collected as synchronized young adults, ~20-50 worms in M9 and frozen in liquid nitrogen.

3.5.5 Total RNA extraction

Total RNA extraction was performed with Trizol reagent (Life Technologies) for worm grind samples and according to the manufactures protocol.

Sample of ~20 worms in M9: Trizol reagent was added to the frozen sample of ~20 worms in M9. To ensure break down of worm bodies, we used 3-4 cycles of freeze-thawing in Trizol, then performed total RNA extraction according to the manufacture's protocol. ~20 young adult worms yield 1-3μg of total RNA.

3.5.6 mRNA and pre-mRNA qRT-PCR

mRNA reverse transcription (RT) was used in heritable RNAi experiment (Fig. A-7b). 1 μg of total RNA was used for the first strand cDNA synthesis with SuperScript III RT kit (Life Technologies) and oligo(dT)20 primer (to enrich for mRNA).

pre-mRNA RT and RNA RT. 2 μg of total RNA was used for the first strand cDNA synthesis with SuperScript III RT kit (Life Technologies) and random hexamer primer mix (to capture pre-mRNA or nascent RNA).

qRT-PCR. qRT-PCR was performed using KAPA SYBR FAST Universal 2× PCR Master Mix (KAPA Biosystems) on a Mastercycler EP Realplex realtime PCR system (Eppendorf) according to the manufacturer's instructions. qPCR primers are listed in Table A-2. Each sample was processed in triplicate. Reported values for the fold change of mRNA and pre-mRNA were calculated using ΔΔCT analysis.

3.5.7 Multigenerational heritable RNAi

Heritable RNAi experiments were conducted as previously described (Gu et al., 2012). *oma-1* RNAi trigger sequence is reported in Table A-2. For *oma-1* RNAi, single nucleotide mismatch at every 30 nt was used to distinguish the trigger sequence from the native *oma-1* gene. RNAi feeding was performed continuously for 2-3 generations until worm population expanded from few L3-L4 worms to a large population of predominantly young adult animals (~7-10 days) on a large *oma-1* RNAi plates. These animals were synchronized by the eggprep and shaking in M9 without food to produce synchronized L1s, which then were released onto large *oma-1* RNAi plates. These animals (continuously exposed to *oma-1* RNAi for about 3-4 generations) were collected at young adult stage and called P0 generation with dsRNA feeding. Sequential F1, F2, F3 (without dsRNA feeding) generations, grown on OP50 food, were collected at young adult stage and called heritable RNAi generations. All samples were ground in liquid nitrogen.

3.5.8 Immunofluorescence (IF)

IF staining of gonad of young adult hermaphrodite animals was performed according to the Schedl lab protocol. The gonads were hand-dissected in 1xPBS with 0.2 mM Levamisole and were immediately transferred into glass culture tubes with the freshly-made cold fixative solution (3% formaldehyde, 6.6 μM K_2HPO_4 (pH7.2), 80% methanol) and incubated at -20°C for 10 min. Fixative solution was removed by pipette and the dissected gonads were washed with the wash buffer (1x PBS, 0.1% Tween 20) three times. Resulted gonads were transferred into a small glass tube and incubated over night at 4C in wash buffer with BSA (1 mg/ml) and primary antibodies. Staining was

performed using primary goat-anti-c-Myc antibody (Abcam, ab9132), 1:400 dilution of the company stock, and mouse-anti-FLAG (Sigma, F1804-200UG) 1:100 dilution. Gonads were washed five times with the wash buffer and incubated in the wash buffer with BSA (1mg/ml) and secondary antibodies for 4hr at room temperature in the dark. Secondary antibodies used: bovine-anti-goat-Alexa594 (Jackson ImmunoResearch Laboratories, 805-585-180) and donkey-anti-mouse-Alexa488 (Jackson ImmunoResearch Laboratories, 715-545-150) with dilution of the company stocks 1:100 and 1:200 respectively. The gonads were washed with the wash buffer five times at room temperature. The DAPI (200 ng/ml) staining was done for 5 min in the wash buffer. The slow fade solution was added. Gonads were placed on a 2% agar pad on a glass slide, covered with a cover slip and used for imaging. Imaging was performed immediately using a Delta Vision deconvolution microscope. Images were deconvoluted using Huygens Essential image analysis software and then were processed and analyzed using ImageJ (Wayne Rasband, NIH). All images are shown as collapsed data stacks.

3.5.9 High-throughput sequencing

Pol II ChIP-seq. Crosslinking, sonication and ChIP were performed using the protocol described in (Kalinava et al., 2017; Ni et al., 2014; Ni et al., 2016). Worm grind sample (~5000 young adult worms) was used as starting material. IP was performed using anti-RNA Pol II S2 (ab5095, Abcam). 5ng or less ChIP DNA was used to prepare DNA library using KAPA Hyper Prep Kit (KAPA Biosystems) according to the manufacturer's instruction.

RNA-seq: Total RNA was extracted as described above from either ~20 worm sample or a worm grind. Ribosomal RNAs (rRNA) were removed using RNase H

enzymatic reaction and gel purified DNA oligos (mixture of 110 oligos, 50nt, listed in Table A-3) that are antisiense to rRNA (protocol adopted from A. Fire lab). Briefly, ~2.5ug of rRNA antisense oligos were mixed with ~0.5-1ug of total RNA in 1x Hybridization Buffer (5µM TrisCl pH 7.4, 100mM NaCl). The sample was denatured at 95 °C for 2 minutes, and then cooled at −0.1 °C /sec to 45°C. rRNA was digested by 10 units of Hybridase Thermostable RNase H (Epicentre) in 1x RNaseH Reaction Buffer (5µM TrisCl, 100mM NaCl, 1µM $MgCl_2$) at 45°C for 1 hr. DNA oligos were removed by TURBO DNase (Invitrogen) according to manufacture's instruction, followed by phenol: chloroform extraction. The yielded RNA was used to prepare RNA-seq library as described in (Ni et al., 2014). A mixture of four different 4-mer barcodes were used for the 5'-end ligation in RNA-seq as indicated in Table A-1.

All libraries were sequenced using Illumina HiSeq 2500 platform, with 50-nt single-end run and dedicated index sequencing. Dedicated 6-mer indexes were used to demultiplex DNA ChIP-seq and RNA-seq libraries for different samples. All libraries with total sequencing depth used in this study are listed in the Table A-1.

3.5.10 Data analysis

Whole genome alignment of the sequencing reads to *C. elegans* genome (WS190 version) was done using Bowtie (0.12.7) (Langmead et al., 2009). Only perfectly aligned reads were used for data analysis. Reads that aligned to N different loci were counted as 1/N. Normalization based on total reads aligned to the whole genome for each library was used for all data analysis, except for the ΔPol II box plot analysis in Fig. 8a, where total reads count of the top 5 percentile of Pol II signal in corresponding library was used as the normalization factor. The three-region Venn diagram was generated using a web-

based software (http://www.benfrederickson.com/venn-diagrams-with-d3.js/). Custom R and python scripts were used in this study. Welch Two Sample t-test was used to calculate all p-values.

4. CHAPTER IV – Concluding remarks and future directions

In this thesis I investigated the requirement of the H3K9me3 heterochromatin in the RNAi-mediated transcription regulation. I identified RNAi-dependent H3K9me3 HMTs and characterized HMT-dependent changes of heterochromatin and transcription at endogenous native nuclear RNAi targets at two stages of RNAi-mediated transcription repression: the initiation and the maintenance. I also confirmed our findings using the dsRNA trigger system targeting endogenous gene *oma-1*. Several conclusions can be drawn from this work.

4.1 MET-2, SET-25 and SET-32 together contribute to all RNAi-directed heterochromatin

This project started with the goal to identify H3K9 HMTs, which contribute to the RNAi-dependent H3K9me3 response in *C. elegans*. The field at that time had limited information about which of the many putative or known H3K9 HMTs function in the RNAi-dependent manner. Various screens identified that SET-25 and SET-32 H3K9 HMTs are potentially required for the nuclear RNAi effects (Ashe et al., 2012). We found that MET-2, SET-25 and SET-32 HMTs together contribute to all dsRNA-directed H3K9me3 response at *oma-1* gene. Furthermore, *set-32; met-2 set-25* triple HMT mutants are responsible for nearly all detectable H3K9me3 levels genome wide of young adult animals. That includes the HRDE-1-dependent H3K9me3 levels in germline at two classes of native nuclear RNAi targets: GRTS and GRH. It is important to note that *set-32; met-2 set-25* triple HMT mutants showed complete loss of H3K9me3 levels at both GRTS and GRH type of native nuclear RNAi targets, while *hrde-1* mutants have only partial loss of H3K9me3 at GRTS and a full loss of H3K9me3 at GRH. These lead to the

conclusion that MET-2, SET-25 and SET-32 HMTs contribute to both RNAi-dependent and RNAi-independent H3K9me3 at GRTS type of targets and to all RNAi-dependent H3K9me3 at GRH type of targets.

4.2 Requirement of H3K9me3 for the maintenance of the RNAi-mediated transcription repression

We observed complete loss of dsRNA-induced H3K9me3 at *oma-1* target gene and at the GRTS or GRH type of endogenous native nuclear RNAi targets in *set-32; met-2 set-25* triple HMT mutants. Yet we observed complete transcriptional silencing at dsRNA target *oma-1* and at all native nuclear RNAi targets in triple HMT mutants. Therefore, RNAi-dependent H3K9me3 at *oma-1* and at GRTS and GRH targets is dispensable for the RNAi-mediated transcription repression. Surprisingly, loss of the RNAi-dependent and RNAi-independent H3K9me3 in *set-32; met-2 set-25* triple HMT mutants at GRTS regions also had no effect on transcription repression. Therefore, maintenance of RNAi-mediated transcriptional silencing is self-sufficient by the nuclear RNAi pathway and can be fully decoupled from the H3K9me3 heterochromatin (Kalinava et al., 2017). Our findings are supported by the results of other groups, where *met-2 set-25* double mutants have been studied. Strong loss of H3K9me3 in *met-2 set-25* double mutants has little effect on repression of LTR retrotransposon class of TEs, which unlike DNA transposons and tandem repeats, remain silent at non-stress condition (20ºC) (Zeller et al., 2016). In addition, H3K9me3 and H3K9me2 heterochromatin marks have distinct distribution in the genome: H3K9me3 are enriched at LTR retrotransposons, while H3K9me2 are enriched at DNA transposons and other repetitive regions (McMurchy et al., 2017). HPL-2, the homolog of HP1 (heterochromatin protein 1), co-

localizes with H3K9me2 and is required for silencing of these regions, but not H3K9me3 regions. It was confirmed that nuclear RNAi pathway plays a central and dominant role in silencing of LTR retrotrasncposons, but not H3K9me3. Therefore, H3K9me3 heterochromatin can be decoupled from the RNAi-mediated silencing, providing a unique opportunity to investigate the mechanism of RNAi-mediated repression in *C. elegans*.

What is the role of the RNAi-independent H3K9me3 at the native nuclear RNAi targets? We performed transcription analysis of native nuclear RNAi targets in HMT+*hrde-1* combination mutants and found enhanced de-silencing of some GRTS regions, but not GRH, when compared to *hrde-1* mutants alone. These results revealed the conditional requirement of MET-2, SET-25 and SET-32 for the transcriptional repression, which is masked by the dominant HRDE-1-dependent silencing mechanism.

Many nuclear RNAi mutants, including *hrde-1*, are sensitive to the heat and display *Mrt* phenotype – a progressive loss of germline. It takes several generations for *hrde-1* mutants to become completely sterile under heat stress (23-25ºC). This progressive loss of germline is also accompanied with a progressive enhancement of transcriptional desilencing in *hrde-1* mutants (Ni et al., 2016; Weiser et al., 2017).

We propose that HRDE-1-dependent silencing is a dominant mechanism, but it has its limitations. Heat stress is one of the conditions that can drive the enhanced desilencing; H3K9me3 is another. Due to the dominant and potent RNAi-mediated silencing mechanism, neither heat stress nor loss of H3K9me3 alone has any effect on transcription repression. But in combination with *hrde-1* mutation, H3K9me3 is required for the maintenance of some level of repression at native nuclear RNAi targets. Future studies of HMT+*hrde-1* combination mutants under the heat stress will determine if

H3K9me3 heterochromatin serves as a backup silencing mechanism to maintain repression of the heat-inducible regions in the absence of HRDE-1.

4.3 Requirement of SET-32 in the transgenerational onset of RNAi-mediated transcriptional repression

Nuclear RNAi efficiently represses many LTR retrotransposons. This repression is maintained over many generations and can be further maintained in the absence of H3K9me3. In order for a retrotransposon to propagate in the host genome and to transmit vertically through germline, it needs to be transcriptionally active in germline. Therefore, efficient initiation of germline nuclear RNAi-mediated transcriptional silencing of TEs is important to preserve genome integrity and stability. Since many LTR retrotransposons are transcriptionally active in *hrde-1* mutants background, we mimicked the initiation of germline nuclear RNAi-mediated silencing by restoring activity of HRDE-1 using CRISPR-mediated gene repair. We tested the requirement of MET-2, SET-25 and SET-32 for the initiation of the RNAi-mediated silencing. Our results showed that SET-32 putative H3K9me3 HMT promotes the onset of RNAi-mediated transcriptional silencing. However, this requirement is temporal and is limited to the early post-repair generations (at least 5 generations).

What is the mechanism for the delayed establishment of silencing in the *set-32* mutant background? Candidate screens identified SET-32, as one of the heterochromatin factors that promotes piRNA-dependent silencing (Ashe et al., 2012). It is possible that SET-32 function in piRNA pathway, which was proposed to precede nuclear RNAi-mediated silencing. PRG-1 is the key component of piRNA pathway in *C. elegans*. However, it is not required for the nuclear RNAi-mediated H3K9me3 or transcriptional

repression (McMurchy et al., 2017; Ni et al., 2014). This can be explained by the HRDE-1-dependent self-sufficient maintenance of silencing, which is past the initiation stage. New approaches that allow investigating the initiation of repression, rather than the maintenance, need to be considered for the future studies to define the role of SET-32 HMT in the piRNA pathway. Furthermore, analyses of siRNA and piRNA profiles at regions with delayed establishment of silencing may help to understand the role of SET-32 in the piRNA and the nuclear RNAi pathways.

4.4 Future directions

Although H3K9me3 heterochromatin can be decoupled from the RNAi-mediated transcriptional regulation, the outstanding question of what is the mechanism of RNAi-mediated silencing is still not resolved. One of the immediate directions is to test other chromatin marks that may function redundantly with H3K9me3 heterochromatin. It is possible that different regions have different redundant mechanisms.

In *C. elegans*, unlike several other organisms, H3K9me3 and H3K27me3 repressive marks are often found at the same genomic regions (Ho et al., 2014). The nuclear RNAi pathway is required for H3K27me3 response at the target genes (Mao et al., 2015) and at the native endo-siRNA target regions, mostly GRH type of targets (Kalinava et al., 2017; Ni et al., 2014). In future it will be important to test transcriptional changes in the combination mutants that have depleted RNAi-mediated H3K9me3 and H3K27me3 responses. Since RNAi-directed H3K27me3 and H3K9me3 are both enriched at GRH type of nuclear RNAi targets, it is possible that both of these heterochromatin marks function redundantly at GRH type of targets.

Histone acetylation, H3K4me3 and H3K36me3 histone modifications accompany and promote active transcription. Therefore, inhibition of establishment of these marks or their active removal can be another model for RNAi-mediated transcriptional repression. Since GRTS regions show very strong transcriptional up-regulation in *hrde-1* mutants, it is possible that nuclear RNAi promotes histone deacetylation or inhibits histone acetylation, H3K4 or H3K36 methylation. In *S. pombe* nuclear RNAi inhibits HDAC activity and recruits H3K9me3 HMT Clr4. In *C. elegans* the role of HDAC (HDA-4) in nuclear RNAi is controversial. In one screen *hda-4* mutants showed heritable RNAi defects (Vastenhouw et al., 2006), in another - not (Ashe et al., 2012). I propose to test the requirement of HDA-4 for the onset of nuclear RNAi-mediated silencing too.

Nuclear RNAi-mediated transcriptional silencing is a complex process. There are still a lot of unknown. This work opened an opportunity to test the mechanism of the onset and the maintenance of the RNAi-mediated transcription regulation. Future studies will define the function of RNAi-directed H3K9me3 and the role of other chromatin factors in the nuclear RNAi pathway.

Appendices A

Table A-1 **List of libraries, sequencing depth and barcodes used in this study**

Experiment	Library name	Seq. depth (reads/ million)	5'-end barcode mix
1. Libraries used in chapter II			
oma-1 **RNAi feeding, 19°C, young adult stage**			
H3K9me3 ChIP-seq, WT	SG0315_lib43	4.9	NA
H3K9me3 ChIP-seq, *set-32*	SG0615_lib32	3.7	NA
H3K9me3 ChIP-seq, *met-2;set-25*	SG0315_lib44	5.4	NA
H3K9me3 ChIP-seq, *met-2;set-25;set-32*	SG1115_lib7	8.7	NA
H3K9me3 ChIP-seq, *hrde-1*	SG0315_lib45	4.3	NA
Pol II (S2) ChIP-seq, WT	SG0315_lib49	5.5	NA
Pol II (S2) ChIP-seq, *set-32*	SG1115_lib9	9.7	NA
Pol II (S2) ChIP-seq, *met-2;set-25*	SG0315_lib50	5.5	NA
Pol II (S2) ChIP-seq, *met-2;set-25;set-32*	SG1115_lib13	9.6	NA
Pol II (S2) ChIP-seq, *hrde-1*	SG0315_lib51	4.4	NA
GFP RNAi feeding, 19°C, young adult stage			
H3K9me3 ChIP-seq, WT	SG0315_lib40	6.5	NA
H3K9me3 ChIP-seq, *set-32*	SG0615_lib33	5.0	NA
H3K9me3 ChIP-seq, *met-2;set-25*	SG0315_lib41	5.2	NA
H3K9me3 ChIP-seq, *met-2;set-25;set-32*	SG1115_lib8	8.8	NA
H3K9me3 ChIP-seq, *hrde-1*	SG0315_lib42	6.8	NA
Pol II (S2) ChIP-seq, WT	SG0315_lib46	6.7	NA
Pol II (S2) ChIP-seq, *set-32*	SG1115_lib10	8.8	NA
Pol II (S2) ChIP-seq, *met-2;set-25*	SG0315_lib47	7.6	NA
Pol II (S2) ChIP-seq, *met-2;set-25;set-32*	SG1115_lib14	6.7	NA
Pol II (S2) ChIP-seq, *hrde-1*	SG0315_lib48	5.5	NA
OP50 feeding, 19°C, young adult stage			
H3K27me3 IP ChIP-seq, WT	SG0315_lib56	3.8	NA
H3K27me3 IP ChIP-seq, *met-2;set-25;set-32*	SG1115_lib16	5.3	NA
H3K27me3 IP ChIP-seq, *hrde-1*	SG0315_lib57	4.2	NA
ChIP-seq Input, WT	SG0315_lib60	2.7	NA
ChIP-seq Input, *set-32*	SG0615_lib16	2.7	NA
ChIP-seq Input, *met-2;set-25*	SG0315_lib62	3.3	NA
ChIP-seq Input, *met-2;set-25;set-32*	SG0615_lib17	1.7	NA
ChIP-seq Input, *hrde-1*	SG0315_lib61	3.0	NA
H3K9me3 IP ChIP-seq, WT	SG0315_lib52	3.4	NA
H3K9me3 IP ChIP-seq, *set-32*	SG0615_lib5	6.8	NA
H3K9me3 IP ChIP-seq, *met-2;set-25*	SG0315_lib54	2.7	NA

Table A-1 **cont.**

H3K9me3 IP ChIP-seq, *met-2;set-25;set-32*	SG0615_lib6	4.0	NA
H3K9me3 IP ChIP-seq, *hrde-1*	SG0315_lib53	3.8	NA
pre-mRNA-seq, WT	SG0315_lib32	1.3	['AGCG','CGTC', 'GTTA','TATG']
pre-mRNA-seq, *set-32*	SG0615_lib30	3.7	['CTGG','ACTG', 'GAAG','TGCC']
pre-mRNA-seq, *met-2;set-25*	SG0315_lib34	2.9	['AGCG','CGTC', 'GTTA','TATG']
pre-mRNA-seq, *met-2;set-25;set-32*	SG0615_lib31	2.7	['CTGG','ACTG', 'GAAG','TGCC']
pre-mRNA-seq, *hrde-1*	SG0315_lib33	2.4	['AGCG','CGTC', 'GTTA','TATG']
mRNA-seq, WT	SG1115_lib27	5.5	['CTGG','ACTG', 'GAAG','TGCC']
mRNA-seq, *set-32*	SG1115_lib42	5.7	['CTGG','ACTG', 'GAAG','TGCC']
mRNA-seq, *met-2;set-25*	SG1115_lib44	4.8	['CTGG','ACTG', 'GAAG','TGCC']
mRNA-seq, *met-2;set-25;set-32*	SG1115_lib43	6.6	['CTGG','ACTG', 'GAAG','TGCC']
mRNA-seq, *hrde-1*	SG1115_lib45	4.4	['CTGG','ACTG', 'GAAG','TGCC']
2. Libraries used in chapter III			
OP50 feeding, 19°C, young adult stage			
RNA-seq, WT	SG0117_lib1	0.7	['CTGG','ACTG', 'GAAG','TGCC']
RNA-seq, *hrde-1*	SG0117_lib2	0.6	['CTGG','ACTG', 'GAAG','TGCC']
RNA-seq, *set-32(ok1457)*	SG0117_lib9	0.7	['CTGG','ACTG', 'GAAG','TGCC']
RNA-seq, *set-32(red11)*	SG0117_lib5	0.9	['CTGG','ACTG', 'GAAG','TGCC']
RNA-seq, *met-2 set-25*	SG0117_lib7	0.8	['CTGG','ACTG', 'GAAG','TGCC']
RNA-seq, *set-32(ok1457); met-2 set-25*	SG0117_lib3	0.9	['CTGG','ACTG', 'GAAG','TGCC']
RNA-seq, *set-32(ok1457); hrde-1*	SG0117_lib10	0.5	['CTGG','ACTG', 'GAAG','TGCC']
RNA-seq, *set-32(red11); hrde-1*	SG0117_lib6	0.9	['CTGG','ACTG', 'GAAG','TGCC']
RNA-seq, *met-2 set-25 hrde-1*	SG0117_lib8	0.6	['CTGG','ACTG', 'GAAG','TGCC']
RNA-seq, *set-32(red11); met-2 set-25 hrde-1*	SG0117_lib4	0.6	['CTGG','ACTG', 'GAAG','TGCC']
Pol II IP ChIP-seq, WT	SG0615_lib46	3.7	NA
Pol II IP ChIP-seq, *hrde-1*	SG0117_lib31	5.7	NA

Table A-1 **cont.**

Pol II IP ChIP-seq, *set-32(red11)*	SG0117_lib27	3.0	NA
Pol II IP ChIP-seq, *met-2 set-25*	SG0615_lib50	3.0	NA
Pol II IP ChIP-seq, *set-32(ok1457); met-2 set-25*	SG1115_lib18	6.1	NA
Pol II IP ChIP-seq, *set-32(red11); hrde-1*	SG0117_lib29	6.1	NA
Pol II IP ChIP-seq, *met-2 set-25 hrde-1*	SG0615_lib8	6.6	NA
Pol II IP ChIP-seq, *set-32(red11); met-2 set-25 hrde-1*	SG0117_lib28	3.1	NA
hrde-1(+^{R}) **post-repair generation, OP50 feeding, 19°C, young adult stage**			
RNA-seq, *hrde-1(+^{R})* F4	SG0117_lib14	0.5	[‘CTGG’,’ACTG’, ‘GAAG’,’TGCC’]
RNA-seq, *hrde-1(+^{R})* F5	SG0117_lib15	0.6	[‘CTGG’,’ACTG’, ‘GAAG’,’TGCC’]
RNA-seq, *set-32(ok1457); hrde-1(+^{R})* F5	SG0117_lib17	1.0	[‘CTGG’,’ACTG’, ‘GAAG’,’TGCC’]
RNA-seq, *set-32(ok1457); hrde-1(+^{R})* F8	SG0117_lib18	1.1	[‘CTGG’,’ACTG’, ‘GAAG’,’TGCC’]
RNA-seq, *set-32(red11); hrde-1(+^{R})* F4	SG0117_lib21	1.2	[‘CTGG’,’ACTG’, ‘GAAG’,’TGCC’]
RNA-seq, *set-32(red11); hrde-1(+^{R})* F5	SG0117_lib22	0.9	[‘CTGG’,’ACTG’, ‘GAAG’,’TGCC’]
RNA-seq, *met-2 set-25 hrde-1(+^{R})* F3	SG0117_lib19	0.8	[‘CTGG’,’ACTG’, ‘GAAG’,’TGCC’]
RNA-seq, *met-2 set-25 hrde-1(+^{R})* F5	SG0117_lib20	1.1	[‘CTGG’,’ACTG’, ‘GAAG’,’TGCC’]
RNA-seq, *set-32(red11); met-2 set-25 hrde-1(+^{R})* F5	SG0117_lib23	0.8	[‘CTGG’,’ACTG’, ‘GAAG’,’TGCC’]

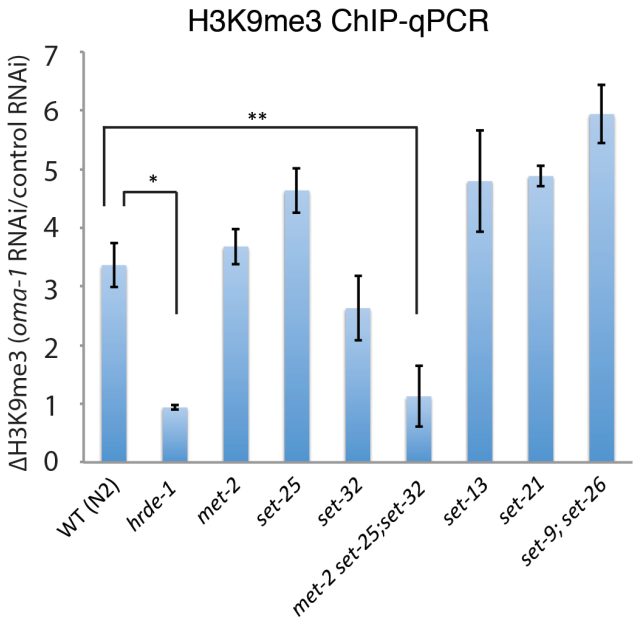

Sample	Fold change repeat 1	repeat 2	repeat 3	Mean Fold change	SD	p-value compared to WT
N2 (WT)	3.7	3.4	3.0	3.4	0.37	n/a
hrde-1	0.9	1.0	0.9	0.9	0.03	0.00035*
met-2	3.5	3.5	4.0	3.7	0.30	ns
set-25	4.6	5.0	4.2	4.6	0.38	ns
set-32	2.6	2.1	3.2	2.6	0.55	ns
met-2 set-25;set-32	0.6	1.6	1.2	1.1	0.52	0.00379**
set-13	4.3	4.3	5.8	4.8	0.86	ns
set-21	5.0	4.7	4.9	4.9	0.17	ns
set-9;set-26	5.7	5.6	6.5	5.9	0.50	ns

***Figure A-1* H3K9me3 ChIP-qPCR analysis of *oma-1* dsRNA-triggered H3K9me3 response in WT and various mutants**

H3K9me3 change at *oma-1* was measured by ChIP-qPCR. ΔΔCT analysis was used to calculate H3K9me3 fold change in various mutants in *oma-1* RNAi compared to corresponding *gfp* RNAi control.

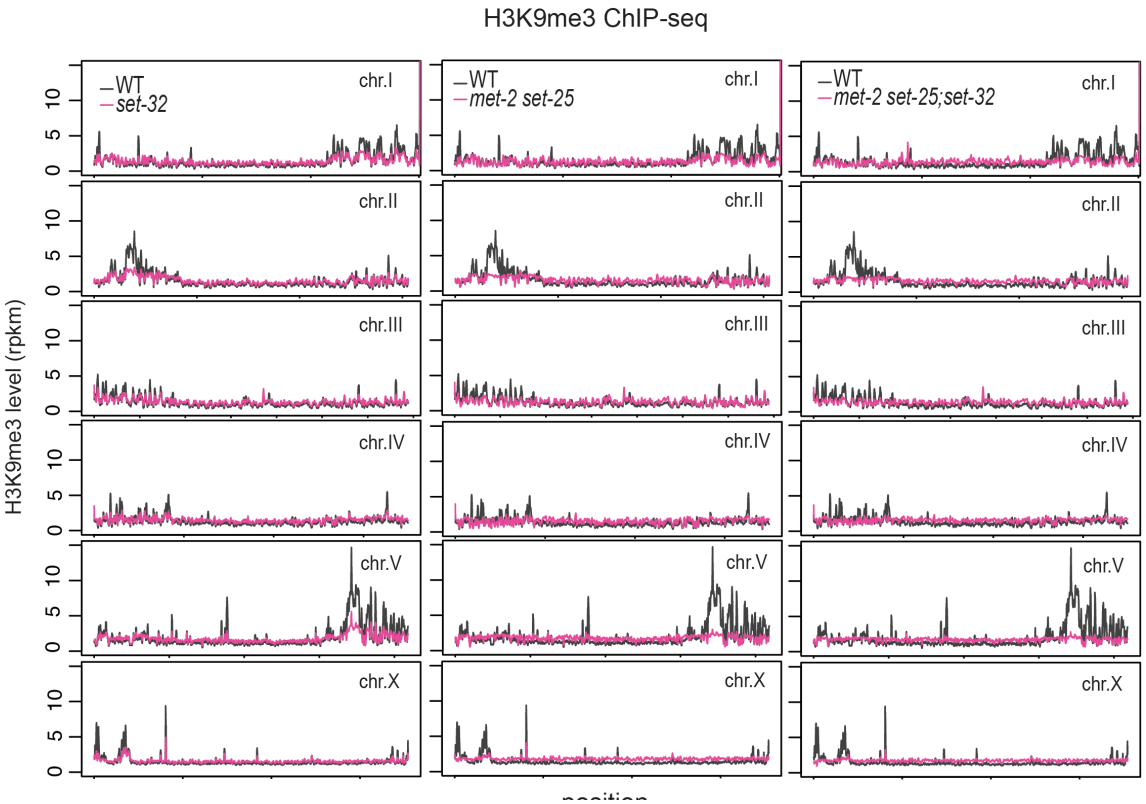

Figure A-2 **H3K9me3 coverage plot of individual chromosome for WT and HMT mutants.**

H3K9me3 levels are plotted as a function of position on all chromosomes for WT and HMT mutants (the panels for chromosome V are also shown in Fig. 4a). A moving average with a sliding window of 50 kb was used to plot H3K9me3 levels.

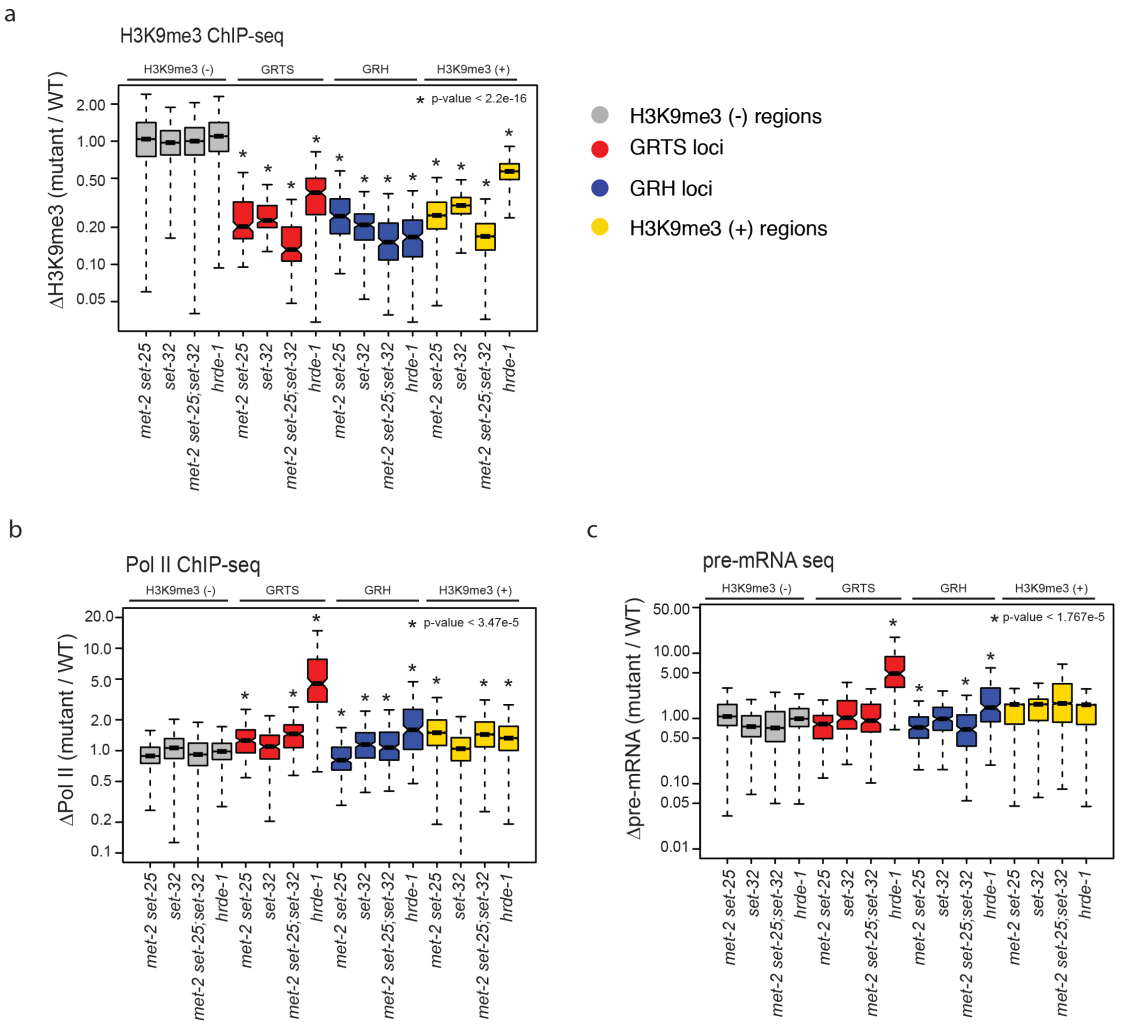

Figure A-3 **Box plot analysis for H3K9me3 and Pol II ChIP-seq and pre-mRNA seq data for native nuclear RNAi targets in WT and HMT mutants**

Boxplot analysis for the ratios between mutant and WT for (a) H3K9me3, (b) Pol II, and (c) pre-mRNA in different subsets of the genome: GRTS loci (191 kb), GRH loci (215 kb), top 5-percentile H3K9me3 regions in WT (H3K9me3(+) regions, 4775 kb), and bottom 5–25-percentile H3K9me3 regions in WT (H3K9me3(−) regions, 20,200 kb).

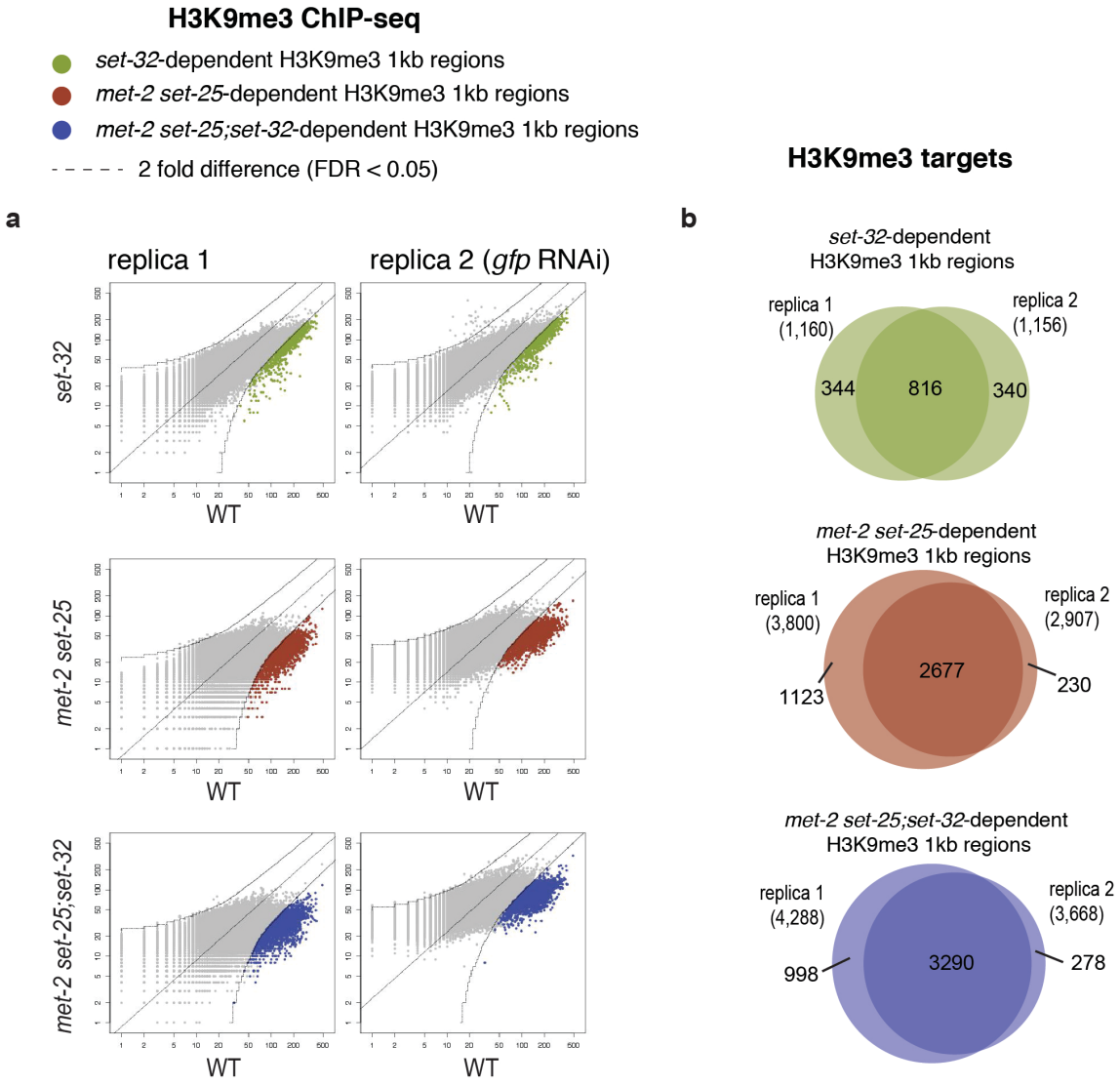

Figure A-4 **Identification of H3K9me3 that is dependent on SET-32, MET-2 SET-25, or MET-2 SET-25;SET-32.**

(a) Whole-genome H3K9me3 scatter plots (1 kb resolution) that compare various HMT mutants with WT. (b) Venn diagram analysis between two biological repeats for H3K9me3 that is dependent on SET-32, MET-2 SET-25, or MET-2 SET-25;SET-32.

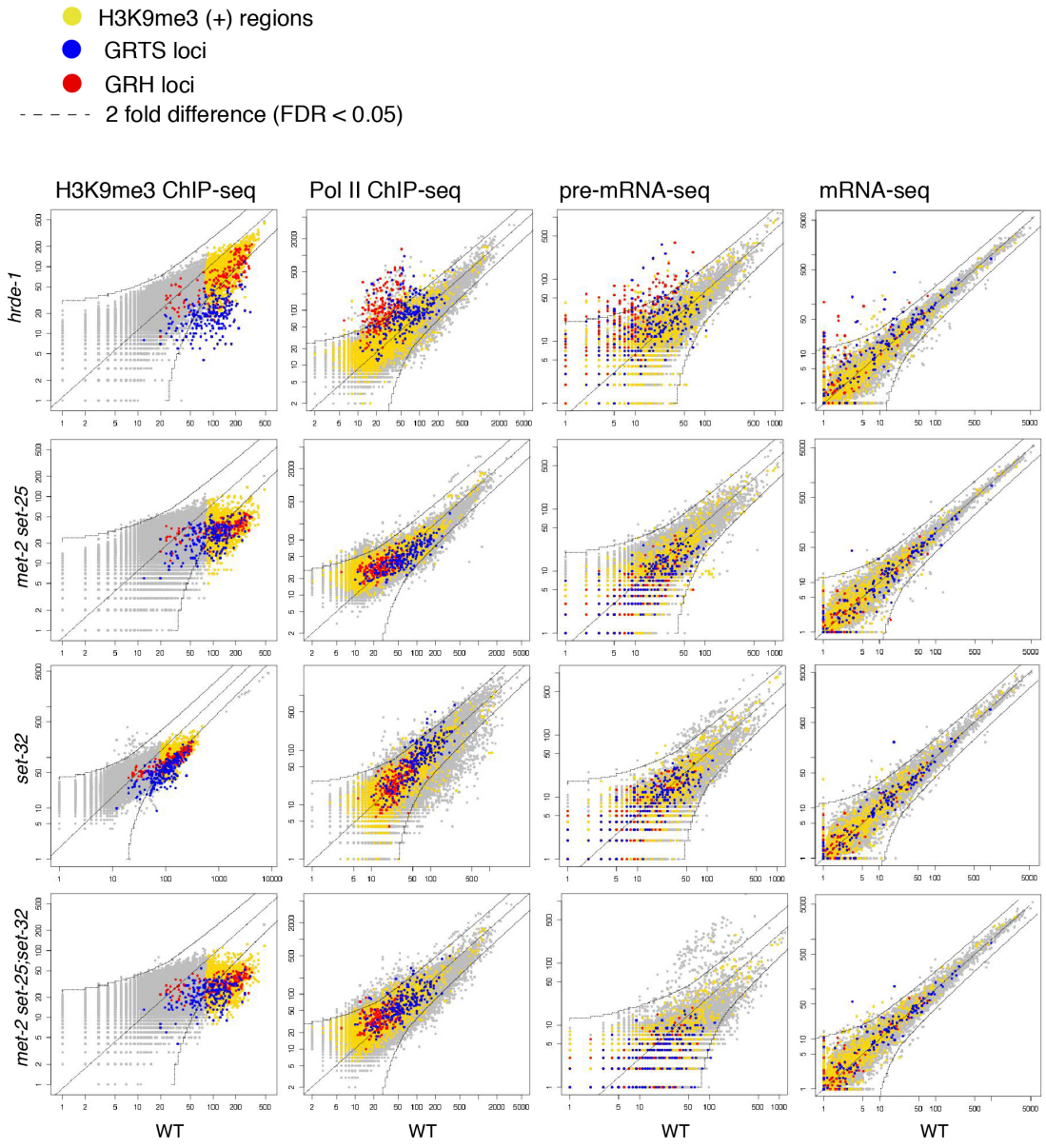

Figure A-5 **Whole-genome scatter plot analysis of H3K9me3, Pol II, pre-mRNA and mRNA sequencing data**

Whole-genome scatter plots (1 kb resolution) that compare various mutants with WT for (a) H3K9me3 ChIP-seq, (b) Pol II ChIP-seq, and (c) pre-mRNA and (d) mRNA-seq (gene-based).

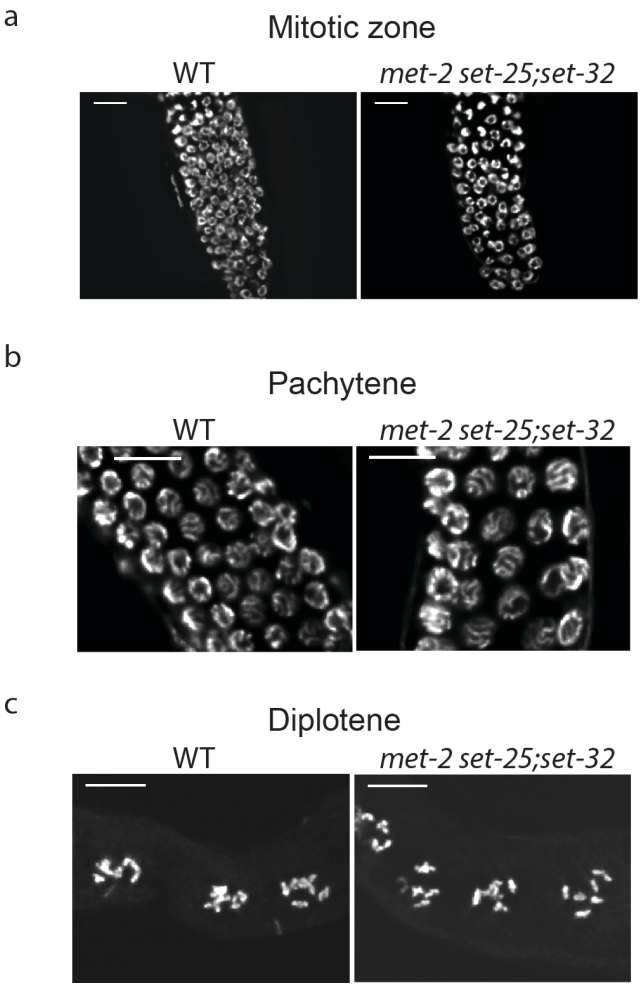

Figure A-6 **DAPI staining of germline nuclei**

DAPI staining of germline nuclei from WT and *met-2 set-25;set-32* mutant adult hermaphrodite. Scale bar: 10 μm.

Table A-2 **Oligonucleotides and other sequences used in this study**

gene name	oligo or plasmid name	sequence	description
oma-1	pSG42	gtCtctcaacgccatgcattggct gacattcgCgatcaaatggagcag cacatcatgactaaCggtcgcatt gcagctcccccgctttctgcGatt cagcatcctttagaaatgtttgcc agAccatcaactccagatgagcca gcggctaaGttgccactaggacca actcctgttagtacCcgtggtcca agatatgagctaccaacgaaAgaa ttgcatgacgcggaaggtgcgatg acTtatccaccgtctcgctggcca ttggatccGtcgatgtttgctcta gacgcttggaatatggcCcatcgg ccagctagtccactcgattcAatg gttttgggttccgctccaaatgct ggTtcgttcggaatgctcggaaag caaaatacCcctggaggagtttct ggatattcatctgcCggatccacg ccttctcaggatctcagttcCtcg tcactcaatgcagcatccgcag	oma-1 dsRNA trigger; chrIV:8,889,833-8,890,353; exclude intron; 478 bp; capital letters are mismatch every ~30nt; vector backbone L4440
hrde-1(tm1200)	SG-386	ttcgtgtcgaagttgtctcg	SG-386 and SG-387 are oligoes for genotyping *hrde-1 (tm1200)*, PCR product for WT and *hrde-1(+R)* is 648 bp, *tm1200* is 272 bp. These primers were used to genotype *hrde-1(+R)* outcomes in CRISPR screen.
hrde-1(tm1200)	SG-387	ttcgtgtcgaagttgtctcg	
met-2(n4256)	SG-778	gtcacatcacctgcatcagc	SG-778 and SG-779 are oligoes for *met-2(n4256)* genotyping, mutant 461bp; WT 1804bp
met-2(n4256)	SG-779	tctattcccaggagccaatg	
met-2(n4256)	SG-834	GTTGGCAGCCGTAATGAAAT	SG-834 and SG-835 are oligos for *met-2(n4256)* genotyping, WT 248bp, mutant no product, primers in the deletion region
met-2(n4256)	SG-835	CGAGCCAGACAGAAATCTCC	

Table A-2 **cont.**

set-25(ok5021)	SG-1318	GACACTCGACCGTTTCCACT	SG-1318 and SG-1319 are *set-25 (ok5021)* genotyping oligos; mutant 732 bp, WT does not have a product (too large)
set-25(ok5021)	SG-1319	ACTCGACGAGGCTCTGAAAC	
set-25(ok5021)	SG-836	ATATGGATGCCCACGAGAAG	SG-836 and SG-837 are oligos for *set-25(n5021)* genotyping, WT is 356 bp, mutant no product, primers in the deletion region
set-25(ok5021)	SG-837	CCGTGAAAAAGAGCATCACA	
set-32 (ok1457)	SG-1144	cggagcaggatttcccgata	SG-1144 and SG-1145, primers to genotype *set-32(ok1457)*, chrI:9519414-9520167 ; WT - 754bp, mutant - 240 bp
set-32 (ok1457)	SG-1145	gggcagttttcgttttcgta	
oma-1	SG-1018	acatgtatttttgctcactgtaa	SG-1018 and SG-1019 are oligos for H3K9me3 qPCR, *oma-1*, gDNA, intron+ex5, chrIV: 8,889,800 - 8,889,957; 158bp
oma-1	SG-1019	ggcctggcaaacatttctaa	
ChIP control region	SG-1044	agccatggcacaaaaagaag	SG-1044 and SG-1045 are oligos for qPCR as H3K9me3 control region (reference), chrII:6,708,915-6,709,320; 201bp
ChIP control region	SG-1045	tgtggcctgagaagacaaaa	
oma-1	SG-1016	ctacaggactctgcccatacg	SG-1016 and SG-1019 are oligos for mRNA qRT-PCR, *oma-1*, chrIV:8,889,697-8,889,956 excluding intron; 261 bp

Table A-2 **cont.**

oma-1	SG-1022	ttaatgacctctgttttaggtg	SG-1022 and SG1023 are oligos for qRT-PCR of *oma-1* pre-mRNA, SG-1022 covers intron-ex6 junction, chrIV: 8890089 - 8890222; 134 bp
oma-1	SG-1023	gaacccaaaaccatcgaatc	
tba-1	SG-1108	TCCAAGCGAGACCAGGCTTCAG	SG-1108 and SG-1109 are oligos for mRNA and pre-mRNA qRT-PCR control; *tba-1*, Chr I: 9786104-9786296; 192 bp
tba-1	SG-1109	TCAACACTGCCATCGCCGCC	
set-9(red8)		ATGGCAGACGGAGAGCATACGCTTCCAGCCGACGAGGAGCTCTTCGAGCAACCACCACgctagctCAACAACAACCCGAAATCGCCGAGCCAATTGTTATGGCTCAAG	Stop codon and a frame shift induced by CRISPR in exon 1 of *set-9* gene, chrIV: 4312497-4312501
set-9(red8)	SG-1128	CGCAATTTTTCCGTCATTTT	SG-1128 and SG-1129 are oligos for *set-9(red8)* genotyping; WT and mutant PCR size is ~ 630bp; mutant cut with NheI to 530bp+100bp.
set-9(red8)	SG-1129	GACTCCTTGAATGGGCTCTG	
set-32(red11)	SG-1173	tcttcgaatatacagacacgaatgttttgaacccgGCTAGCAtgctccgcaagaaacattgcgaaagcatgtattatgtctcaaaaggaagagaat	HR oligo for generating *set-32* loss of function mutation. Low case indicate the flanking sequences. Upper case indicate a new sequence insertion into the exon 3 (chrI: 9519901-9519989), that introduce a stop codon, frame shift and a NheI site for genotyping.
set-32(red11)	SG-1144	cggagcaggatttcccgata	SG1144 + SG1145 are oligos for set-32(red11) genotyping; WT and mutant PCR sizes are ~760bp, mutant NheI cut to ~235+525bp .

Table A-2 **cont.**

set-32(red11)	SG-1145	gggcagttttcgttttcgta	
set-32::cMyc (red10)	SG-1159	AGTGGGAAAGTTGGCACAAGAACA TCTGCGAACCTCTTgaacaaaaac tGatAtcagaagaggatctgTCAT GCAACGACGATGTAGTTGTTTTAG ATTAAGTG	repair template oligo to insert c-myc sequence before the last 10 amino acid of SET-32. 38 nt HR sequence + c-myc sequence (30 nt, with a EcoRV site, inserted between +3 and +4 position of seed) + 36 nt HR-seq (upper case of the flanking sequences). CRISPR seed sequence is disrupted by the c-myc sequence. There are 10 amino acids downstream to the Myc sequence of native SET-32. Internal myc design is used because (1) presumed higher HR frequency (2) low conservation for the last 10 amino acid sequence.
set-32::cMyc (red10)	SG-1161	AGCTGTTCGCCGAATTTAGA	SG-1161 and 1162 are used to genotype *set-32::cMyc (red10)*. WT and *set-32::cMyc (red10)* have PCR product ~ 610 bp, *set-32::cMyc (red10)* cut with EcoRV: 430+180 bp.
set-32::cMyc (red10)	SG-1162	CGTTTCGAATGGGTTCGTAT	
hrde-1::SF (red3)		TCGTTTCATCGTTTCTTATTTCAG TCAAACATGGactataaagacgat gatgataaaggatcagctgcttca tggtcacatccacaattcgaaaaa ggaggaggatcaggaggaggatca ggaggaggatcatggtcacatcca caattcgaaaaagCaGACTTGCTC GACAAAATTATGGGAAGTTCG	repair oligo to insert SF tag into 5' end of hrde-1. The repair oligo disrupt the PAM site by mutating C to A, which leads to a synonymous mutation (GCC->GCA, Ala, at position 2). Upper case - flanking sequence, lower case – insertion with SF tag.

Table A-2 **cont.**

hrde-1::SF (red3)	SG-865	AGCTTGTCATGTACTGTTCTCA	SG-865 and SG-866 are genotyping primers for *hrde-1::SF(red3)*. Product sizes for WT and *hrde-1::SF(red3)* are 600 bp and 750 bp, respectively.
hrde-1::SF (red3)	SG-866	TCAGGACGGTAAAGCTTTTGT	
hrde-1(+R)		taatcgtatgTggaaaccg	Seed sequence for crRNA targeting *hrde-1(tm1200)* mutation. It was used for all CRISPR experiments to repair hrde-1(tm1200) to the wild-type *hrde-1* sequence.
hrde-1(+R)	SG-1292	aaggagaagttgcccaggag	primers SG1292+SG1293 to generate dsDNA repair template for *hrde-1 (tm1200)*; PCR product in WT is 424bp, with 34-35 pb of homology arms. However, SG386+SG387 oligos were used to genotype the positive *hrde-1(+R)* outcomes.
hrde-1(+R)	SG-1293	atctcggtacctgtcgttgc	
hrde-1	SG-518	CCACATTCCCACGTCTTTCT	qRT-PCR primers for *hrde-1*. SG-518 and SG-519 amplify a region (chrIII:4175030-4175318) of *hrde-1* gene that are deleted in *hrde-1(tm1200)* mutant. PCR product is 289bp in WT.
hrde-1	SG-519	AAGTCTCTCGAGTCGGAACG	
Cer8, GRTS example	SG-1299	ggtctggtgaatgccaagat	*cer8* qRT-PCR primers (SG1299+1300) product size 104bp, specific to the *cer8* copy at chrV: 5179680-5191222
Cer8, GRTS example	SG-1300	aagcccgtacgcgagtagta	

Table A-2 **cont.**

GHR example	SG-1301	AGGGAACAACAGGAACATGC	GRH example qRT-PCR primers (SG1301+1302) product size 99bp, specific to region at the examlary GRH chrV:5465000-5485000
GRH example	SG-1302	GTGTTTGTGAACGTGGCAAG	

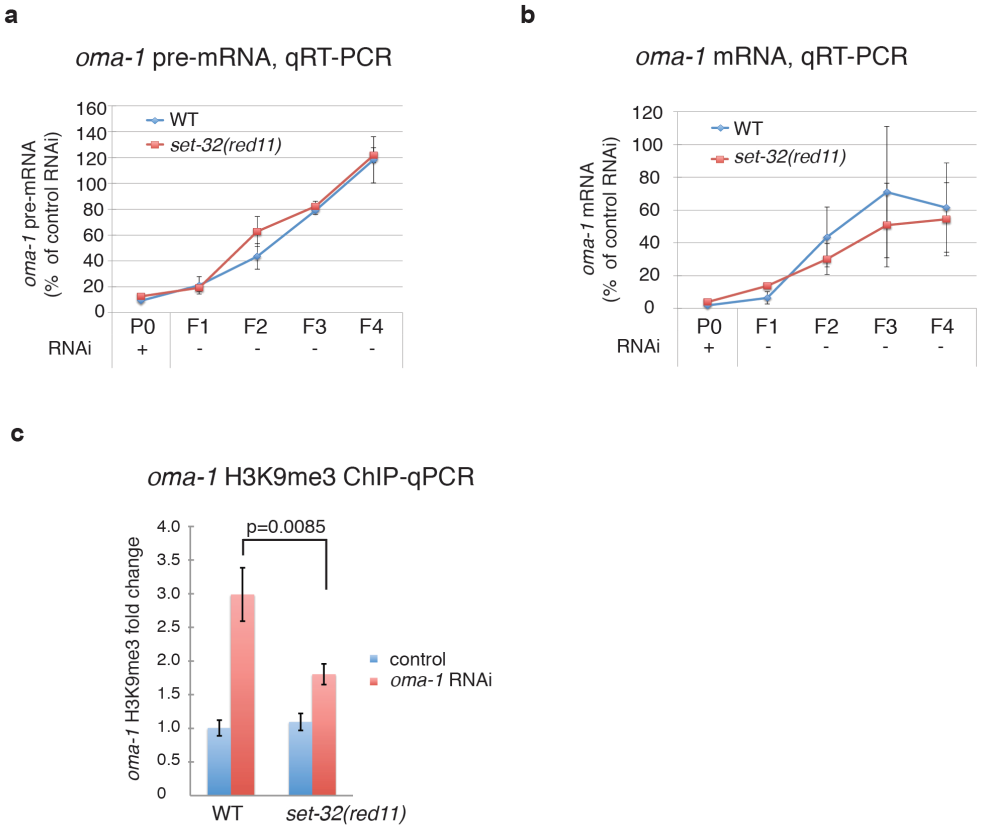

Figure A-7* Test of *set-32 (red11)* mutants for heritable RNAi and dsRNA-induced transcriptional silencing and H3K9me3 at *oma-1

(a) pre-mRNA and (b) mRNA levels of *oma-1* RNAi samples, normalized to the control RNAi are plotted as a function of generations for WT or *set-32(red11)* mutant strains. (c) H3K9me3 ChIP-qPCR analysis of *oma-1* dsRNA-triggered H3K9me3 response in WT and *set-32(red11)* mutant strains.

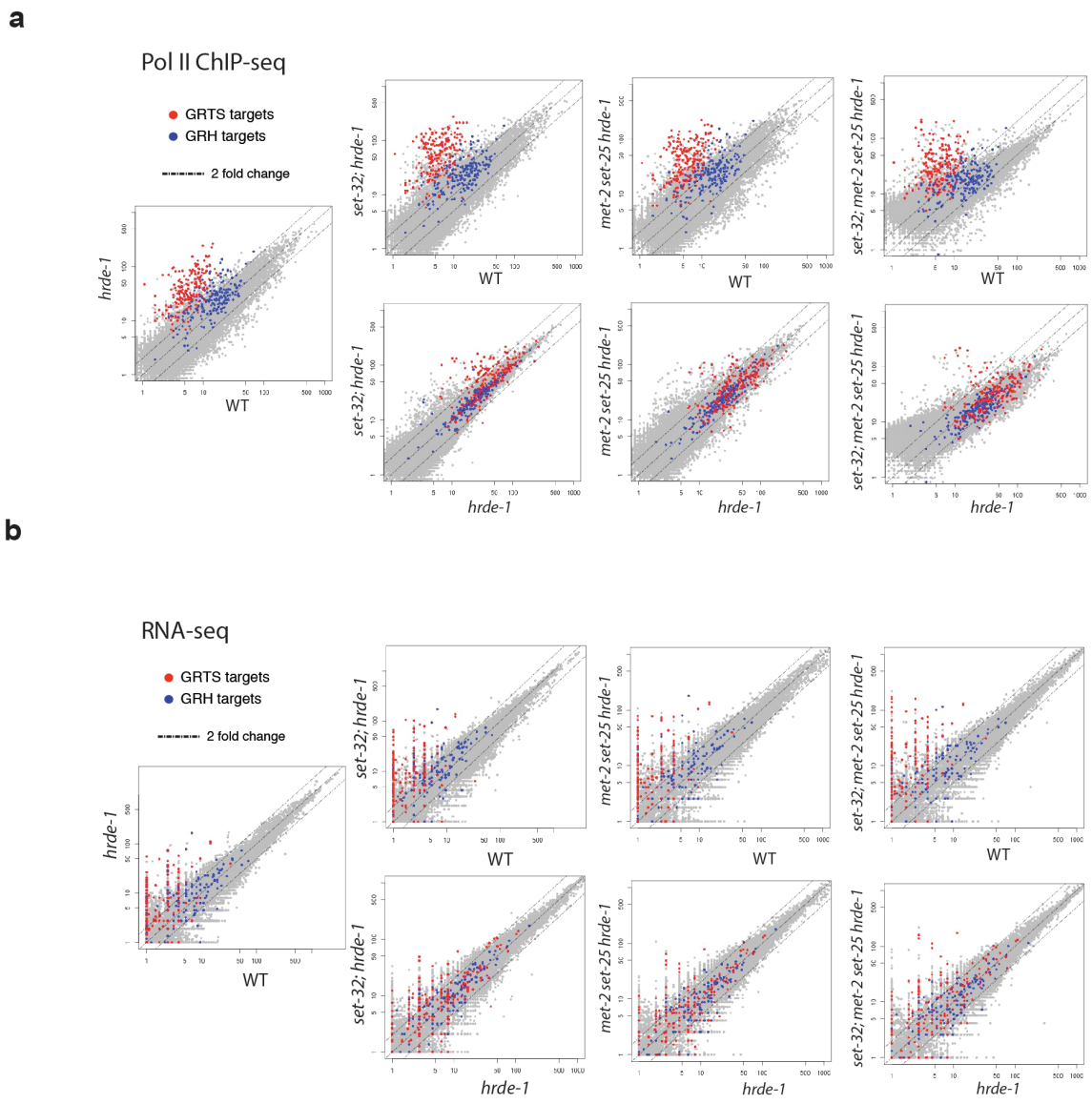

Figure A-8 **Whole-genome scatter plots (1 kb resolution) that show the additive de-silencing effect in various combination mutants of *set-32*, *met-2*, *set-25* and *hrde-1***

Scatter plots (1 kb resolution) that compare various combination mutants with WT or *hrde-1* for (a) Pol II ChIP-seq, (b) RNA-seq whole genome analysis.

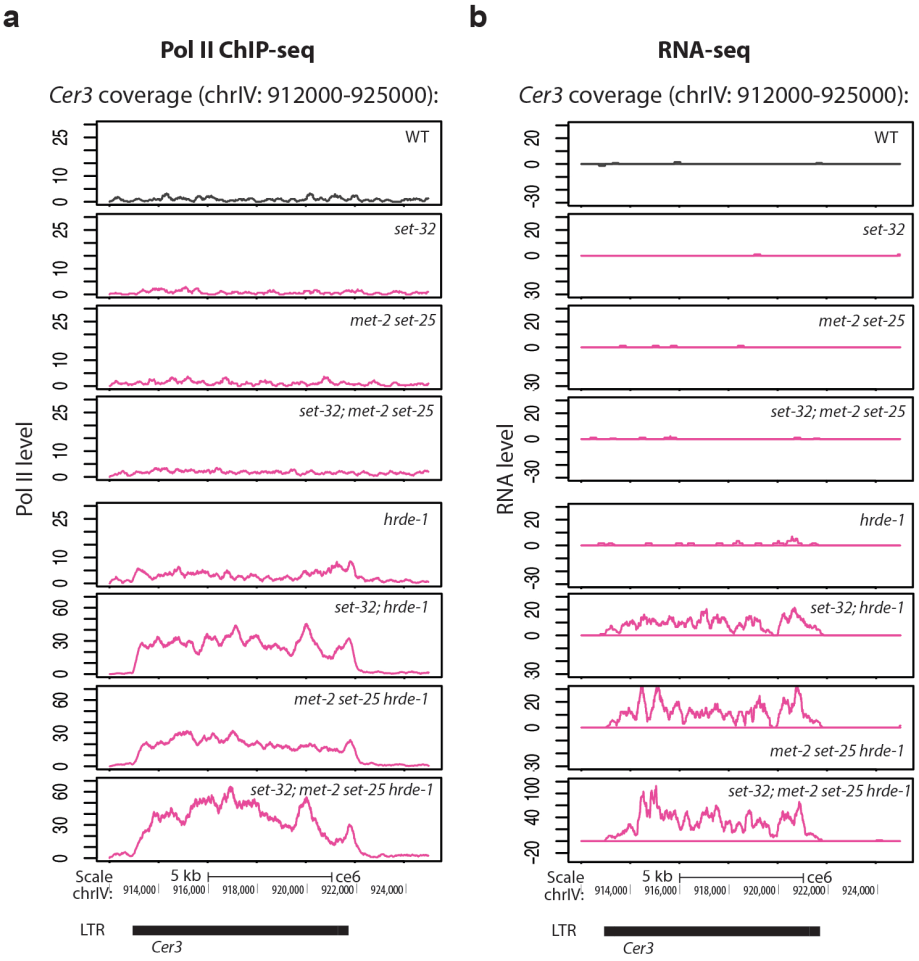

Figure A-9 **Pol II and RNA profile characterization of *Cer3* locus in WT and various mutants**

Coverage plot of (a) Pol II and (b) RNA levels at *Cer3* locus. For RNA coverage plots, sense reads are plotted above the $y = 0$ line (antisense bellow). This is an expanded version (with additional mutants) of the figure Fig. 10b,c.

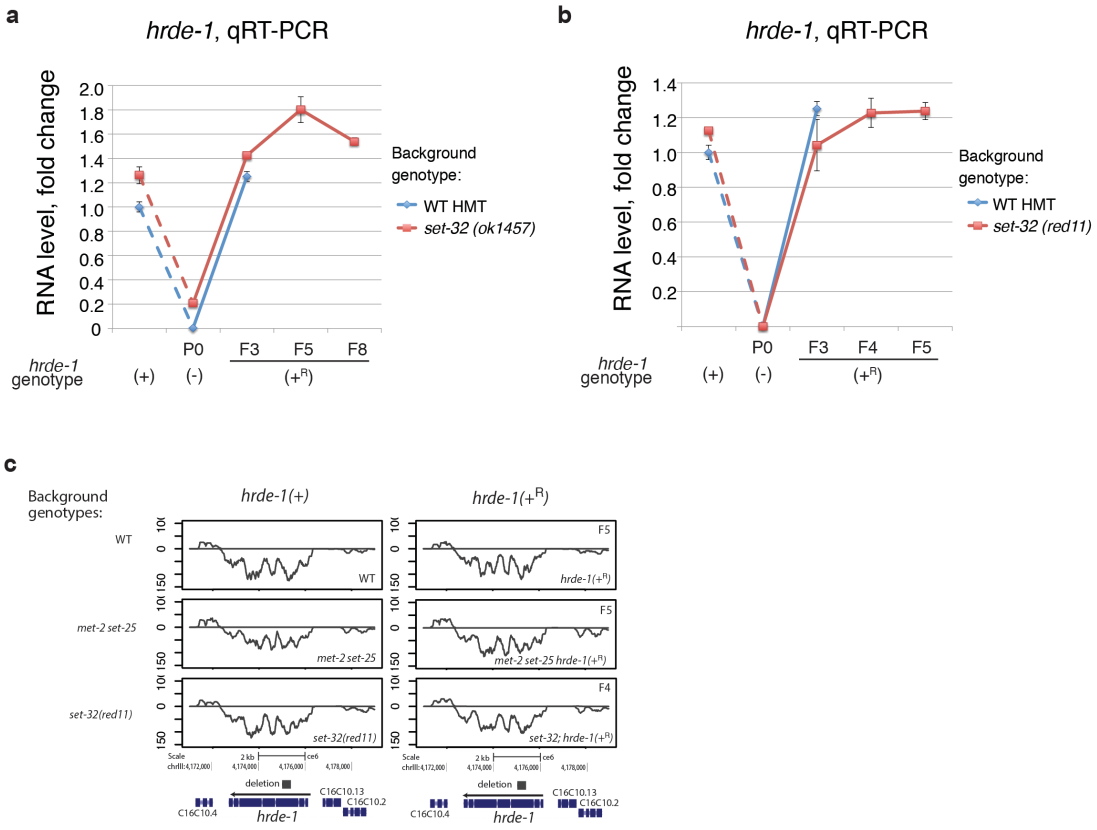

Figure A-10 **HRDE-1 expression at RNA level is fully recovered after *hrde-1* gene repair**

RNA levels measured by qRT-PCR at *hrde-1* gene before and after *hrde-1* repair in multigenerational experiments of (a) *set-32(ok1457)* mutant background and WT HMT background control samples, (b) *set-32(red11)* mutant background and WT HMT background control samples, (c) coverage plot of RNA levels at *hrde-1* gene in *hrde-1(+)* control samples and post-repair samples of WT HMT genetic background and various HMT mutant backgrounds. Sense reads are plotted above the $y = 0$ line (antisense bellow).

Table A-3 **List of sequences of 50-mer DNA oligonucleotides used for rRNA depletion**

Sequence:
caaaaaactcaatcaaaggatagtctcaacagatcgcagtataaaaggac
tgctctactgaatacaacaccttgaccaagagaccaagtcgtatgcaagt
gatttagcgccccgacattgaaccagagtgatctggcgttggcaagcgtc
gcagaattcactacgacgccaaggccatacatagggcataagctctcgtg
ttgccacgagatagagatgcctcccgacaccgggaagcaagaaattttcg
ccttgacaaggcgagattctaacttagaggcgttcagttataatctctca
aatggtagcttcagaccattgatctgtcgatcaagtttatgaaccaaatg
tttgaacccgctgttcctctcgtactaagcaggattactttcgcaataac
aagtcaacagtagggtaaaactaacctgtctcacgacggtctaaacccag
ctcacgttccctattagtgggtgaacaatccaacgcttggcgaattctgc
ttcgcaatgataggaagagccgacatcgaaggatcaaaaagcaacgtcgc
tatggacgcttggctgccacaagccagttatccctgtggtaacttttctg
acacctcttacctgaaacaatcaggattaaaaggatcgataggccacgct
ttcgcggtctgtactcgtactgaaagtcaagatcaagcaagcttttgccc
ttttgctctacgagaggtttccgtcctctctgagctcgccttaggacacc
tacgttacgatttgatagatgtaccgccccagtcaaactccccgcttgac
actgtcttcgaggagagtcacggtgccataaaatggctccgcttaatgct
tcgaaaaaaggccgtgaagccaattctcttttaaccgaataagtaaagag
tcgatgaaagtggtggtatttcactgtcgtccgaagactcccacctatgc
tacacctctcatgactcttcacaatgtcaaactagagtcaagctcaacag
ggtcttctttccccgctatttttgccaagcccgttcccttggctgtggtt
tcgctagaaagtagttagggacagtaggaatctcgttaatccattcatgc
gcgtcaacaattaaatgacgaggcatttggctaccttaagagagtcatag
ttactcccgccgtttacccgcgcttactcgaattactacgatttaacatt
cagagcactgggcagaaatcagtgacagtcaacgtccgcaaggaccatct
gtcacctctgttttaattagacagtcggattccctgagtccgtaccggtt
ccagtacggttgtttagatgagcgatcaggatactagaaccgaggtccaa
gcacacaccagaaagcgtccgcaagcaagcacaatcactagtccgccatc
aacccgaaagtatcaagcagacagaactgcgccggacaagcatcaaccaa
ctggccaaccgttccaaccactggagccaatccttttcccgaagttacgg
atctagtttgccgacttcccttacctacattattctatcgactagaggct
gttcaccttggagacctaatgcggatatcggtacgattgagtgcaaatta
atagcctcccttggtgttttaagggccgttcaaagagcacgagacaccac
agaaaccgcggtgcttttcggaaacaacgtccccatctctggctgaacca
attccagggagtccgttccttaactagagaagaaaactctagctcggtct
ttgagcgactaaccaagttcgaatgcgttaccgcgcttgtgctccgaaga
acacaatctttgcatctcagttagggaatattaaccctattccctttcga
caagcggggactaaaagcaagctttcgccaccgatgatacaaggcgttc

Table A-3 **cont.**

gccagtaccttaggatcgactgacccacatccaactactgttcacgtgga
acccttctccacttcagtcttcaaggatcgaacttgaatatttgctacta
ccattacgatctgcactgacggaagctccagccgagcctacgctcatagc
cttcaacgcaaccgccacgaccttcctactcgttacgacctggcgctaga
caacgcacatgtcgcaacggcggagtataggtctctcgcttaagcgccat
ccattttcagggctagttgattcggcaggtgagttgttacacactcctta
gcggataccgacttccatggccaccgtcctgctgtcaatatcaaccaaca
ccttttatggggtctcatgagcgagaagttaggcaccttaactccacgtt
tggttcatcccacagcgccagttctgcttaccaaaaatggcccacttgga
cctcgcattcacgttgacagttcactaaagaaactgcaacttcatatcca
ttgaaagtttgagaataggttgaggacattacgtccccaaggcctctaat
cattagctttaccgaatataactgcctgagatccagctatcctgagggaa
acttcggaaggaaccagctactagatggttcgattagtctttcgccccta
tacccaagtctatcgatcgatttgcacgtcagaaccgatacggacttcca
ccagagtttcctctggcttcatcctgctcaggcatagttcaccatctttc
gggtcgtttgccaactgctcaacctctgcacagtcacaagtgacacgcac
agggccgtggtgcgctgcactccgaagaacacagatcccacgtcggccaa
ttcgagactgacctttactttcatttcgccgcaaggttttaacacccttt
gactcgcagtagacaagcactccgcaatccgtgtttcaagacgggtcgga
aacgtcgtcgactttcacaccgacgtcacacacactagcgtaactaaacg
ctagccgccacgaacccactaccgccagcaagacaccttctcttgcgaga
tgggcaacactgtcgggctagaacgagcagccaacgccgtcggcgtagca
taggaaacgacacccggcaacgatcacaactaagcgaccagtcaccaagc
ttgtctccaagcaacatcaactgtctccggttccactccagcgatttcac
gttctcttgaactctctcttcaaagtcctttgcaactttccctcacggta
cttgttcgctatcgcaatcgagtcgatatttagccttagatgaagtttat
cacccactttaggctgcactttcaagcaacccgactccaaggagcaagcg
aaccaacagtgccgctatccagaacggggctcgcaccctctctggtttat
ggcctcaatcgtaaggacttcggacatacgacactgctggaaacttacac
ctatacgccacatttcgaagcagccaaagactgatcgattcggcgctggg
ctcttcccgtttcactcgccgttactaagggaatccttttagtttcttt
tcctccgctaaatgatatgcttaagttcagcgggtaatcacgactgagtt
caggttgagcgatgatccagctgcaggttcacctacagctaccttgttac
gacttttacccggttcaaaccaatgcgataaaaatggtttccgcaacaac
gaagtcgttaaacctcgaagcgacagtccccactcttctcgaatcagttc
agtcccggatagcgacgggcggtgtgtacaaagggcagggacgtaatcaa
cgtgagctgatgactcacacttactaggcattcctcgtttaagggcaata
attacaataccctatcccggacatggaagaatttcaacggtttaccgata
cctttcggcataggaaaaacccgctgactccaccagtgtagcacgcgtgc

Table A-3 **cont.**

agccccggacatctaagggcatcacagacctgttatcgctcaatctcgtg
cggctaaacaccgcttatccctctaagaagttatacgaacccgaagattc
gccaactatttagcaggctagagtctcgctcgttatcggaataaaccaga
caaatcactccaccaactaagaacggccatgcaccaccaaccaccaaatc
gagaaagagctttcaatctgtcagtcctaatggtgtccggaccgggtgag
ttttcccgtgttgagtcaaattaagccgcaagctccacgccttgtggtgc
ccttccgtcaatttctttaagtttcagctttgcaaccatactacccccgg
aaccgaaagactttcgtttccggatagctcctcggcagggcaaaaaccct
ccgaatcgcgagatggcatcgtttacggtcagaactagggcggtatctaa
tcgccttcgaacctctgactttcgttcttgattaatgaagacattcttgg
caaatgctttcgctgttgggcgtctcactacggtccacgaatttcacctc
tcgcgtaatgatacgaatgcccccggtttgtccctcttaaccattaaatc
agttctagaaccaacaaaaagaaccgaagtcctgtttcattattccatga
tgagctattcaagcaagcgcttgtattgagcactctgatttattcaaggt
aaacctgctggcagttgaagggcgaacccaacctcaaaccagcaaattag
aagtcacgaccacagttgacgcaaattgcgaactgcggcacgtaacctag
atccaactacgagcttttaaccgcagcaataacgagatacactaggaga
cgaagaatcatttgtattcaactcattgaaataactcatccaaaaggatg
agtctttatatttttagtcactatctcatactcaacagtggataagtttc
gcgcctgctgccttccttggacgtggtagccgtttctaaggctccctctc
cggagtcgaacccttattctccgttacccgtaacaaccatggtagtccaa
taaactaccatctagttgaaagggcagacacccttccggatagagtcag
tcgaaactgacagtaaactgctttattcagagtcaacaaacaacgtccga
aaacgtttggtctgttctaataattgcaccccgccttgcgttggggtata
gttgcatgtattagctccagtatttccgcagttatccatatgaggatccc
ggataaggtgatatctgctctaatgagccgtacgcaatttcattgatgaa
tcaaagcatgcatggcttaatcttttacttgagcatatcgcgctgacaga
atcaatcaggtataacaaccctgaaccagacgtaccaactggaggcccag
ttggtgctatgcgttcgaaatttcaccactctaagcgtctgcaattcgtg
agcttacaacatccaggattcccaggccgtctccgatccaagtactaact
ggactcaacgttgcttaacttgccagatcggacgggatggcgtgcattca
acgtgatatggtcgtaagcctgcgttcttcatcgatactcgatgcaaccg
cgcggctgctggcaccagacttgccctctccttgctactccatcgctgaa

References

Alcazar, R.M., Lin, R., and Fire, A.Z. (2008). Transmission dynamics of heritable silencing induced by double-stranded RNA in Caenorhabditis elegans. Genetics *180*.
Ameyar-Zazoua, M., Rachez, C., Souidi, M., Robin, P., Fritsch, L., Young, R., Morozova, N., Fenouil, R., Descostes, N., Andrau, J.*, et al.* (2012). Argonaute proteins couple chromatin silencing to alternative splicing. Nat Struct Mol Biol *19*, 998-1004.
Andersen, E.C., and Horvitz, H. (2007). Two C. elegans histone methyltransferases repress lin-3 EGF transcription to inhibit vulval development. Development (Cambridge, England) *134*, 2991-2999.
Aravin, A.A., Sachidanandam, R., Bourc'his, D., Schaefer, C., Pezic, D., Toth, K.F., Bestor, T., and Hannon, G.J. (2008). A piRNA pathway primed by individual transposons is linked to de novo DNA methylation in mice. Mol Cell *31*, 785-799.
Arribere, J.A., Bell, R.T., Fu, B.X., Artiles, K.L., Hartman, P.S., and Fire, A.Z. (2014). Efficient marker-free recovery of custom genetic modifications with CRISPR/Cas9 in Caenorhabditis elegans. Genetics *198*.
Ashe, A., Sapetschnig, A., Weick, E.M., Mitchell, J., Bagijn, M.P., Cording, A.C., Doebley, A.L., Goldstein, L.D., Lehrbach, N.J., Le Pen, J.*, et al.* (2012). piRNAs can trigger a multigenerational epigenetic memory in the germline of C. elegans. Cell *150*, 88-99.
Audergon, P.N., Catania, S., Kagansky, A., Tong, P., Shukla, M., and Pidoux, A.L. (2015). Epigenetics. Restricted epigenetic inheritance of H3K9 methylation. Science *348*.
Bagijn, M.P., Goldstein, L.D., Sapetschnig, A., Weick, E.M., Bouasker, S., Lehrbach, N.J., Simard, M.J., and Miska, E.A. (2012). Function, targets, and evolution of Caenorhabditis elegans piRNAs. Science *337*, 574-578.
Bayne, E.H., and Allshire, R.C. (2005). RNA-directed transcriptional gene silencing in mammals. Trends in Genetics *21*, 370-373.
Bernstein, B.E., Caudy, A.A., Hammond, S.M., and Hannon, G.J. (2001). Role for a bidentate ribonuclease in the initiation step of RNA interference. Nature *409*, 363-366.
Bessler, J.B., Andersen, E.C., and Villeneuve, A.M. (2010). Differential localization and independent acquisition of the H3K9me2 and H3K9me3 chromatin modifications in the Caenorhabditis elegans adult germ line. PLoS Genet *6*.
Brennecke, J., Malone, C.D., Aravin, A.A., Sachidanandam, R., Stark, A., and Hannon, G.J. (2008). An epigenetic role for maternally inherited piRNAs in transposon silencing. Science *322*, 1387-1392.
Brenner, S. (1974). The genetics of Caenorhabditis elegans. Genetics *77*.
Buckley, B.A., Burkhart, K.B., Gu, S.G., Spracklin, G., Kershner, A., Fritz, H., Kimble, J., Fire, A., and Kennedy, S. (2012). A nuclear Argonaute promotes multigenerational epigenetic inheritance and germline immortality. Nature *489*, 447-451.
Buhler, M., Haas, W., Gygi, S.P., and Moazed, D. (2007). RNAi-dependent and -independent RNA turnover mechanisms contribute to heterochromatic gene silencing. Cell *129*, 707-721.
Buhler, M., Spies, N., Bartel, D.P., and Moazed, D. (2008). TRAMP-mediated RNA surveillance prevents spurious entry of RNAs into the Schizosaccharomyces pombe siRNA pathway. Nat Struct Mol Biol *15*, 1015-1023.

Bühler, M., Verdel, A., and Moazed, D. (2006). Tethering RITS to a nascent transcript initiates RNAi- and heterochromatin-dependent gene silencing. Cell *125*, 873-886.
Burkhart, K.B., Guang, S., Buckley, B.A., Wong, L., Bochner, A.F., and Kennedy, S. (2011). A pre-mRNA-associating factor links endogenous siRNAs to chromatin regulation. PLoS Genet *7*.
Burton, N.O., and Burkhart, K.B. (2011). Nuclear RNAi maintains heritable gene silencing in Caenorhabditis elegans. Proceedings of the ….
Carmell, M.A., Girard, A., van de Kant, H.J., Bourc'his, D., Bestor, T.H., de Rooij, D.G., and Hannon, G.J. (2007). MIWI2 is essential for spermatogenesis and repression of transposons in the mouse male germline. Dev Cell *12*, 503-514.
Castel, S.E., and Martienssen, R.A. (2013). RNA interference in the nucleus: roles for small RNAs in transcription, epigenetics and beyond. Nature reviews Genetics *14*, 100-112.
Castellano, L., and Stebbing, J. (2013). Deep sequencing of small RNAs identifies canonical and non-canonical miRNA and endogenous siRNAs in mammalian somatic tissues. Nucleic Acids Res *41*, 3339-3351.
Chandler, V.L. (2010). Paramutation's properties and puzzles. Science *330*, 628-629.
Chu, Y., Yue, X., Younger, S.T., Janowski, B.A., and Corey, D.R. (2010). Involvement of argonaute proteins in gene silencing and activation by RNAs complementary to a non-coding transcript at the progesterone receptor promoter. Nucleic Acids Res *38*, 7736-7748.
Corsi, A.K., Wightman, B., and Chalfie, M. (2015). A Transparent window into biology: A primer on Caenorhabditis elegans. WormBook : the online review of C elegans biology, 1-31.
Cuerda-Gil, D., and Slotkin, R.K. (2016). Non-canonical RNA-directed DNA methylation. Nature plants *2*.
Das, P.P., Bagijn, M.P., Goldstein, L.D., Woolford, J.R., Lehrbach, N.J., Sapetschnig, A., Buhecha, H.R., Gilchrist, M.J., Howe, K.L., Stark, R.*, et al.* (2008). Piwi and piRNAs act upstream of an endogenous siRNA pathway to suppress Tc3 transposon mobility in the Caenorhabditis elegans germline. Mol Cell *31*, 79-90.
de Vanssay, A., Bougé, A.L., Boivin, A., Hermant, C., Teysset, L., Delmarre, V., Antoniewski, C., and Ronsseray, S. (2012). Paramutation in Drosophila linked to emergence of a piRNA-producing locus. Nature *490*, 112-115.
Dernburg, A.F., Zalevsky, J., Colaiácovo, M.P., and Villeneuve, A.M. (2000). Transgene-mediated cosuppression in the C. elegans germ line. Genes & development *14*, 1578-1583.
Eissenberg, J.C., James, T.C., Foster-Hartnett, D.M., Hartnett, T., Ngan, V., and Elgin, S.C. (1990). Mutation in a heterochromatin-specific chromosomal protein is associated with suppression of position-effect variegation in Drosophila melanogaster. Proceedings of the National Academy of Sciences of the United States of America *87*, 9923-9927.
Ekwall, K., Nimmo, E.R., Javerzat, J.P., Borgstrøm, B., Egel, R., Cranston, G., and Allshire, R.C. (1996). Mutations in the fission yeast silencing factors clr4+ and rik1+ disrupt the localisation of the chromo domain protein Swi6p and impair centromere function. J Cell Sci *109*, 2637-2648.
Elbashir, S.M., Lendeckel, W., and Tuschl, T. (2001). RNA interference is mediated by 21- and 22-nucleotide RNAs. Genes & development *15*.

Ellermeier, C., Higuchi, E.C., Phadnis, N., Holm, L., Geelhood, J.L., Thon, G., and Smith, G.R. (2010). RNAi and heterochromatin repress centromeric meiotic recombination. Proceedings of the National Academy of Sciences of the United States of America *107*, 8701-8705.
Fire, A., Xu, S., Montgomery, M.K., Kostas, S.A., Driver, S.E., and Mello, C.C. (1998). Potent and specific genetic interference by double-stranded RNA in Caenorhabditis elegans. Nature.
Fultz, D., Choudury, S.G., and Slotkin, R.K. (2015). Silencing of active transposable elements in plants. Current Opinion in Plant Biology *27*, 67-76.
Gagnon, K.T., and Corey, D.R. (2012). Argonaute and the nuclear RNAs: new pathways for RNA-mediated control of gene expression. Nucleic acid therapeutics *22*, 3-16.
Garrigues, J.M., Sidoli, S., Garcia, B.A., and Strome, S. (2015). Defining heterochromatin in C. elegans through genome-wide analysis of the heterochromatin protein 1 homolog HPL-2. Genome Res *25*.
Gaydos, L.J., Rechtsteiner, A., Egelhofer, T.A., Carroll, C.R., and Strome, S. (2012). Antagonism between MES-4 and Polycomb repressive complex 2 promotes appropriate gene expression in C. elegans germ cells. Cell Rep *2*, 1169-1177.
Greer, E.L., Beese-Sims, S.E., Brookes, E., Spadafora, R., Zhu, Y., and Rothbart, S.B. (2014). A histone methylation network regulates transgenerational epigenetic memory in C. elegans. Cell Rep *7*.
Grewal, S.I., and Jia, S. (2007). Heterochromatin revisited. Nature reviews Genetics *8*, 35-46.
Gu, S.G., and Fire, A. (2010). Partitioning the C. elegans genome by nucleosome modification, occupancy, and positioning. Chromosoma *119*.
Gu, S.G., Pak, J., Guang, S., Maniar, J.M., Kennedy, S., and Fire, A. (2012). Amplification of siRNA in Caenorhabditis elegans generates a transgenerational sequence-targeted histone H3 lysine 9 methylation footprint. Nature genetics *44*, 157-164.
Guang, S., Bochner, A.F., Burkhart, K.B., Burton, N., Pavelec, D.M., and Kennedy, S. (2010). Small regulatory RNAs inhibit RNA polymerase II during the elongation phase of transcription. Nature *465*, 1097-1101.
Guang, S., Bochner, A.F., Pavelec, D.M., Burkhart, K.B., Harding, S., and Lachowiec, J. (2008). An Argonaute transports siRNAs from the cytoplasm to the nucleus. Science *321*.
Gullerova, M., and Proudfoot, N.J. (2008). Cohesin complex promotes transcriptional termination between convergent genes in S. pombe. Cell *132*, 983-995.
Haag, J.R., and Pikaard, C.S. (2011). Multisubunit RNA polymerases IV and V: purveyors of non-coding RNA for plant gene silencing. Nat Rev Mol Cell Biol *12*, 483-492.
Hall, I.M., Shankaranarayana, G.D., Noma, K., Ayoub, N., Cohen, A., and Grewal, S.I. (2002). Establishment and Maintenance of a Heterochromatin Domain. Science *297*.
Hammond, S.M. (2005). Dicing and slicing: The core machinery of the RNA interference pathway. FEBS Letters *579*.
Hammond, S.M., Bernstein, E., Beach, D., and Hannon, G.J. (2000). An RNA-directed nuclease mediates post-transcriptional gene silencing in Drosophila cells. Nature *404*.
Hammond, S.M., Boettcher, S., Caudy, A.A., Kobayashi, R., and Hannon, G.J. (2001). Argonaute2, a link between genetic and biochemical analyses of RNAi. Science *293*.

Hirsh, D., Oppenheim, D., and Klass, M. (1976). Development of the reproductive system of Caenorhabditis elegans. Dev Biol *49*.
Ho, J.W., Jung, Y.L., Liu, T., Alver, B.H., Lee, S., Ikegami, K., Sohn, K.A., Minoda, A., Tolstorukov, M.Y., Appert, A.*, et al.* (2014). Comparative analysis of metazoan chromatin organization. Nature *512*, 449-452.
Holoch, D., and Moazed, D. (2015). RNA-mediated epigenetic regulation of gene expression. Nature reviews Genetics *16*, 71-84.
Houri-Ze'evi, L., Korem, Y., Sheftel, H., Faigenbloom, L., Toker, I.A., and Dagan, Y. (2016). A tunable mechanism determines the duration of the transgenerational small RNA inheritance in C. elegans. Cell *165*.
Huang, X.A., Yin, H., Sweeney, S., Raha, D., Snyder, M., and Lin, H. (2013). A major epigenetic programming mechanism guided by piRNAs. Dev Cell *24*, 502-516.
Irvine, D.V., Zaratiegui, M., Tolia, N.H., Goto, D.B., Chitwood, D.H., Vaughn, M.W., Joshua-Tor, L., and Martienssen, R.A. (2006). Argonaute Slicing Is Required for Heterochromatic Silencing and Spreading. Science *313*, 1134-1137.
Izumi, N., and Tomari, Y. (2014). Diversity of the piRNA pathway for nonself silencing: worm-specific piRNA biogenesis factors. Genes & development *28*, 665-671.
Johnson, W.L., Yewdell, W.T., Bell, J.C., McNulty, S.M., Duda, Z., O'Neill, R.J., Sullivan, B.A., and Straight, A.F. (2017). RNA-dependent stabilization of SUV39H1 at constitutive heterochromatin. eLife *6*.
Kalinava, N., Ni, J.Z., Peterman, K., Chen, E., and Gu, S.G. (2017). Decoupling the downstream effects of germline nuclear RNAi reveals that H3K9me3 is dispensable for heritable RNAi and the maintenance of endogenous siRNA-mediated transcriptional silencing in Caenorhabditis elegans. Epigenetics Chromatin *10*, 6.
Kennerdell, J.R., and Carthew, R.W. (1998). Use of dsRNA-mediated genetic interference to demonstrate that frizzled and frizzled 2 act in the wingless pathway. Cell *95*.
Ketting, R.F., and Plasterk, R.H. (2000). A genetic link between co-suppression and RNA interference in C. elegans. Nature *404*, 296-298.
Kim, D.H., Villeneuve, L.M., Morris, K.V., and Rossi, J.J. (2006). Argonaute-1 directs siRNA-mediated transcriptional gene silencing in human cells. Nat Struct Mol Biol *13*, 793-797.
Knight, S.W., and Bass, B.L. (2001). A Role for the RNase III Enzyme DCR-1 in RNA Interference and Germ Line Development in Caenorhabditis elegans. Science *293*, 2269–2271.
Kuramochi-Miyagawa, S., Watanabe, T., Gotoh, K., Totoki, Y., Toyoda, A., Ikawa, M., Asada, N., Kojima, K., Yamaguchi, Y., Ijiri, T.W.*, et al.* (2008). DNA methylation of retrotransposon genes is regulated by Piwi family members MILI and MIWI2 in murine fetal testes. Genes & development *22*, 908-917.
Langmead, B., Trapnell, C., Pop, M., and Salzberg, S.L. (2009). Ultrafast and memory-efficient alignment of short DNA sequences to the human genome. Genome Biol *10*.
Le Thomas, A., Rogers, A.K., Webster, A., Marinov, G.K., Liao, S.E., Perkins, E.M., Hur, J.K., Aravin, A.A., and Toth, K.F. (2013). Piwi induces piRNA-guided transcriptional silencing and establishment of a repressive chromatin state. Genes & development *27*, 390-399.

Le Thomas, A., Stuwe, E., Li, S., Du, J., Marinov, G., Rozhkov, N., Chen, Y.C., Luo, Y., Sachidanandam, R., Toth, K.F.*, et al.* (2014). Transgenerationally inherited piRNAs trigger piRNA biogenesis by changing the chromatin of piRNA clusters and inducing precursor processing. Genes & development *28*, 1667-1680.
Lee, H.C., Gu, W., Shirayama, M., Youngman, E., Conte, D., Jr., and Mello, C.C. (2012). C. elegans piRNAs mediate the genome-wide surveillance of germline transcripts. Cell *150*, 78-87.
Leopold, L.E., Heestand, B.N., Seong, S., Shtessel, L., and Ahmed, S. (2015). Lack of pairing during meiosis triggers multigenerational transgene silencing in Caenorhabditis elegans. Proc Natl Acad Sci USA *112*.
Luteijn, M.J., van Bergeijk, P., Kaaij, L.J., Almeida, M.V., Roovers, E.F., Berezikov, E., and Ketting, R.F. (2012). Extremely stable Piwi-induced gene silencing in Caenorhabditis elegans. EMBO J *31*, 3422-3430.
Maniar, J.M., and Fire, A.Z. (2011). EGO-1, a C. elegans RdRP, modulates gene expression via production of mRNA-templated short antisense RNAs. Current biology : CB *21*, 449-459.
Mao, H., Zhu, C., Zong, D., Weng, C., Yang, X., and Huang, H. (2015). The Nrde pathway mediates small-RNA-directed histone H3 lysine 27 trimethylation in Caenorhabditis elegans. Current biology : CB *25*.
Martienssen, R., and Moazed, D. (2015). RNAi and heterochromatin assembly. Cold Spring Harb Perspect Biol *7*.
McMurchy, A.N., Stempor, P., Gaarenstroom, T., Wysolmerski, B., Dong, Y., Aussianikava, D., Appert, A., Huang, N., Kolasinska-Zwierz, P., Sapetschnig, A.*, et al.* (2017). A team of heterochromatin factors collaborates with small RNA pathways to combat repetitive elements and germline stress. eLIfe *6:e21666*.
Mette, M.F., Aufsatz, W., Winden, J.v.d., Matzke, M.A., and Matzke, A.J.M. (2000). Transcriptional silencing and promoter methylation triggered by double-stranded RNA. The EMBO Journal *19*, 5194-5201.
Moazed, D. (2009). Small RNAs in transcriptional gene silencing and genome defence. Nature *457*, 413-420.
Mohn, F., Sienski, G., Handler, D., and Brennecke, J. (2014). The rhino-deadlock-cutoff complex licenses noncanonical transcription of dual-strand piRNA clusters in Drosophila. Cell *157*, 1364-1379.
Montgomery, M.K., Xu, S., and Fire, A. (1998). RNA as a target of double-stranded RNA-mediated genetic interference in Caenorhabditis elegans. Proceedings of the National Academy of Sciences of the United States of America *95*, 15502-15507.
Morris, K.V., Chan, S.W., Jacobsen, S.E., and Looney, D.J. (2004). Small interfering RNA-induced transcriptional gene silencing in human cells. Science *305*, 1289-1292.
Napoli, C., Lemieux, C., and Jorgensen, R. (1990). lntroduction of a Chimeric Chalcone Synthase Gene into Petunia Results in Reversible Co-Suppression of Homologous Genes Ín trans. The Plant Cell *2*, 279-289.
Ni, J.Z., Chen, E., and Gu, S.G. (2014). Complex coding of endogenous siRNA, transcriptional silencing and H3K9 methylation on native targets of germline nuclear RNAi in C. elegans. BMC Genom *15*.

Ni, J.Z., Kalinava, N., Chen, E., Huang, A., Trinh, T., and Gu, S.G. (2016). A transgenerational role of the germline nuclear RNAi pathway in repressing heat stress-induced transcriptional activation in C. elegans. Epigenetics & chromatin *9*, 1.
Paix, A., Folkmann, A., Rasoloson, D., and Seydoux, G. (2015). High efficiency, homology-directed genome editing in Caenorhabditis elegans using CRISPR-Cas9 ribonucleoprotein complexes. Genetics *201*.
Pak, J., and Fire, A. (2007). Distinct Populations of Primary and Secondary Effectors During RNAi in C. elegans. Science *315*.
Partridge, J.F., DeBeauchamp, J.L., Kosinski, A.M., Ulrich, D.L., Hadler, M.J., and Noffsinger, V.J. (2007). Functional separation of the requirements for establishment and maintenance of centromeric heterochromatin. Mol Cell *26*, 593-602.
Pek, J.W., and Kai, T. (2011). A role for vasa in regulating mitotic chromosome condensation in Drosophila. Current biology : CB *21*, 39-44.
Ragunathan, K., Jih, G., and Moazed, D. (2015). Epigenetics. Epigenetic inheritance uncoupled from sequence-specific recruitment. Science *348*.
Rajeevkumar, S., Anunanthini, P., and Sathishkumar, R. (2015). Epigenetic silencing in transgenic plants. Frontiers in plant science *6*, 693.
Robert, V.J., Sijen, T., van Wolfswinkel, J., and Plasterk, R.H. (2005). Chromatin and RNAi factors protect the C. elegans germline against repetitive sequences. Genes & development *19*, 782-787.
Rozhkov, N.V., Hammell, M., and Hannon, G.J. (2013). Multiple roles for Piwi in silencing Drosophila transposons. Genes & development *27*, 400-412.
Sander, J.D., and Joung, J.K. (2014). CRISPR-Cas systems for editing, regulating and targeting genomes. Nature Biotechnology *32*, 347–355.
Seth, M., Shirayama, M., Gu, W., Ishidate, T., Conte, D., and Mello, C.C. (2013). The C. elegans CSR-1 argonaute pathway counteracts epigenetic silencing to promote germline gene expression. Dev Cell *27*.
Shirayama, M., Seth, M., Lee, H.C., Gu, W., Ishidate, T., and Conte, D. (2012). piRNAs initiate an epigenetic memory of nonself RNA in the C. elegans germline. Cell *150*.
Shiu, P.K., and Hunter, C.P. (2017). Early Developmental Exposure to dsRNA Is Critical for Initiating Efficient Nuclear RNAi in C. elegans. Cell Rep *18*, 2969-2978.
Sienski, G., Donertas, D., and Brennecke, J. (2012). Transcriptional silencing of transposons by Piwi and maelstrom and its impact on chromatin state and gene expression. Cell *151*, 964-980.
Sijen, T., Fleenor, J., Simmer, F., Thijssen, K.L., Parrish, S., Timmons, L., Plasterk, R.H., and Fire, A. (2001). On the Role of RNA Amplification in dsRNA-Triggered Gene Silencing. Cell *107*, 465–476.
Sijen, T., Steiner, F.A., Thijssen, K.L., and Plasterk, R.H. (2007). Secondary siRNAs Result from Unprimed RNA Synthesis and Form a Distinct Class. Science *315*.
Slotkin, R.K. (2014). The epigenetic control of the Athila family of retrotransposons in Arabidopsis. Epigenetics *5*, 483-490.
Slotkin, R.K., and Martienssen, R. (2007). Transposable elements and the epigenetic regultation of the genome. Nature Reviews Genetics *8*, 272-285.
Snyder, M.J., Lau, A.C., Brouhard, E.A., Davis, M.B., Jiang, J., and Sifuentes, M.H. (2016). Anchoring of heterochromatin to the nuclear lamina reinforces dosage compensation-mediated gene repression. PLoS Genet *12*.

Spieth, J., Lawson, D., Davis, P., Williams, G., and Howe, K. (2014). Overview of gene structure in C. elegans. WormBook : the online review of C elegans biology, 1-18.
Spracklin, G., Fields, B., Wan, G., Vijayendran, D., Wallig, A., Shukla, A., and Kennedy, S. (2017). Identification and Characterization of C. elegans RNAi Inheritance Machinery. Genetics.
Tabara, H., Grishok, A., and Mello, C. (1998). RNAi in C. elegans: soaking in the genome sequence. Science *282*, 430-431.
Tabara, H., Sarkissian, M., Kelly, W., Fleenor, J., Grishok, A., Timmons, L., Fire, A., and Mello, C. (1999). The rde-1 gene, RNA interference, and transposon silencing in C. elegans. Cell *99*, 123-132.
Timmons, L., and Fire, A. (1998). Specific interference by ingested dsRNA. Nature *395*, 854.
Towbin, B.D., González-Aguilera, C., Sack, R., Gaidatzis, D., Kalck, V., Meister, P., Askjaer, P., and Gasser, S.M. (2012). Step-wise methylation of histone H3K9 positions heterochromatin at the nuclear periphery. Cell *150*, 934-947.
Tschiersch, B., Hofmann, A., Krauss, V., Dorn, R., Korgel, G., and Reuter, G. (1994). The protein encoded by the Drosophila position- effectvariegationsuppressor gene Su(var)3-9 combines domains of antagonistic regulators of homeoticgene complexes. The EMBO Journal *13*, 3822-3831.
Tuschl, T., Zamore, P.D., Lehmann, R., Bartel, D.P., and Sharp, P.A. (1999). Targeted mRNA degradation by double-stranded RNA in vitro. Genes & development *13*.
Vastenhouw, N.L., Brunschwig, K., Okihara, K.L., Muller, F., Tijsterman, M., and Plasterk, R.H. (2006). Gene expression: long-term gene silencing by RNAi. Nature *442*.
Verdel, A., Jia, S., Gerber, S., Sugiyama, T., Gygi, S., Grewal, S.I., and Moazed, D. (2004). RNAi-mediated targeting of heterochromatin by the RITS complex. Science *303*, 672-676.
Volpe, T., Schramke, V., Hamilton, G., White, S., Teng, G., Martienssen, R., and Allshire, R. (2003). RNA interference is required for normal centromere function in fission yeast. Chromosome Res *11*, 137-146.
Wassenegger, M., Heimes, S., Riedel, L., and Sänger, H.L. (1994). RNA-directed de novo methylation of genomic sequences in plants. Cell *76*, 567-576.
Wei, W., Ba, Z., Gao, M., Wu, Y., Ma, Y., Amiard, S., White, C.I., Rendtlew Danielsen, J.M., Yang, Y.G., and Qi, Y. (2012). A role for small RNAs in DNA double-strand break repair. Cell *149*, 101-112.
Weiser, N.E., Yang, D.X., Feng, S., Kalinava, N., Brown, K.C., Khanikar, J., Freeberg, M.A., Snyder, M.J., Csankovszki, G., Chan, R.C.*, et al.* (2017). MORC-1 Integrates Nuclear RNAi and Transgenerational Chromatin Architecture to Promote Germline Immortality. Dev Cell *41*, 408-423 e407.
Yamanaka, S., Mehta, S., Reyes-Turcu, F.E., Zhuang, F., Fuchs, R.T., Rong, Y., Robb, G.B., and Grewal, S.I. (2013). RNAi triggered by specialized machinery silences developmental genes and retrotransposons. Nature *493*, 557-560.
Yigit, E., Batista, P.J., Bei, Y., Pang, K.M., Chen, C.C., Tolia, N.H., Joshua-Tor, L., Mitani, S., Simard, M.J., and Mello, C.C. (2006). Analysis of the C. elegans Argonaute family reveals that distinct Argonautes act sequentially during RNAi. Cell *127*, 747-757.

Zamore, P.D., Tuschl, T., Sharp, P.A., and Bartel, D.P. (2000). RNAi: Double-Stranded RNA Directs the ATP-Dependent Cleavage of mRNA at 21 to 23 Nucleotide Intervals. Cell *101*, 25-33.
Zeller, P., Padeken, J., Schendel, R., Kalck, V., Tijsterman, M., and Gasser, S.M. (2016). Histone H3K9 methylation is dispensable for Caenorhabditis elegans development but suppresses RNA:DNA hybrid-associated repeat instability. Nature Genetics *48*.
Zhang, K., Mosch, K., Fischle, W., and Grewal, S.I. (2008). Roles of the Clr4 methyltransferase complex in nucleation, spreading and maintenance of heterochromatin. Nature structural & molecular biology *15*, 381-388.
Zhuang, J.J., Banse, S.A., and Hunter, C.P. (2013). The Nuclear Argonaute NRDE-3 Contributes to Transitive RNAi in Caenorhabditis elegans. Genetics *194*, 117-131.